



## รายงานวิจัยฉบับสมบูรณ์

โครงการ: การศึกษาคุณลักษณะ การกระจาย และการประยุกต์ใช้ฮอร์โมน นิวโรเปปไทด์เอฟ ต่อการเจริญเติบโต การพัฒนารังไข่ และการ ตกไข่ ของกุ้งก้ามกราม

Project: Characterization and localization of neuropeptide F, and its applications in growth, ovarian maturation and spawning of the female freshwater prawn, *Macrobrachium rosenbergii* 

## โดย

รองศาสตราจารย์ ดร.ยสวันต์ ตินิกุล และคณะ ภาควิชากายวิภาคศาสตร์ คณะวิทยาศาสตร์ มหาวิทยาลัยมหิดล

มิถุนายน 2560

# รายงานวิจัยฉบับสมบูรณ์

โครงการ: การศึกษาคุณลักษณะ การกระจาย และการประยุกต์ใช้ฮอร์โมน นิวโรเปปไทด์เอฟ ต่อการเจริญเติบโต การพัฒนารังไข่ และการ ตกไข่ ของกุ้งก้ามกราม

Project: Characterization and localization of neuropeptide F, and its applications in growth, ovarian maturation and spawning of the female freshwater prawn, *Macrobrachium rosenbergii* 

### โดย

รองศาสตราจารย์ ดร. ยสวันต์ ตินิกุล และคณะ ภาควิชากายวิภาคศาสตร์ คณะวิทยาศาสตร์ มหาวิทยาลัยมหิดล

สนับสนุนโดยสำนักงานกองทุนสนับสนุนการวิจัย และ มหาวิทยาลัยมหิดล (ความเห็นในรายงานนี้เป็นของผู้วิจัย สกว. และมหาวิทยาลัยมหิดล ไม่จำเป็นต้องเห็นด้วยเสมอไป)

#### **ACKNOWLEDGEMENTS**

In this project, I would like to acknowledge the support of many people, without whom this work would not have been accomplished. First, I would like to express my gratefulness and deep appreciation to Prof. Dr. Prasert Sobhon, for encouragement and excellent suggestions. My grateful appreciation is also extended to Prof. Dr. Peter J Hanna for their constructive comments and valuable guidance. I wish to express my gratefulness to Dr. Kaset Amantakul and Dr. Sompong Yoongtong, Vice President, and Dr. Mondhakarn Oprasertsawat, Assistant to President for Nakhonsawan Campus, Nakhonsawan Province, for providing the opportunities for me to conduct researches and valuable advices. I am extremely grateful to my oversea research collaborators, Prof. Dr. Joffre Mercier, Brock University, Canada and Assoc. Prof. Dr. Scott Cummins, at the University of the Sunshine Coast, Queensland, Australia, for their kindness, sharing his knowledge, and constructive advice on my project.

My special thank is expressed to Asst. Prof. Dr. Ruchanok Tinikul for her kindness, helpful suggestions, and supportive encouragement. In addition, my special gratitude is also extended to Dr. Thanapong Kruangkum, Dr. Jaruwan Ponjaroen, Ms. Sirorat Thongrod and Mr. Attakorn Engsusophon for their helps, valuable advices, and companionships. I would also like to thank Assoc. Prof. Dr. Prasert Meeratana and Mr. Tanes Poomtong for their assistance and useful suggestions. I also thank Center of Nanoimaging (CNI), Olympus Bioimaging Centers, and Central Instrumental Facility (CIF) at Faculty of Science, Mahidol University for the use of a confocal microscope and technical assistance. I would like to thank members at the Electron Microscopy and Cell Biology Laboratories (EM), as well as chair and staffs at Department of Anatomy, Faculty of Science, Mahidol University, for their assistance and provide laboratory spaces.

I would like to acknowledge the financial support from a TRF Research Career Development Grant (RSA grant) to me (co-funded by the Thailand Research Fund and Mahidol University, grant no. RSA5780011), and a Distinguished Research Professor Grant to Prof. Prasert Sobhon (jointly funded by the Thailand Research Fund, the Commission on Higher Education, and Mahidol University). Last of all, but the most on my mind, I am wholeheartedly grateful to my dearest mother, Mrs. Sirikul Tinikul, my daughter and family for their endless love, trust, and encouragement during my project study, which enables me to carry out and overcome all obstacles. Words are never enough to express how grateful I am for what they have done for me.

Assoc. Prof. Dr. Yotsawan Tinikul

### บทคัดย่อ

รหัสโครงการ: RSA5780011

**ชื่อโครงการ :** การศึกษาคุณลักษณะ การกระจาย และการประยุกต์ใช้ฮอร์โมนนิวโรเปปไทด์เอฟ

ต่อการเจริญเติบโต การพัฒนารังไข่ และการตกไข่ ของกุ้งก้ามกราม

ชื่อนักวิจัย: รศ.ดร.ยสวันต์ ตินิกุล

ภาควิชากายวิภาคศาสตร์ คณะวิทยาศาสตร์ มหาวิทยาลัยมหิดล

อีเมล์: yotsawan.tin@mahidol.ac.th, anatch2002@gmail.com

ระยะเวลาโครงการ : 15 มิถุนายน 2557 ถึง 16 มิถุนายน 2560

กุ้งก้ามกราม (Macrobrachium rosenbergii) เป็นสัตว์น้ำที่มีคุณค่าสูงทางเศรษฐกิจของประเทศไทยซึ่งมีการ ้ เพาะเลี้ยงกันอย่างกว้างขวางในแถบภูมิภาคเอเชียและประเทศไทย ปัญหาและอุปสรรคที่มักพบในการเพาะเลี้ยงกุ้งก้ามกราม ในปัจจุบัน โดยเฉพาะประสิทธิภาพในการผลิตพ่อพันธุ์และแม่พันธุ์ที่สามารถผลิตเซลล์สืบพันธุ์และตัวอ่อนก็ยังมีอยู่มาก ้ เนื่องจากการเลี้ยงในสภาพกักขังและมีประชากรหนาแน่นทำให้กุ้งเกิดความเครียดโดยปล่อยฮอร์โมนความเครียด ทำให้กุ้งลด ประสิทธิภาพในการสืบพันธุ์ลง นอกจากนี้การตัดตาแม่พันธุ์กุ้ง เพื่อกระตุ้นการพัฒนาของรังไข่ การฟักออกเป็นตัวของลูกกุ้งให้ เร็วขึ้น ซึ่งวิธีการเหล่านี้นอกจากจะเป็นวิธีการทรมานกุ้งแล้ว ยังส่งผลต่ออายุขัยและจำนวนครั้งของการสืบพันธุ์ของแม่พันธุ์กุ้ง และปริมาณของลูกกุ้งในแต่ละครั้งด้วย ซึ่งวิธีการเหล่านี้อาจจะไม่เป็นที่ยอมรับในอนาคต อีกทั้งอาหารสำเร็จที่ใช้เลี้ยงพ่อและ แม่พันธุ์กุ้งอาจจะไม่เหมาะสมที่จะกระตุ้นให้กุ้งมีประสิทธิภาพในการสืบพันธุ์ได้ ดังนั้นวัตถุประสงค์หลักของโครงการวิจัยนี้คือ ทำการศึกษาคุณลักษณะ การกระจาย ตรวจสอบผลของนิวโรเปปไทด์เอฟ (NPF) ต่อวงจรการพัฒนาของรังไข่และการตกไข่ ของกุ้งก้ามกรามเพศเมีย นอกจากนี้เราได้ศึกษาระดับ การปรากฏและการกระจายของสารสื่อประสาทและความสัมพันธ์ที่ เป็นไปได้กับ NPF ต่อการพัฒนาของระยะตัวอ่อนในกุ้งก้ามกราม โดยผู้วิจัยพบว่า NPF ประกอบด้วยสองกลุ่มหลัก คือ Long NPF (MrNPF-I, MrNPF-II, MrNPF-III) และ Short NPF โดยยังพบว่า การแสดงออกของยืน NPF และการกระจายตัวของ NPF ซึ่งเป็นยืนเป้าหมายโดยใช้วิธี RT-PCR และ Immunohistochemistry มีการแสดงออกในเนื้อเยื่อหลายแห่งด้วยกัน อาทิ สมอง ปมประสาทช่องอก ปมประสาทลำตัว และ รังไข่ นอกจากนี้ยังได้ทำการกระตุ้นพ่อแม่พันธุ์กุ้งด้วย NPF พบว่า NPF ทำ ให้วงจรการพัฒนาของรังไข่และการตกไข่สั้นลง และส่วนค่า GSI และ oocyte diameter มีค่าเพิ่มขึ้นเมื่อเทียบกับกลุ่มควบคุม อย่างมีนัยสำคัญทางสถิติ นอกจากนี้ยังพบว่าสารสื่อประสาทมีการกระจายตัว และมีผลต่อการพัฒนาของตัวอ่อนด้วย อย่างไรก็ ตาม หน้าที่หลักของ NPF และความสัมพันธ์ของ NPF กับสารสื่อประสาท ในการควบคุมการพัฒนาของรังไข่และการพัฒนา ของตัวอ่อนในเชิงลึกยังต้องมีการศึกษาเป็นลำดับต่อไป จากการวิจัยในครั้งนี้มีประโยชน์อย่างมากในการได้รับองค์ความรู้ พื้นฐานใหม่ที่สำคัญที่เกี่ยวข้องกับระบบและหน้าที่ของ NPF ในกุ้งก้ามกรามเพศเมีย และอาจจะสามารถนำ NPF มา ประยุกต์ใช้ในการกระตุ้นการพัฒนาของรังไข่และการฟักออกเป็นตัวของลูกกุ้งก้ามกรามให้เร็วขึ้นแทนการใช้วิธีตัดตาได้ใน อนาคต

คำสำคัญ: นิวโรเปปไทด์เอฟ, ซีโรโทนิน, โดพามีน, ระบบประสาท, รังไข่, วงจรการพัฒนาของรังไข่, การตกไข่ ตัวอ่อน, กุ้งก้ามกราม

#### **Abstract**

Project Code: RSA5780011

Project Title: Characterization and localization of neuropeptide F, and its applications in growth,

ovarian maturation and spawning of the female freshwater prawn, Macrobrachium

rosenbergii

Investigators: Assoc. Prof. Dr. Yotsawan Tinikul

Department of Anatomy, Faculty of Science, Mahidol University

**E-mail Address :** yotsawan.tin@mahidol.ac.th, anatch2002@gmail.com

Project Period: 15 June 2014 to 16 June 2017

The giant freshwater prawn, Macrobrachium rosenbergii, is one of the most commercially important freshwater crustacean species cultured in Thailand. The prawn aquaculture has lower productivity due to disease problems and the fecundity of female broodstocks which leads to the production of gametes, embryos larvae declines due to culture in captivity with a high population density, which may cause the release of stress hormones. At present, the best food that has been used for feeding prawns and shrimps in farms, but they are expensive and inconvenient in storage and feeding. Alternatively, the use of hormones could be one way to stimulate ovarian maturation and spawning. Neuropeptide F (NPF) is a neuropeptide with an RxRFamide carboxy terminus, and has been proposed to play an important role in feeding, energy homeostasis, and reproduction in invertebrates. In this proposal, we investigated the characterization, expression, distribution of NPF in the central nervous system and ovary, and its role in controlling ovarian maturation and spawning in the female freshwater prawn, M. rosenbergii. There were four putative NPFs identified using transcriptomic analysis of cDNA from our research group, and we further validated the data in this study using molecular cloning and RT-PCR techniques. They were designated as MrNPF-I, MrNPF-III and a short NPF (sNPF). The sequencing results showed that the deduced amino acid sequences of all MrNPF isoforms were similar to the sequence data obtained from transcriptomic analysis. Thus, this can ascertain the NPF sequences in female M. rosenbergii. We further produced, tested the specificity of MrNPF antibody and used it for further immunohistochemical studies. MrNPF-ir was distributed extensively in neurons, fibers, and neuropils in the brain, SEG, thoracic ganglia and abdominal ganglia. MrNPF-immunoreactivity (-ir) was detected in the ovaries and was more intense in the early- and mid-stages of ovarian development, and suddenly decreased in the mature stages. By RT-PCR, MrNPF transcript levels also increased during the early- and middle stages of ovarian development, and suddenly fell at late stage. MrNPFtreated prawns showed significantly decreased ovarian maturation periods, and increased GSI, OD, Vg levels compared with those of control groups. MrNPF also caused significantly earlier spawning compared with the control groups, and the numbers of eggs per spawn among experimental groups were higher compared with those of the controls. However, the mean fecundity between MrNPF-treated prawns and controls did not differ significantly. In addition to the investigation of the effects of MrNPF on female ovarian maturation and spawning, we further investigated whether NPF is involved in controlling embryonic development and/or in relation to major neurotransmitters. First, we examined the expression and changes in the levels, and possible actions of major neurotransmitters (5-HT and DA) in this grant, since we believed that 5-HT and DA could be the first hierarchical molecules in regulation of NPF in reproduction and probably embryonic development. The 5-HT concentrations gradually increased from the pale yellow egg to orange egg stages, and reaching a maximum at the black egg stage, while DA concentrations were much lower in the early embryos than those of 5-HT (P < 0.05). 5-HT was firstly detected in the early embryonic stages, whereas DA developed later than 5-HT. Functionally, 5-HT-treated prawns produced embryos with significantly shortened lengths of early embryonic stages, whereas DAtreated prawns lengthened the period of mid-embryonic stage onwards. However, the expression and precise action of NPF and mechanisms between 5-HT/DA and NPF in the regulation of ovarian maturation and embryonic development of this female prawn needed to be clarified by further studies. Finally, the results of this project should improve the basic knowledge of NPF and neuroendocrine-hormonal regulation in the prawn reproduction, and in finding the way to enhance the prawn reproduction for aquaculture.

**Keywords**: Neuropeptide F; Neurotransmitter; Ovarian maturation; Spawning; Central nervous system, Embryonic development; Freshwater prawn; *Macrobrachium rosenbergii* 

### 1. Objectives

**Overall objectives:** To characterize and localize neuropeptide F, and investigate its functions on ovarian maturation, spawning, and growth in the female freshwater prawn, *M. rosenbergii*.

**Specific Objectives**: In order to reach the above goals, the following specific objectives are formulated as the bases for the experimental designs:

- To identify and characterize the female *M. rosenbergii* neuropeptide F by a molecular cloning, high performance liquid chromatography (HPLC), mass spectrometry (MS) and/or other related techniques;
- 2. To localize and map NPF in the nervous system and gonadal tissues by immunohistochemistry;
- 3. To investigate the effects of NPF on ovarian maturation, spawning, and growth by bioassays; and
- 4. To study the existence, distribution and possible relationship of major neurotransmitters and NPF during reproduction and embryonic development.

# PART I. Identification and characterization of neuropeptide F in the female *M.*rosenbergii

1.1 Identification and characterization of NPF encoding gene.

#### 1.1.1 Specimen collection and preparation

Mature females *M. rosenbergii* were obtained from the culture ponds in Ayuthaya province and from Burapha University, Bang saen, Chonburi province. The size of the selected prawns was 15-20 cm in length, and 50-60 g in body weight. The animals were kept in tanks with continuous aeration, and water was changed every 2 days. The animals were acclimated under a photoperiod 12:12 h light-dark at room temperature for a week. The animals were fed twice a day with commercial pelleted feed. First, the prawns were anesthetized on ice and cut into three parts at an imaginary line from left to right mandible and cephalothoraco-abdominal junction. The anterior part was further dissected for eyestalks and brain, the middle part for subesophageal and thoracic ganglia, and the posterior part for abdominal ganglia. In addition, gonads (ovary), muscles (walking and swimming legs), and gastrointestinal tract, were dissected during the processes. All dissected tissues were immediately frozen and stored in liquid nitrogen until used.

#### 1.1.2 RNA extraction and transcriptomic analysis

Female *M. rosenbergii* issues, including eyestalks, CNS (pooled brain, thoracic ganglia, and abdominal ganglia), and ovaries were collected. Total RNA was isolated using TriPure isolation reagent (Roche, IN, USA) following the manufacturer's protocol. The quality and concentration of total RNA was determined by gel electrophoresis and spectrophotometry (NanoDrop 1000; Thermo Fisher Scientific, DE, USA). The dried form of total RNA was sent to BGI (Hong Kong), for *de novo* RNA-seq transcriptomes (http://bgiamericas.com/). Briefed method, the complementary DNA (cDNA) was first synthesized, and then mRNA was purified by subjecting to oligo-dT selection before performing the fragmentation into a small fragment. The fragmented cDNA samples were subsequently repaired and ligated with adapter. Double-stranded cDNAs were constructed by reversed-transcription of selected fragments. A duplex-specific nuclease and PCR amplification were then used for normalizing and constructing the cDNA libraries, respectively. Ultimately, samples were subjected to an Illumina HiSeq 2000 instrument (Illumina Inc.) for sequencing. After obtained the read data, *de novo* assemblies were then performed.

#### 1.1.3 RNA extraction and RT-PCR

Total RNA were extracted using TRIzol<sup>®</sup> reagent (Invitrogen, USA). These tissues were homogenized and processed according to the direction supplied with the kit. The yield of isolated RNA was determined as described in **1.1.2**. RT-PCR technique was used to synthesize first strand cDNA from the total RNA extraction. A 20-μl reaction volume for the first strand cDNA was carried out following the manufacturer's protocols. Each reaction contains 1-5 μg of total RNA, 1 μl of 0.5 μg/ml gene specific primer (reverse primer), 4 μl of 5x first strand buffer, 2 μl of 0.1 M DTT, 1 μl of 10 mM dNTP mix, and 1 μl of 200 units reverse transcriptase (RevertAidTM Reverse Transcriptase, Fermentus) were used as the reverse transcriptase enzyme. The reaction product was used as templates for cDNA amplification in PCR experiments.

#### 1.1.4 Primer designs

To validate the MrNPF-I, MrNPF-II, MrNPF-III and a short NPF (sNPF) genes, and gene specific primers were designed based on the sequence identified from transcriptomic analysis (Suwansa-Ard et al., 2015). Primers were synthesized by the Bioservice Unit, National Science and Technology Development Agency (NSTDA), Bangkok, Thailand.

#### 1.1.5 PCR experiments

The amplifications of specific cDNA sequences were performed in an Eppendorf thermal cycler. Each 25  $\mu$ l of the PCR reaction mixture contains approximately 1  $\mu$ l of 50-100 ng DNA template, 2.5  $\mu$ l of 10x PCR buffer, 400  $\mu$ M dNTP mix, 2 mM MgCl<sub>2</sub>, 400 nM of each primer, 1  $\mu$ l of 5 unit/ $\mu$ l of Taq DNA polymerase (Fermentus). A precise selection of optimal times, temperatures and numbers of cycles were performed depending on the DNA being amplified and the primers chosen.

#### 1.1.6 cDNA Cloning and sequencing

The amplified PCR fragments were cloned into TA cloning kit pGEMT easy® (Promega, USA). Transformation process were performed in competent *E. coli* cells, strain XL1(Blue), by CaCl₂/heat shock method. Microbiological techniques were used for growing the bacterial cells in amplicillin selected media. Finally, the plasmid DNA containing the genes of interest was isolated from *E. coli* using a miniprep procedure. The nucleotide sequences of cDNA obtained above were also determined (Macrogen Inc., Korea).

#### Results:

#### Identification and characterization of NPF encoding genes.

In this study, the aim of the first part was to identify and characterize neuropeptide F (MrNPF) in female *M. rosenbergii*, in order to obtain the real NPF sequences for further using for the antibody characterization and production, as well as for investigating their biological functions in female *M. rosenbergii*.

According to our research group, four putative NPFs were identified using transcriptomic analysis of cDNA from female *M. rosenbergii* tissues (including eyestalks, CNS and ovaries) with precursor encoding genes (Suwansa-Ard et al., 2015). These were included three isoforms of MrNPFs which were classified as long NPFs and a short NPF. They were designated as MrNPF-II, MrNPF-III, and a short NPF (sNPF). We further validated the data in this study and results of NPF precursor genes by using molecular cloning and RT-PCR techniques. The gene specific primers designed for each NPF gene and MrNPF-I, MrNPF-II, MrNPF-III and a MrsNPF encoding gene were amplified from cDNA extracted from the CNS and ovaries. The sequencing results showed that the deduced amino acid sequences of all MrNPF isoforms were similar to the sequence data obtained from transcriptomic analysis. Therefore, this can ascertain the NPF sequences in female *M*.

rosenbergii. The nucleotide and deduced amino acid sequences of all NPF isoforms were demonstrated in Figs 1-4. The mature sequence of active MrNPFs were predicted by analyzing the deduced amino acid sequences with signal IP 4.1 program and Neuropred program (http://neuroproteomics.scs.illinois.edu /neuropred.html), and this was summarized in Table 1. All of mature MrNPFs sequences had a consensus C-terminal RxRF sequence, as presented in invertebrate NPFs (Nassel and Wegener 2011).

Precursor proteins of long MrNPF-I, MrNPF-III gave rise a single active peptide sequence. The putative MrNPF-I precursor protein consisted of 90 amino acids, containing a 29 residue N-terminal signal peptide followed by the active peptide sequences. A single dibasic cleavage site was found at Lys63Arg. Therefore, predicted active peptide sequences for MrNPF-I was 32 amino acids length (Fig. 1). The putative MrNPF-II precursor had 127-amino acid length with a prediction of 29 residue N-terminal signal peptide and Lys86Arg dibasic cleavage site. This resulted in an active peptide consisting of 61 amino acids residues Fig. 2). Whereas the MrNPF-III precursor was predicted to have a short 23 residue N-terminal signal peptide and dibasic cleavage site at Lys86Arg with a 61-amino acid length of mature NPF sequence (Fig. 3).

The MrsNPF precursor was predicted to have multiple cleavage sites. It contained 25 residue N-terminal signal peptide and 7 positions of mono- and dibasic cleavage sites to give rise four active peptides (Fig. 4 and Table 1). These were included with three sNPFs containing a conserved sNPF motif (1: GGGGPPSMRLRF-NH<sub>2</sub> 2: TPALRLRF-NH<sub>2</sub> 3: APALRLRF-NH<sub>2</sub>) and one longest peptide of sNPF (GGGSIRSWQQVSQRSEPSLRLRY- NH<sub>2</sub>)

M Y Q R V G Q V W A A I L

gtgggcgtggtcgtcgtcatgcagcgtcatgcagatgggcggagttgagggcaaacccgaccca

V G V V V S V M Q M G G V E G K P D P

acgcagctggcggcatggctgatgccctcaagtacctgcaggagctcgacaaatattac

T Q L A A M A D A L K Y L Q E L D K Y Y

tcccaggtgtcacgacccagattcggaaaacgcagcagtatgccgtcctcctggtgat

S Q V S R P R F G K R S E Y A V P P G D

gttctgatggaagccagcgagagactcatggagaactttggcacgcaggaggtgaattccc

V L M E A S E R L M E T L A R R R -

**Fig. 1** Nucleotide and amino acid sequences of putative MrNPF-I precursor. Predicted signal sequence is indicated as bold letters. Dibasic cleavage site and amidation site are given by dark gray and black highlights. The mature sequence of MrNPF-I consisting of 32 amino acids is in light gray highlight.

Fig. 2 Nucleotide and amino acid sequences of putative MrNPF-II precursor. Predicted signal sequence is indicated as bold letters. Dibasic cleavage site and amidation site are given by dark gray and black highlights. The mature sequence of MrNPF-II consisting of 69 amino acids is in light gray highlight.

m R N Y A L T S

gcagcagtggtggtggccgtcctcctggtctcgacggcgtcctcggcgagaacgggcaac

A A V V V A V L L V S T A S S A R T G N

gccgccgagaccctgcaggccatgcgcgaggccgacctcgcaggaatcctgggctcgcc

A A E T L Q A M R E A D L A G I L G S A

gaggtaccctaccggtctaatatcttcaagtcacccgttgagctcaggcagtac

E V P Y P S R P N I F K S P V E L R Q Y

ttggatgcgcttaacgcttattatgccatcgctggacggccaggttcggtaagcggcc

L D A L N A Y Y A I A G R P R F G K R G

ggcgccatgccccagcggtcatcctcacacgacgacctcctcgactactgacgaaggaat

G A M P Q R S S S H D D L L D Y -

Fig. 3 Nucleotide and amino acid sequences of putative MrNPF-III precursor. Predicted signal sequence is indicated as bold letters. Dibasic cleavage site and amidation site are given by dark gray and black highlights. The mature sequence of MrNPF-III consisting of 61 amino acids is in light gray highlight.

a agtttccacgacaagaagtccgaggctatgggcgttgggcgttctcaaatggtgcacgMGVGVLKWCT  $\tt gcgggggtattctgctcatcttagcccaggtggcatccacggtgccaactccacct$ A G V F C C L I L A Q V A S T V P T P P gactacgatgctgccctcagcgacatgtacgacctgctgtcccacggcgtggagaggcgc D Y D A A L S D M Y D L L S H G V E R R gggggggggggggggcggccgccgtccatgcgactgagattcggcaagagaggcggaggaagc G G G G P P S M R L R F <mark>G K R G G G S</mark> attaggtcctggcagcaggtgtcccagaggtctgaaccttcgctcagactccgctacggc I R S W Q Q V S Q R S E P S L R L R Y G aagaqaaccgtcgacqaggctgaacccctcctcgatcacgacttggtccgaaaagaccgc K R T V D E A E P L L D H D L V R K D R T P A L R L R F G K R T S S D Y L Q D D gcctacgacgcagcagatttcatccgccaagaccgggctcccgccctcagactccgcttt A Y D A A D F I R Q D R A P A L R L R F ggcaaaagagacgtctcatacggacaggacgaagaagcatcaaccggcagccacgagcag G K R D V S Y G Q D E E A S T G S H E Q 

**Fig. 4** Nucleotide and amino acid sequences of putative sMrNPF precursor. Predicted signal sequence is indicated as bold letters. Dibasic cleavage site and amidation site are given by dark gray and black highlights. Four isoforms of mature sequences are in light gray highlight.

Table 1 Mature sequences of MrNPF and MrsNPF

NPF	Mature sequences
MrNPF-I	KPDPTQLAAMADALKYLQELDKYYSQVS <b>R</b> P <b>RF</b> -NH <sub>2</sub>
MrNPF-II	KPDPTQLAAMADALKYLQELDKYYSQVSRPSPRSAPGPASQIQALEKTLKFLQL
	QELGKLYSLRARPRF-NH <sub>2</sub>
MrNPF-III	ARTGNAAETLQAMREADLAGILGSAEVPYPSRPNIFKSPVELRQYLDALNAYYA
	IAGRPRF-NH <sub>2</sub>
sNPF	GGGGGPPSM <b>R</b> L <b>RF</b> -NH <sub>2</sub>
	TPALRLRF-NH <sub>2</sub>
	APALRLRF-NH <sub>2</sub>
	GGGSIRSWQQVSQRSEPSLRLRY-NH <sub>2</sub>

Furthermore, the MrNPF-I (KPDPTQLAAMADALKYLQELDK YYSQVSRPRF-NH<sub>2</sub>) and sNPF isoform (TPALRLRF-NH<sub>2</sub>, APALRLRF-NH<sub>2</sub>) were then selected to custom synthesize by GenScript company (USA). The synthesized MrNPF-I was used for polyclonal antibody production. While the biological functional assays were investigated with MrNPF-I.

# PART II. To localize and map NPF in the nervous system and gonadal tissues by immunohistochemistry

#### 2.1 Antibody and peptide

The polyclonal antibody against MrNPF peptide was produced following the protocol described previously by Tinikul et al (2011) and Thongrod et al (2017). Briefly, two male New Zealand white rabbits were approved and obtained by the Animal Care Unit, Faculty of Science, Mahidol University. The antiserum was produced by immunizing rabbits with synthetic MrNPF (GenScript, Piscataway, NJ, USA) that was conjugated to bovine serum albumin (BSA) using N-(3-dimethylaminopropyl)-N'-ethylcabodiimide hydrochloride (Sigma-Aldrich, St. Louis, MO, USA). For immunization, animals were injected subcutaneously with initial 500 µg conjugated proteins, mixed with Freund's complete adjuvant. A further three boosting injections were given with 250 µg of conjugated proteins mixed with Freund's incomplete adjuvant. Immunizations were performed at two week intervals. Blood was collected two weeks after the final injections, and following centrifugations. The antiserum was collected and stored at -20°C until used.

#### 2.2 Testing of antibody specificity by dot blot analysis

Dot blots were performed to test specificity of the antibody against MrNPF (Thongrod et al. 2017). Briefly, the synthetic peptide, MrNPF peptide (2 µg/ml) were spotted onto nitrocellulose membranes and dried at room temperature for 45 min. Non-specific bindings were blocked by the blocking solution containing 4% skimmed milk in TPBS (0.1% Tween 20 in 0.1 M phosphate-buffered saline), at room temperature for 2 h. After washing, the membranes were incubated in the primary antibody, anti-MrNPF, which was pre-absorbed with BSA at a concentration of 200 mg/ml, then incubated overnight at 4°C. Subsequently, the membranes were washed three times with TPBS, at room temperature, for 10 min each. Then HRP-conjugated goat anti-rabbit IgG (Southern Biotech, Birmingham, AL, USA), diluted at 1:4000 in blocking solution, was added to the membranes, and incubated at room temperature for 2 h. The membranes were gently washed three times in PBST. The signals were then developed using an ECL kit (Amersham Pharmacia Biotech, Buckinghamshire, UK), and the membranes exposed to film, before developing. Controls were performed by substituting primary antibodies with pre-immune rabbit serum, or by pre-absorption of the primary antibody with excesses of synthetic MrNPF's.

#### 2.3 Testing of antibody specificity by Western blotting

The Western blotting was used to ascertain antibody specificity. Briefly, 5 µg of BSA and BSA-conjugated MrNPF's, were separated by 12.5% SDS-PAGE. After electrophoresis, the resolved proteins were transferred onto nitrocellulose membranes. The membrane was then washed with TPBS (0.1% Tween 20 in 0.1 M phosphate-buffered saline). Non-specific binding was blocked with 4% skimmed milk in TPBS, for 2 h at room temperature, with gentle shaking. The membranes were subsequently incubated with primary antibody anti-MrNPF, preabsorbed with BSA (diluted 1:500) at a concentration of 150 mg/ml, overnight at 4°C, with gentle shaking. After washing three times with TPBS, the membranes were incubated with secondary antibody (HRP-conjugated goat anti-rabbit IgG, Southern Biotech, Birmingham, AL, USA), diluted 1:2000, at room temperature for 2 h. The membranes were gently washed three times in TPBS. The signal was developed using an ECL kit (Amersham Pharmacia Biotech, Buckinghamshire, UK), and exposed to film, before developing. Negative controls were performed by substituting primary antibody with pre-immune rabbit serum, or by absorption of the pre-absorbed primary antibody with excess of synthetic MrNPF's.

#### 2.4 Immunohistochemistry

The detection of immunofluorescence by the whole-mounts was based on the protocol of Tinikul et al. (2011, 2017). After fixation, the whole-mounts of the CNS were washed with 0.1 M PBS for 6 h, by changing the washing solution every 30 min. Each CNS was desheathed using microforceps and pre-incubated with 4% Triton X-100-PBS (10% NGS, 4% Triton X-100 in PBS) at 4 °C for 24 h. The tissues were then washed three times with 0.1 M PBS, by changing the washing solution every 15 min. The CNS whole-mounts were then permeabilized with Dent's solution (80% ethanol, 20% DMSO) at -20 °C for 8 h, and washed five times with 0.1 M PBS by changing the washing solution every 15 min. The CNS whole-mounts were incubated in the primary antibody (rabbit anti-MrNPF diluted 1:100), in 2% NGS, 0.4% Triton X-100, in PBS, at 4 °C for 6-7 days with gentle shaking. The CNS whole-mounts were then washed five times with PBST by changing the washing solution every 20 min, and followed by two washings with 0.1 M PBS by changing the washing solution every 15 min. The CNS whole-mounts were then incubated in the second antibody, Alexa 488-conjugated goat anti-rabbit IgG (Molecular Probes, Eugene, Oregon, USA), diluted 1:500 in 5% NGS, 0.4% Triton X-100, in 0.1 M PBS, at 4 °C for 72 h, with gentle shaking. In addition, the nuclei of cells in the CNS and ovaries were counterstained with ToPro-3 (Molecular Probes, Eugene, Oregon,

USA), diluted 1:2000 in blocking solution. The whole-mounts were then washed with PBST for 2 h with six changes, and subsequently with PBS for 1 h with three changes. They were subsequently dehydrated through increasing concentrations of ethanol (50%, 70%, 80%, 90%, 95%, 3×100%), and cleared in methyl salicylate for 30-45 min. Controls were performed by replacing the primary antibodies with pre-immune rabbit serum, or by pre-absorption of the primary antibody with excesses of synthetic MrNPFs.

#### 2.5 Confocal laser scanning microscopy and image analysis

The whole-mounts and sections of the CNS prepared for immunofluorescence detection, were viewed and photographed with an Olympus Fluoview 1000 laser-scanning confocal microscope (Olympus America, Center Valley, PA). The tissues were scanned sequentially for each fluorophore to obtain separate images for each label and an overlay image of all three channels for each optical section. These projected images were produced using subsets of the z-stacks. Furthermore, the digital images were exported and converted from the Olympus confocal system as .tiff images, and then transferred into Photoshop CS software (Adobe Systems Inc., San Jose, CA, USA) to adjust contrast and brightness to obtain optimal clarity. In addition, negative controls for each fluorochrome were scanned using the same parameter settings.

#### Results

#### Testing the specificity of MrNPF antibody

In this part, specificity of anti-MrNPF-I antibody was rigorously tested against synthetic NPF-Is, FMRFamide, KISS1 and KISS2 peptides by Thongrod et al. (2017). The anti-MrNPF-I showed no cross-reaction with the synthetic FMRFamide, KISS1 and KISS2 peptides, while anti-FMRFamide showed very low reactivity against MrNPF-I. Preabsorption of anti-MrNPF-I with MrNPF-I reduced the intensity of the MrNPF-I dot appreciably, while preabsorption with FMRFamide did not. Preabsorption of anti-FMRFamide with MrNPF-I totally abolished the reactivity of the antibody against MrNPF-I (Fig. 5). Anti-MrNPF-I showed strong reactivity to both LvNPF-I and MrNPF-I peptides, and also to protein extract from the CNS. For immunohistochemical testing, anti-MrNPF-I showed intense staining in the olfactory neuropil (ON), but no reactivity was detected when anti-MrNPF-I was preabsorbed with MrNPF-I peptide (Fig. 5). These results confirmed that anti-MrNPF-I is strictly specific to MrNPF-I and strongly cross-reacting with LvNPF-I (Thongrod et al., 2017). Thus, this antibody was used for

subsequent immunoperoxidase and immunofluorescence detections. Since the amino acid sequences of MrNPF-I and –II are identical, except for the insert in the mid region of the latter as mentioned earlier, we assume that anti-MrNPF-I can detect both isoforms and henceforth will be referred to as MrNPFs (Thongrod et al., 2017, Fig. 5). The pre-immune serum did not show any positive result. Therefore, this antibody was used for examining the neuroanatomical distribution of MrNPF peptide in the CNS and ovary of this prawn.

#### Expression and distribution of MrNPF immunoreactivity in the brain and ventral nerve cord

In *M. rosenbergii*, the supraesophageal ganglion (brain) is composed of three major regions: medial protocerebrum which contains anterior medial protocerebral neuropils (AMPNs), posterior medial protocerebral neuropils (PMPNs), protocerebral bridge (PB), central body (CB) and neuronal clusters 6, 7 and 8; deutocerebrum containing several neuropils including medial antenna I neuropil (MAN), lateral antenna I neuropil (LAN), olfactory neuropil (ON) and olfactory globular tract neuropil (OGTN), and neuronal clusters 9, 10, 11, 12 and 13; tritocerebrum which contains tegumentary neuropil (TN) and antenna II neuropil (AnN) and neuronal clusters 14, 15, 16 and 17 (Fig. 6).

In medial protocerebrum, there was strong MrNPF-immunoreactivity (-ir) in many medium-sized neurons within cluster 6 (Fig. 6). Intense immunoreactive fibers were observed in AMPN and PMPN neuropils and moderately intense immunoreactive fibers were also detected in PT, PB, and CB neuropils. In the deutocerebrum, and very strong MrNPF immunoreactive fibers were observed in the neuropils of ON and OGTN, and detected in medium-sized neurons of clusters 9, 11 (Fig. 6). In the tritocerebrum strong MrNPF-ir neurons were detected in clusters 14, 15, 16 (Fig. 8f) and intense immunoreactive fibers in the TN and AnN (Fig. 6). In the CEG, SEG, thoracic ganglia and abdominal ganglia, MrNPF-ir was detected in neurons and fibers (Figs. 7-8). In the thoracic ganglia, MrNPF-ir was detected in medium-sized neurons in ventromedial cell clusters along the midline of each thoracic ganglion, as exemplified by MrNPF-ir neurons in T2, T3 and T4 (Fig. 7). MrNPF-ir fibers were detected in the abdominal ganglia (A1-A6; (Fig. 8).

This study may provide some clues demonstrating the types and characteristics of MrNPF, as well as their specific localizations in the nervous system and ovary during ovarian maturation cycle, implicating their important involvements in female prawn growth and reproduction, as shown in the bioassay results.

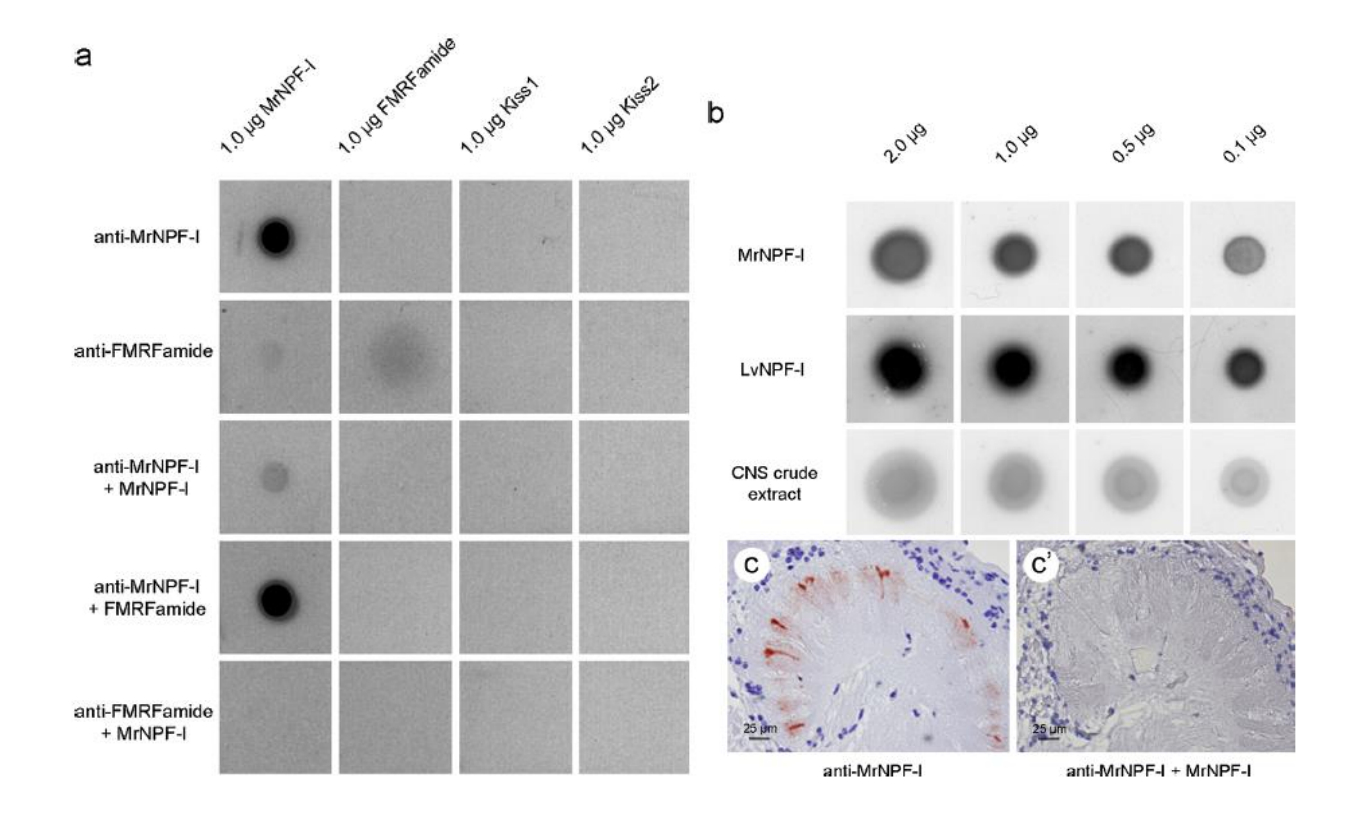


**Fig. 5** From Thongrod et al. (2017), specificity test of anti-MrNPF-I antibody. (a) Cross-reactivity tests of anti-MrNPF-I and anti-FMRFamide with synthetic MrNPF-I, FMRFamide, KISSI and KISSII peptides. The anti-MrNPF-I shows no cross-reaction with synthetic FMRFamide, KISSI and KISSII peptides, and the preabsorption with MrNPF-I largely abolishes its reactivity to MrNPF-I. (b) Anti-MrNPF-I show strong immunoreactivity to NPF-I of *L. vannamei* as intense as NPF-I of *M. rosenbergii*, and also a presumptive NPF protein in the CNS extract.(c) Intense immunoreactivity of anti-MrNPF-I in the olfactory neuropil (ON), no reactivity was seen when using anti-MrNPF-I preabsorbed with the peptide. These results show that anti-MrNPF-I is specific to NPFs. These results were performed and these figures were made by Thongrod et al. (2017).

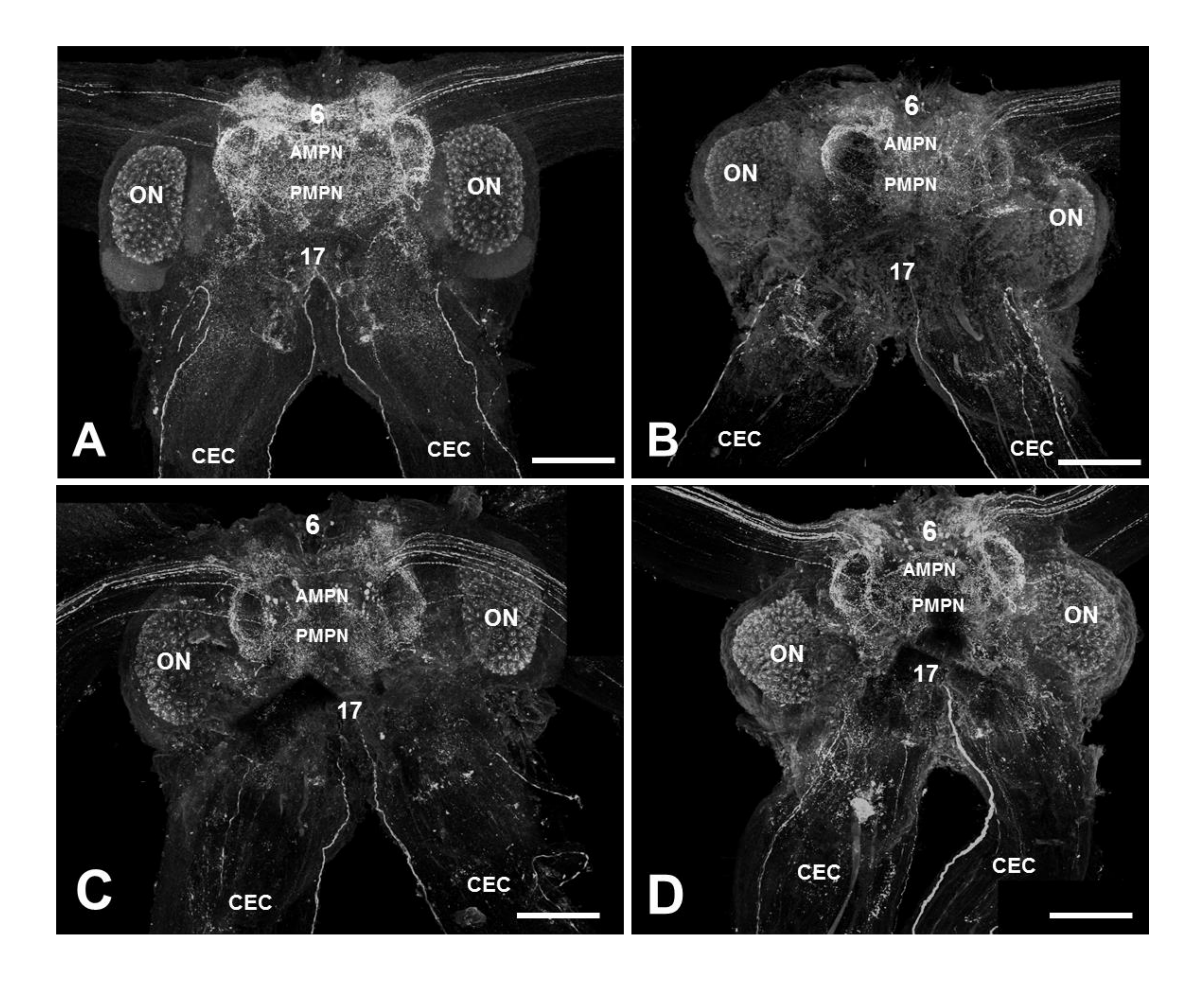


Fig. 6 Immunofluorescence detection of MrNPF-ir (green) in the brain during various ovarian stages, and cell nuclei are counterstained with ToPro-3 (red). The numbers 6 and 17 represent the neuronal clusters 6 and 17 in the brain, respectively. A, stage I; AMPN anterior medial protocerebral neuropil; B, stage II; C, stage III; CEC, circumesophageal ganglia; D, stage IV; ON, olfactory neuropils; PMPN, posterior medial protocerebral neuropil. Scale bar: 400 μm

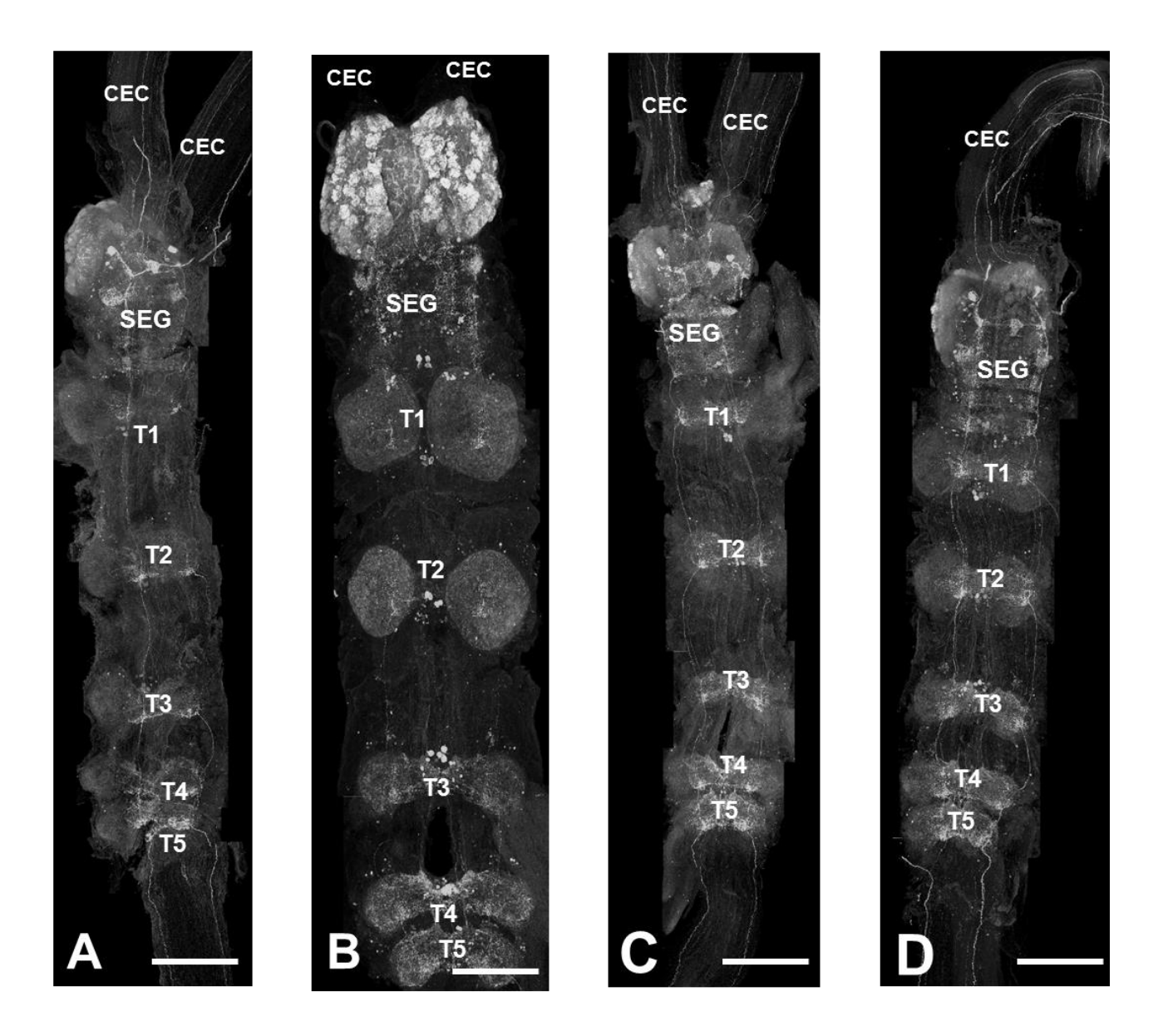
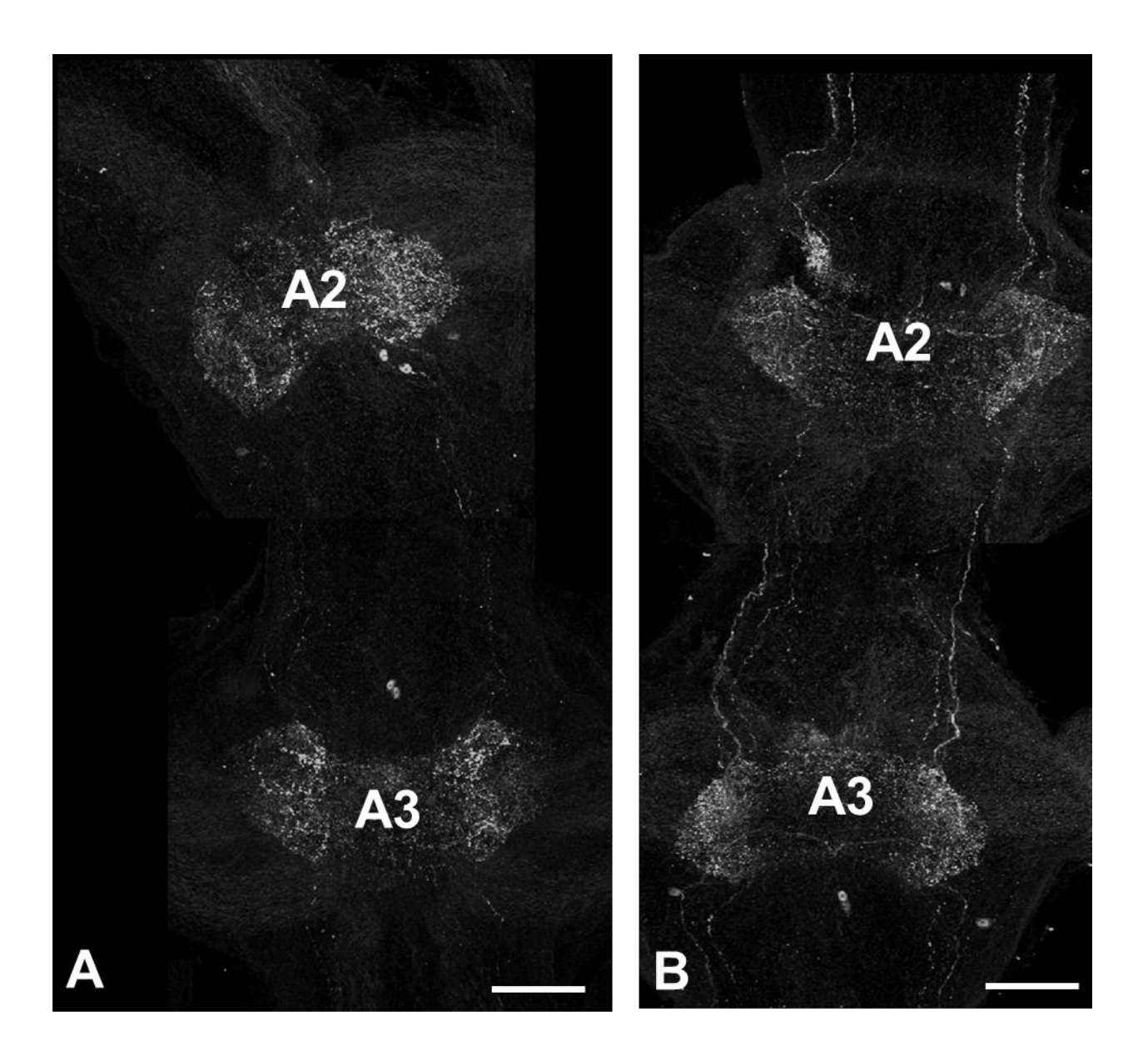


Fig. 7 Immunofluorescence detection of MrNPF-ir (green) in the thoracic ganglia during various ovarian stages, and cell nuclei are counterstained with ToPro-3 (red). A, stage I; B, stage II; C, stage III; CEC, circumesophageal ganglia; D, stage IV; T1-T5, first thoracic ganglion to fifth thoracic ganglion; SEG, subesophageal ganglia. Scale bar: 400 μm



**Fig. 8** Immunofluorescence detection of MrNPF-ir (green) in the abdominal ganglia during various ovarian stages, and cell nuclei are counterstained with ToPro-3 (red). A, stage I; A2 and A3, second and third abdominal ganglia; B, stage IV. Scale bar: 400 μm

#### **Discussion**

In the present project, our recent transcriptomic (Suwansa-ard et al. 2015) and molecular analyses (Thongrod et al., 2017; Tinikul et al., 2017) showed that MrNPF-I and II active peptides show high sequence similarity (>90%) with L. vannamei NPF-I and-II, whereas the MrNPF-III active peptide shows high similarity (66%) with mollusk neuropeptide Y. Moreover, a precursor of short NPF (sNPF) transcript was identified from the eyestalk and CNS transcriptomes; and this sNPF precursor is predicted to be cleaved at multiple sites to give rise to four active short peptides. In the present project, we validated the sequences of the two isoforms of NPFs and found that the full sequences are identical with those predicted from our earlier transcriptomic analysis (Suwansa-ard et al. 2015). It was found that the MrNPF-I, -II precursor proteins, encoded by separate genes, showed high similarity to other prawns NPFs, including L. vannamei and M. marginatus (Christie et al. 2011), while the mature NPF-I is almost identical except for four amino acids (threonine (T), alanine (A), aspartic acid (D) and lysine (K) instead of serine (S), asparaging (N), glutamic acid (E) and asparagine (N), respectively) at the mid region of the peptide (Thongrod et al., 2017). The MrNPF-II is almost identical to the NPF-II of M. marginatus and L. vannamei except for 3 amino acids in the mid region and 1 amino acid in the insert part of the mature peptide. Hence this would confirm that the active peptides of all arthropods and crustaceans are highly conserved.

Several studies have reported regarding expression and distribution of NPF for *Drosophila* and insect NPFs by several techniques, including immunohistochemical and RT-PCR. The NPFs and their receptors were detected in the brain, SEG, ventral nerve cord and midgut of larval *Drosophila* (Carlsson et al. 2013). In *L. vannamei* and *M. marginatus*, the NPF was only determined and it was reported that both NPF-I and -II are broadly distributed in the CNS and the optic ganglia of the eyestalk, brain, thoracic and abdominal ganglia (Christie et al. 2011). In comparison, the intensity of MrNPF -I and -II transcripts in various parts of the freshwater prawn CNS are similar to that of the two

penaeus shrimps with the highest intensity in the brain and thoracic ganglia with the NPF-I showing 5 to 7-fold higher expression than NPF-II. Interestingly, we detected that NPF-I was strongly expressed in the ovary in the present project (Suwansa-ard et al. 2015; Thongrod et al., 2017; Tinikul et al., 2017). Therefore, the wide spread expression of NPFs in ovaries implicate distinct role of NPF in reproduction and may be in controlling feeding, however, this needs to be performed by further studies.

In the supraesophageal ganglion (brain), the strong expression in neurons of cluster 6 and fibers within neuropils of AMPN, PMPN, PT, PB, CB of the medial protocerebrum implicates further that these peptides may help integrating the photoreception by the forebrain (protocerebrum) and the olfactory reception by the midbrain (deutocerebrum). Indeed, the strong intensity of NPFs detected in the neurons of clusters 9, 11 and fibers of the ON and OGTN neuropils, which are the key structures of the midbrain that receive olfactory stimuli (Kruangkum et al. 2013), further supports the notion that MrNPFs may play a central role in mediating the reception of food odor as widely known in *Drosophila* (Nässel and Wegener 2011), as well as integrating between visual and olfactory perceptions.

To our current knowledge, we believe that because of their highly conserved sequences the NPFs must play roles in several physiological processes of this female prawn. However whether NPF should play important role, such as integration in controlling the motor function of the feeding and digestive organs remains unclear which should be further investigated.

# PART III. Investigation of effects of MrNPF on female ovarian maturation and spawning by Bioassays

#### 3.1. Experimental animals and acclimatization

Mature female freshwater prawns (weighing 30-45 g) were obtained from a local market (Phran Nok market, Bangkok, Thailand). The prawns were kept in indoor circular plastic tanks, each 1.50 m in diameter with water depth at 0.80 m, and about 30% of water changed every 2 days. The prawns were fed commercial food pellets (Charoen Pokphand Group, Thailand) twice per day. Aeration was given all day. Small plastic cages were added in every tank for molting animals to hide and to avoid being killed due to the cannibalistic behavior of this species. Male and female prawns were stocked at a ratio of 1:5, respectively, in the same tank. The prawns were acclimatized under a photoperiod of 12:12 h light-dark for a week before starting the experiments.

#### 3.2. Histological examination and determination of ovarian stages

The maturation stages of ovaries during the ovarian cycle were examined directly, and classified based on the criteria described previously (Meeratana and Sobhon 2007; Tinikul et al., 2008). Ovaries were fixed in Bouin's fixative and processed for paraffin embedding, as described previously (Tinikul et al., 2015), in order to evaluate the histology. The sections were cut at 5-6 micron thicknesses from each ovary, after which they were deparaffinized and stained with hematoxylin and eosin (H&E). The sections were mounted with Permount (Bio-Optica, Milan, Italy), and viewed under a Nikon ECLIPSE E600 light microscope. Then images were photographed using a Nikon digital DXM1200 camera.

#### 3.3. Peptides and antibodies

The MrNPF used in this study was MrNPF (KPDPTQLAAMADALKYLQELDKYYSQVSRPRFamide) peptide identified and characterized from the eyestalks and CNS transcriptomes by our research group (Suwansa-ard et al., 2015). This peptide was custom synthesized (GenScript, Piscataway, NJ, USA). In addition, a polyclonal antibody against MrNPF was produced and its specificity was also tested rigorously (Thongrod et al., 2017). Briefly, female New Zealand white rabbits (8 week-old) were obtained from the Animal Care Unit, Faculty of

Science, Mahidol University, and used for production of anti-MrNPF with the approval of Animal Ethics Committee, Faculty of Science, Mahidol University.

#### 3.4. In vivo effects of MrNPF on ovarian maturation and spawning

The doses of MrNPF used in this work were based on the stimulatory effects of L. vannamei NPF (Christie et al., 2011; Tinikul et al., 2015), with some modifications. In this study, in order to investigate the effects of MrNPF on ovarian maturation and early spawning, we employed two doses, 10<sup>-6</sup> and 10<sup>-5</sup> mol/prawn of MrNPF. All injections were given at 4-day intervals. The injections were performed via an intramuscular site at the second abdominal segment using 1 ml syringes fitted with a 26 G × 1/2 (0.45 × 12 mm) thin-wall needle. The measurement of total length and weight of the prawns were performed on every treatment day prior to injections. MrNPF synthetic peptide was dissolved in 0.9% normal saline. For ovarian maturation assay, the prawns were divided into 4 groups of about 45 animals each, and treated as follows: (1) the non-injected control group (C); (2) the sham control: (3 and 4) the groups injected with MrNPF at doses of 10<sup>-6</sup> and 10<sup>-5</sup> mol/prawn, respectively. For spawning assay, we divided prawns into four groups: (1) the non-injected control group (C); (2) the sham control; (3 and 4) the groups injected with MrNPF at doses of 10<sup>-6</sup> and 10<sup>-5</sup> mol/prawn. Prawns in each group were identified by tying plastic loops of different colors around one eyestalk. At least, five prawns in each group were randomly selected and sacrificed at 4-day intervals to examine a gonado-somatic index (GSI = [ovarian weight (g)/body weight (g)] × 100), and oocyte diameters (OD) were carefully measured as described previously (Tinikul et al., 2015). One hundred oocytes were randomly selected at each ovarian stage in each prawn in at least three separate ovarian regions, were examined under the light microscope. Diameters of the one hundred oocytes with full nuclear profiles were measured, and the data expressed as a mean ± SD for each treatment group. The experiment was performed in duplicate. GSI and OD values of the MrNPF-injected groups and the control groups were then analyzed and compared by statistical analyses. The rest of the prawns were allowed to proceed until they spawned in order to determine the spawning duration. Pieces of ovary were subsequently fixed in Bouin's solution, paraffin-embedded, sectioned, stained with H&E, and examined under the light microscope, in order to determine the stages of ovarian maturation and oocyte diameters.

#### 3.5. Hemolymph vitellogenin (Vg) levels after treatment with MrNPF

An anti-vitellin antibody was produced from female M. rosenbergii, and the tests of its specificity and cross reactivity were rigorously performed by Western blot analysis as reported earlier (Soonklang et al., 2012), and the protocol for quantification of hemolymph Vg levels in M. rosenbergii was based on the report of Tinikul et al. (2015) with some modifications. The hemolymph of MrNPFinjected groups and the control groups was collected from the hemolymph sinus at 4-day intervals. The hemolymph vitellogenin (Vg) levels was evaluated by an indirect ELISA technique. Briefly, a 100 μl of hemolymph was centrifuged, and the supernatants collected and stored at -20 °C until used. Microtiter plates were coated with 100 µl of hemolymph supernatant diluted in coating buffer for 2 h at 37 °C. Non-specific bindings were blocked with a blocking buffer containing 0.25% bovine serum albumin (BSA) in 0.01 M PBS, at 37 °C for 2 h. After washing three times, the plates were incubated in anti-vitellin diluted 1:2000 in a diluent containing 0.25% BSA in 0.01 M PBS. Aliquots of 100 µl of primary antibody were added to the wells and the plates incubated at 37 C for 2 h, and then incubated with goat-anti rabbit-HRP (Southern Biotech, Birmingham, USA), diluted 1:4000, at 37 °C, for 1 h. Further, the plates were washed and the color was developed by adding TMB substrate for 15 min, and the reaction was stopped by adding 1 M HCl. The Vg concentrations were calculated from a standard curve established from measurements using purified vitellin. Determinations of hemolymph Vg levels were performed in duplicate. The OD's were read at 450 nm using an automatic spectrophotometer. A negative control sample was prepared in parallel using rabbit pre-immune serum in place of primary antibody.

#### 3.6. Immunohistochemistry in various ovarian stages

The female prawns (n = 5 each) of the four stages of the ovarian maturation cycle were anesthetized on ice for 15-20 min and the ovaries were dissected out and immediately fixed with 4% paraformaldehyde in 0.1 M PBS for MrNPFs for 12-16 h at 4 °C. The ovaries were cut at a 6 μm thickness and mounted on coated slides. The sections were deparaffinized and rehydrated through a graded series of ethyl alcohol, and then processed for immunohistochemistry. The method for immunohistochemical detections was based on that described previously (Tinikul et al., 2015; 2016) with some modifications. For the immunolocalization of MrNPF, rehydrated ovarian sections were incubated with 1% glycine in PBS, and non-specific binding was blocked by the blocking solution containing 10% NGS in PBST. The sections were then incubated with rabbit anti-MrNPF diluted 1:100

in the blocking solution, and then incubated in secondary antibody, Alexa488-conjugated goat antirabbit IgG (Molecular Probes, Eugene, OR, USA), diluted 1:200. In addition, the nuclei in ovarian sections were counterstained with ToPro-3 (Molecular Probes) diluted 1:4000 in blocking solution. The sections were mounted in Vectashield (Vector Laboratory, Burlingame, CA, USA). They were then viewed and images captured using an Olympus FV1000 confocal laser scanning microscope. Negative controls were performed by replacing the primary antibody with the pre-immune rabbit serum, or pre-absorption of the primary antibody with excess of synthetic MrNPF.

#### 3.7 Expression of MrNPF gene in various ovarian stages by RT-PCR

Mature female prawns were anesthetized in ice for 10-15 min. The different stages of ovaries were carefully collected. The protocol for examination of expression of *MrNPF* gene was based on previous reports (Tinikul et al., 2017). All tissues were immediately immersed in liquid nitrogen and store at -80 °C until used. Each sample was homogenized and the total RNA was isolated using Trizol<sup>®</sup> reagent (Invitrogen, CA, USA), following the manufacturer's protocol. The purity and quantity of total RNA were determined by spectrophotometer at 260 and 280 nm. The total RNA was treated by DNase I enzyme (Invitrogen, Carlsbad, CA, USA) to remove genomic DNA following the manufacturer's protocol. First stranded cDNA was synthesized by reverse transcription using SuperScript<sup>TM</sup> III Reverse Transcriptase (Invitrogen, CA, USA) with random hexamer primers. The cDNA was then amplified using Platinum<sup>®</sup> Taq Polymerase (Invitrogen, CA, USA) with *MrNPF* specific primers. RT-PCR products were then separated by 1.5% agarose gel electrophoresis. Beta-actin gene was used as the normalization control and the expression levels of *MrNPF* were normalized against beta-actin.

#### 3.8. Statistical analyses

Data were presented as means  $\pm$  SEM. The data were then analyzed for statistical differences with a SPSS program, using one-way analysis of variance (ANOVA) and Duncan's multiple range test. A probability value less than 0.05 (P<0.05) indicated a significant difference.

#### Results

#### The expression of MrNPF in various stages of ovaries

In the ovaries, the oogonia and early previtellogenic oocytes (Oc1) were not immunoreactive when detected with anti-MrNPF as a probe (Fig. 9A). Intense MrNPF-ir was observed in the cytoplasm of late previtellogenic and early vitellogenic oocytes (Oc2 and Oc3) (Fig. 9B), the epithelium and smooth muscle cells of the oviduct (Fig. 9C-D) and the capsule of ovaries (Fig. 9D-E). In contrast, MrNPF-ir appeared much weaker in late vitellogenic oocytes (Oc4 and mOc) (Fig. 9E). The control sections of oocytes and follicular cells showed no positive staining (Fig. 9F). Using RT-PCR, *MrNPF* transcript was detected in the total extract of various stages of ovaries (Fig. 9G-H). The detection of beta-actin gene expression (used as a positive control and as for normalization of the *MrNPF* expression), was identified in all tissues with equal intensity in all samples. The expression of the mRNA of *MrNPF* was most intense in the ovarian stage III (Fig. 9G, Iane 3), and less intense in the early stages of ovaries (stages I and II), while almost absent in mature ovaries (stage IV) (Fig. 9H).

#### Effects of MrNPF on ovarian development

In this study, the ovarian maturation period of the prawns treated with MrNPF at both doses of  $10^{-6}$  or  $10^{-5}$  mol/prawn were  $28.6 \pm 4.28$  and  $29.76 \pm 5.7$  days, respectively, which were significantly shorter (P<0.05) than that of the controls (i.e.,  $39.2 \pm 4.66$  days) (Fig. 10A). Moreover, the percentage of prawns that attained various ovarian stages at 16 days after the first MrNPF injections showed that in non-injected and sham control groups, most female prawns developed to ovarian stage II (30% and 35%, respectively) and stage III (15% and 20%, respectively), whereas the rest remained at stage I (Fig. 10B). By contrast, 30% of prawns injected with a dose of  $10^{-6}$  mol/prawn, showed the ovaries at stage III. In addition, the prawns injected with doses of  $10^{-6}$  mol/prawn exhibited 50% and 60% ovarian stage IV (Fig. 10B). These data indicated that MrNPF at doses of  $10^{-6}$  or  $10^{-6}$  mol/prawn shortened ovarian maturation period by nearly 10-12 days or about 30%, particularly at the lower dose of  $10^{-6}$  mol/prawn.

At days 1 and 4 after treatment, the GSI values of the controls and MrNPF-injected groups at both doses were all low and not significantly different (P < 0.05) (Fig. 11A). At day 8 post-injection, the GSI values of both groups of MrNPF-injected prawns trended to have slightly higher GSI values, but still with no significant difference from the control groups (P > 0.05). On days 12 and 16, both groups of injected prawns exhibited significantly higher GSI values compared with the control group

(P<0.05) (Fig. 11A). During the experiments, female prawns also exhibited the increase of weight  $(30.14 \pm 4.62 \text{ g})$ , but were not statistically significant compared with the control  $(30.53 \pm 3.39 \text{ g})$ . In addition, mean oocyte diameters (OD) of vitellogenic oocytes (Oc3) and mature oocytes (Oc4) in both groups of treated prawns increased significantly when compared with the control groups (P<0.05) (Fig. 11B). MrNPF-injected prawns, whose ovaries were determined to be at stage IV by external observations, underwent spawning on the following night. All prawns tolerated the injected doses of MrNPF without showing any abnormal behavior.

#### Assessment of ovarian histology

Examination of ovarian histology of the MrNPF-injected and control groups was conducted to ascertain the degree of the ovarian maturation. On days 1 and 4, there were no difference in the ovarian histology in the control groups (Fig. 12A), and the MrNPF-treated groups as the ovaries contained mostly early previtellogenic oocytes (Oc1) and few late previtellogenic oocytes (Oc2) (Fig. 12B). Distinct differences were observed at day 12 and 16 when the ovaries of the control group contained mostly previtellogenic oocytes (Oc2) (Fig. 12C), while the ovaries of the MrNPF-treated groups with doses of 10<sup>-5</sup> or 10<sup>-6</sup> mol/prawn contained mostly early vitellogenic oocytes (Oc3) and late vitellogenic oocytes (Oc4) with numerous lipid droplets. In addition, the diameters of oocytes in the MrNPF-injected groups were larger than those of the control groups (Fig. 12D).

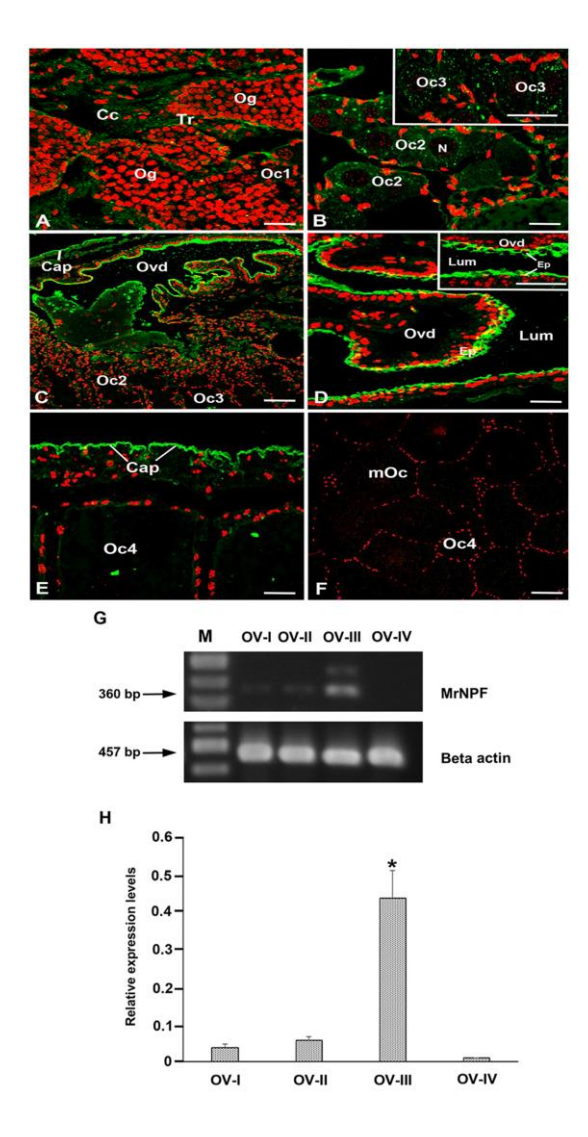
#### Hemolymph Vg concentrations after treatment with MrNPF

Vg concentrations in the non-injected control group, gradually increased from day 0 to about days 36-40 which were from 26.33  $\pm$  4.77 to 266.7  $\pm$  14.38 µg/ml, respectively (Fig. 12E). The Vg concentrations in the MrNPF-treated prawns with  $10^{-5}$  and  $10^{-6}$  mol/prawn showed significant increases from ovarian stage I (19.8  $\pm$  4.1 and 23.75  $\pm$  4.83 µg/ml) to peak at stage IV (348.5  $\pm$  13.1 and 327.2  $\pm$  14.9 µg/ml), respectively, compared with the control group (266.7  $\pm$  14.38 µg/ml) (P<0.05). The Vg concentrations after injection with  $10^{-5}$  or  $10^{-6}$  mol/prawn of MrNPF were approximately 1.3 and 1.2 times higher than that of the control group at ovarian stage IV (P<0.05) (Fig. 12E).

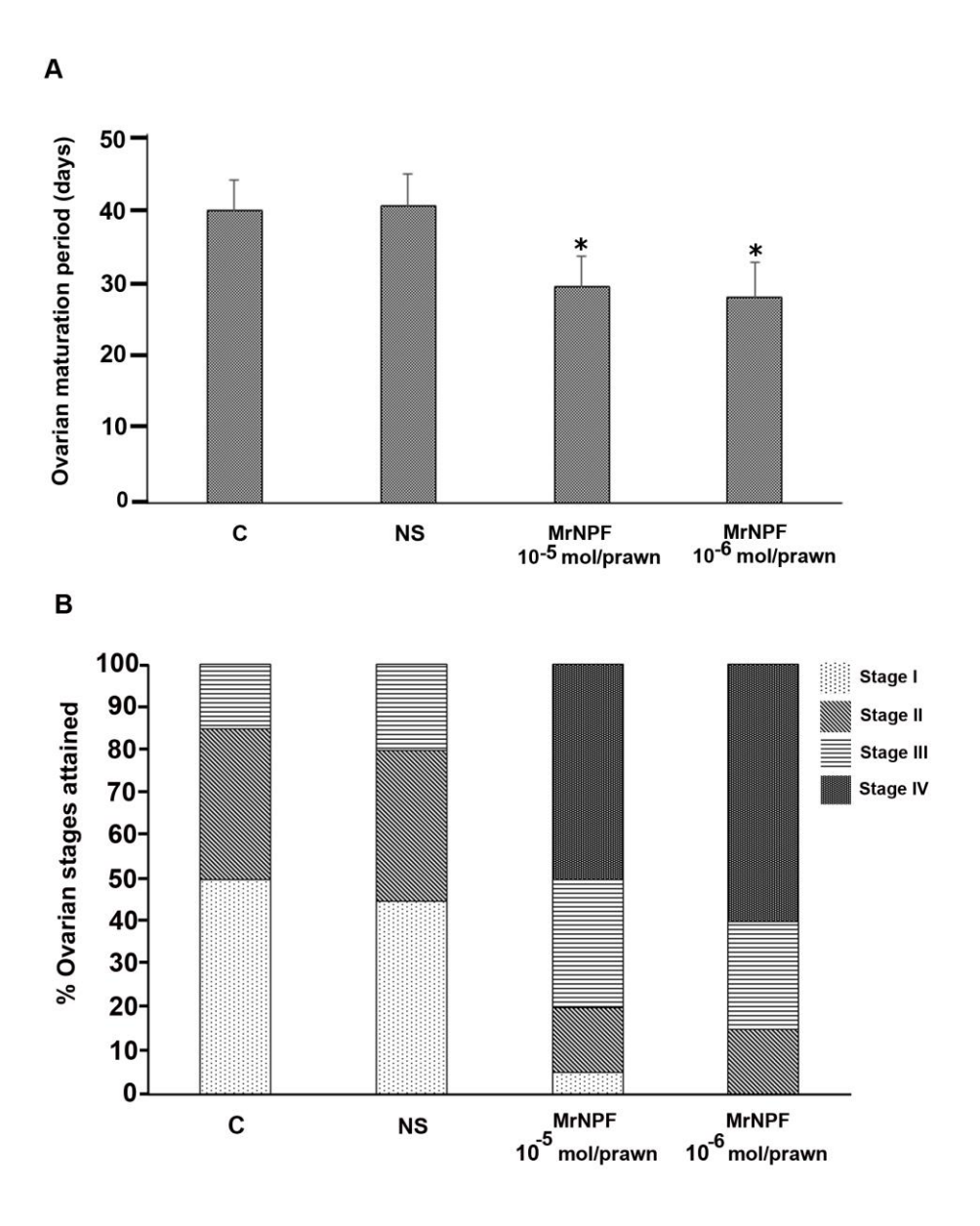
#### Effects of MrNPF on spawning

The durations of spawning, the quality of spawned eggs and the percentage of fertilized eggs from MrNPF-treated groups and control groups were also investigated (Fig. 13, 14). Interestingly, the durations of spawning of MrNPF-injected groups at doses of  $10^{-5}$  or  $10^{-6}$  mol/prawn were much shorter (1.01  $\pm$  0.32 and 1.25  $\pm$  0.58 days, respectively), than the control group (2.79  $\pm$  0.74 days) (P<0.05) (Fig. 13A). Our data strongly indicated that both doses of MrNPF could shorten the duration of early spawning by nearly three times.

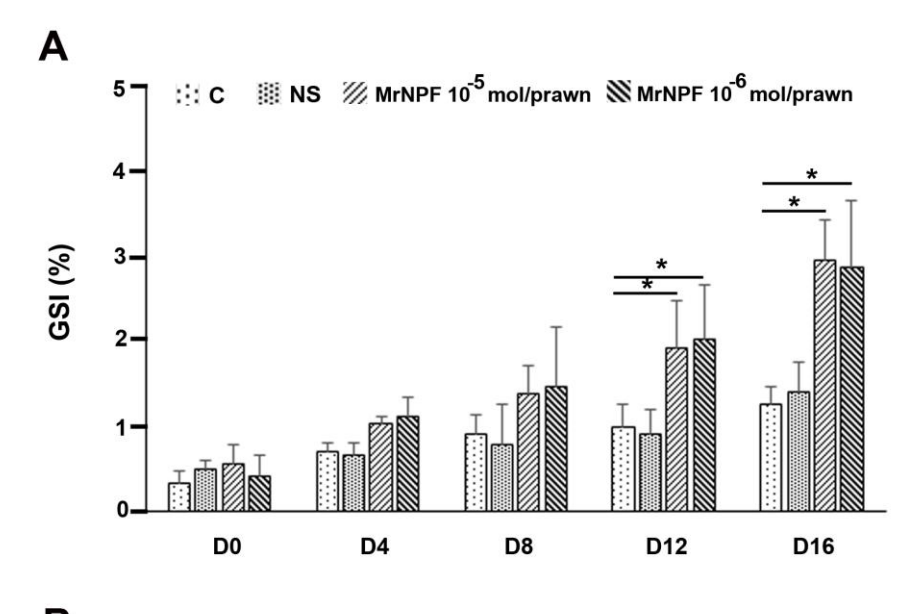
The number of eggs per spawn from both groups of MrNPF-treated groups were about 12 x 10<sup>4</sup> and 14 x 10<sup>4</sup> eggs per prawn, respectively, and these values were not significantly different from the both control groups (12 x 10<sup>4</sup> and 16 x 10<sup>4</sup> eggs per prawn, respectively) (*P*>0.05) (Fig. 13B). The percentages of fertilized eggs were about 97.5% and 98.7% for prawns treated with 10<sup>-5</sup> and 10<sup>-6</sup> mol/prawn of MrNPF (Fig. 14A), which were not statistically different from the controls (98.4% and 99.1%, respectively). The sizes of eggs from female prawns that received both doses of MrNPF were not statistically different, compared with those of the control groups (*P*>0.05). In addition, the percentages of spawners was about 95% in the non-injected group and 100 % for the sham group, compared with 100 % for prawns receiving both doses of MrNPF (Fig. 14B).



**Fig. 9.** Expression of MrNPF-immunoreactivities (-ir) and relative mRNA levels of *MrNPF* gene expression against beta-actin gene in the four ovarian stages of female *M. rosenbergii*. (A) Control section of the early oocytes (Oc1) showing no immunoreactivity. (B) MrNPF-ir appeared more intense in early to mid-oocyte steps (Oc2 and Oc3) in ovarian stages II and III. (C-D) Intense MrNPF-ir is also present in the Ep of oviduct, smooth muscle and the capsule (E). (F) No immunoreactivity was observed in the late oocytes (Oc4) in ovarian stage IV of the control section. (G) Upper row showed the expression of *MrNPF* gene, which was strongly detected by RT-PCR in the ovarian stage III containing mostly Oc2 and Oc3. Bottom row indicates beta-actin gene expression in corresponding tissues. (H) Histograms indicate relative expression of *MrNPF* normalized by beta-actin gene in different ovarian stages, with ovarian stage III showing highest levels, while ovarian stage IV having the lowest levels. Each bar is mean ±SD of three replicates. Bars with superscript '\*' differ significantly from other stages of ovaries at P < 0.05. M = marker. Cap, capsule; Cc, central core of oocyte pouch; Ep, epithelium; Lum, lumen; mOc, mature oocyte; Ovd, oviduct; Tr, trabecular; Oc1, early previtellogenic oocyte; Oc2, late previtellogenic oocyte; Oc3, early vitellogenic oocyte; Oc4, late vitellogenic oocyte; OV-II, ovarian stage II; OV-III, ovarian stage III; OV-IV, ovarian stage IV. Scale bars=100 μm.



**Fig. 10** Effects of MrNPF on the ovarian maturation period of female *M. rosenbergii*. (A) Histograms demonstrating that prawns treated with MrNPF at doses of  $10^{-5}$  and  $10^{-6}$  mol/prawn showed significant shortening ovarian maturation period, compared with the control group. (B) The example of percentages of ovarian stages that the female prawns attained at 16 days after the first injection. After injections with MrNPF at doses of  $10^{-5}$  and  $10^{-6}$  mol/prawn, the prawns ovaries showed significant progress of maturation to reach from stage III to stage IV, faster when compared with the control groups. Each measurement is expressed as a mean  $\pm$  S.E.M. Asterisks indicate significant differences (P<0.05) with respect to the control groups. Stage I, ovarian stage II; Stage III, ovarian stage III; Stage IV, ovarian stage IV.



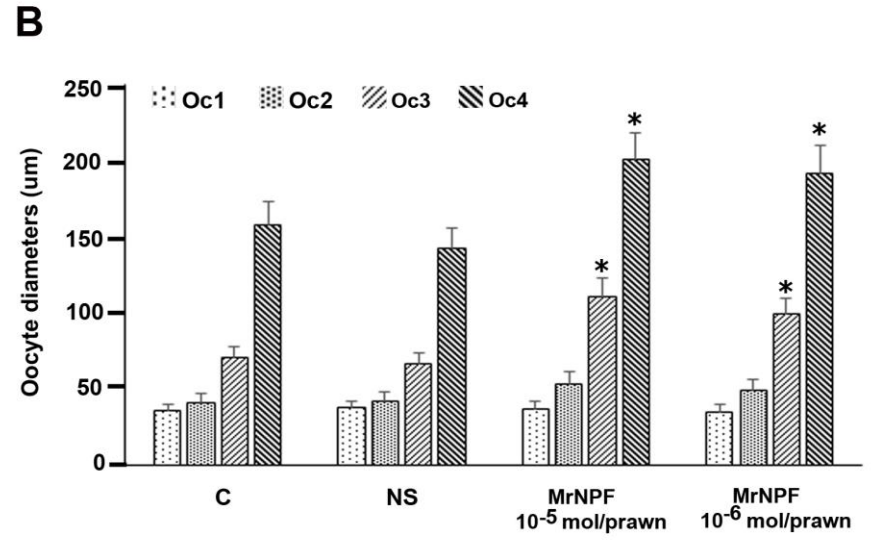


**Fig. 11** Effects of MrNPF on gonado-somatic index and oocyte diameter values of female *M. rosenbergii*. (A) Mean gonado-somatic index (GSI) values after the MrNPF injections, evaluated at 0, 4, 8, 12 and 16 days. The MrNPF-injected groups (with 10<sup>-5</sup> and 10<sup>-6</sup> mol/prawn), showed significant increases of GSI by days 12 and 16, compared with the control groups. (B) Histograms showing the oocyte diameters after injections with MrNPF compared with the control groups. Asterisks indicate significant differences, compared with the control group (*P*<0.05).

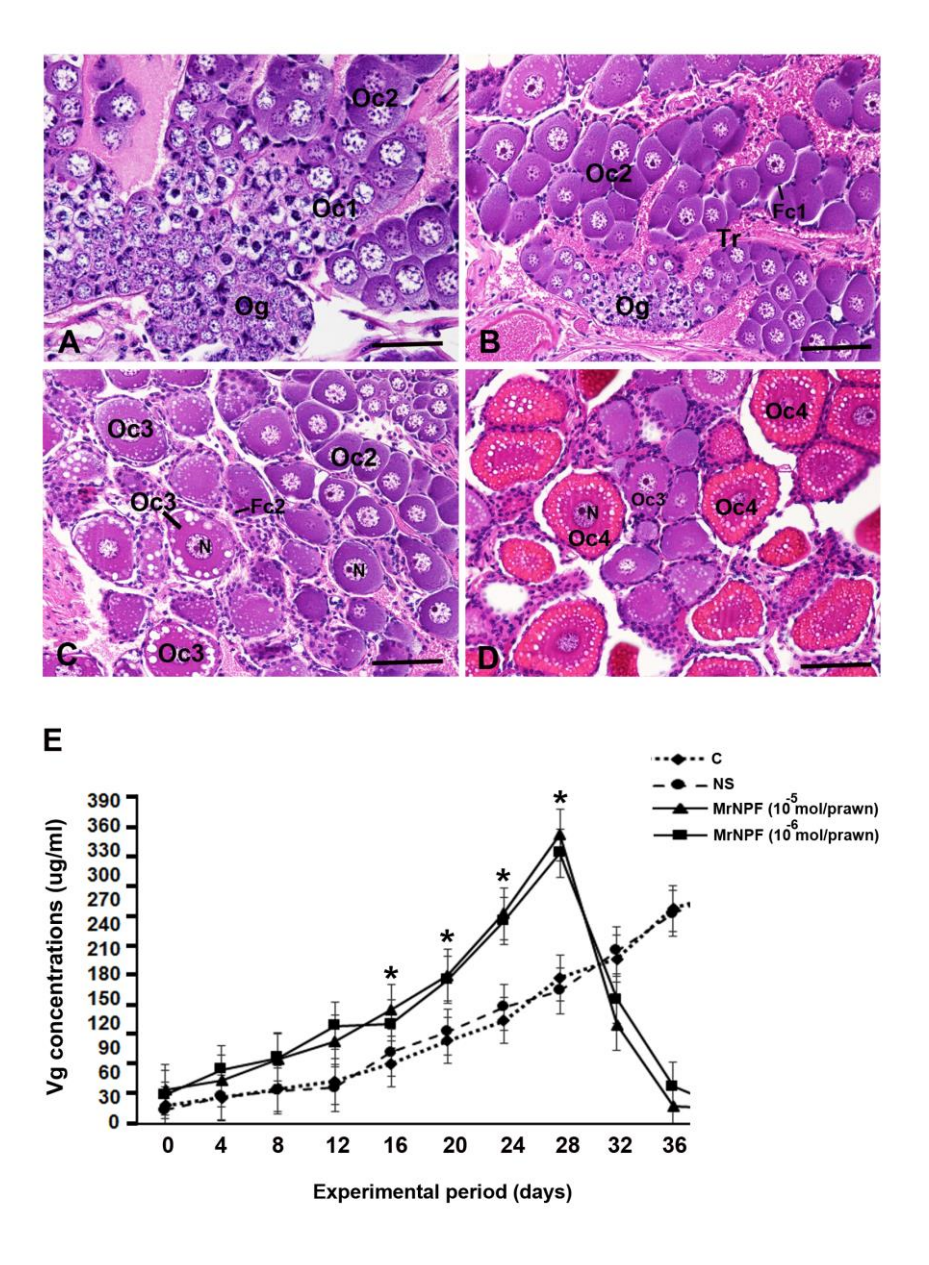


**Fig. 12** Effects of MrNPF on ovarian histology and hemolymph Vg concentrations of female *M. rosenbergii*. A, B) The examples of ovaries of the control group at day 4 (A), and of MrNPF-injected group at a dose of 10<sup>-6</sup> mol/prawn (B), showing there is no histological difference in both groups. C-D) Ovaries of MrNPF-injected groups at 10<sup>-6</sup> mol/prawn contained mostly the late stage oocytes (Oc4) at day 16 (D), while they were only early stage oocytes (Oc1, Oc2) in the control groups (C). (E) A graph showing hemolymph Vg concentrations during the experimental period following treatments with both doses of MrNPF and control groups. The concentrations are expressed as μg/ml. Each measurement is expressed as mean ± S.E.M. Asterisks indicate significant differences (*P*<0.05), comparing the experimental groups and the control groups. Fc1 and Fc2, follicular cell types 1 and 2; Og, oogonia; Oc1, early previtellogenic oocyte; Oc2, late previtellogenic oocyte; Oc3, early vitellogenic oocyte; Oc4, late vitellogenic oocyte; mOc, mature oocyte; n, nucleus; Tr, trabeculae. Scale bars=100 μm.

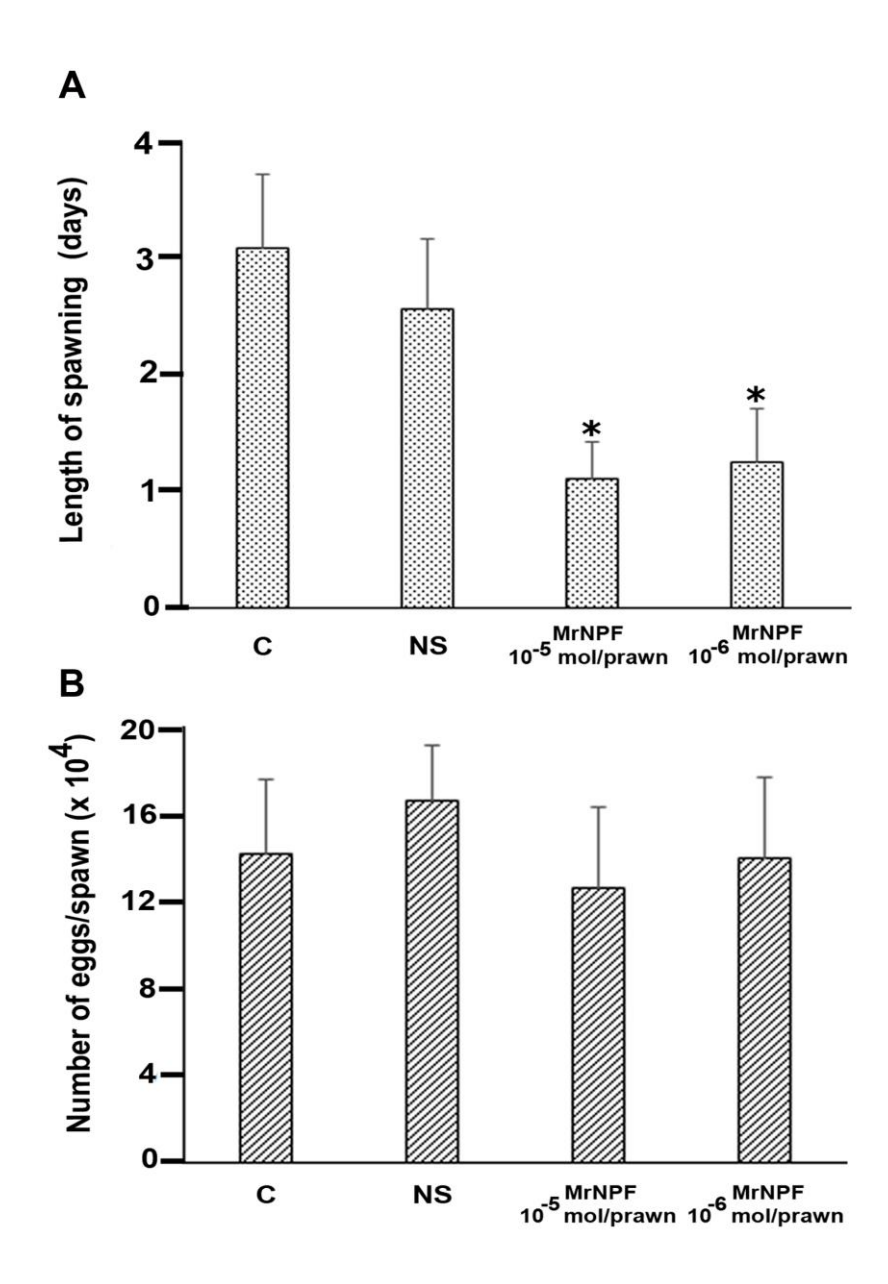


**Fig. 13** Effects of MrNPF on the spawning period and the numbers of eggs per spawn of female M. rosenbergii. (A) Histograms demonstrating that prawns injected with MrNPF at doses of  $10^{-5}$  and  $10^{-6}$  mol/prawn showed significantly shorter spawning time, compared with the control group. (B) Numbers of eggs per spawned after injection with doses of MrNPF at doses of  $10^{-5}$  and  $10^{-6}$  mol/prawn compared with the controls. The data are presented as mean  $\pm$  S.E.M. Asterisks indicate significant differences (P<0.05).

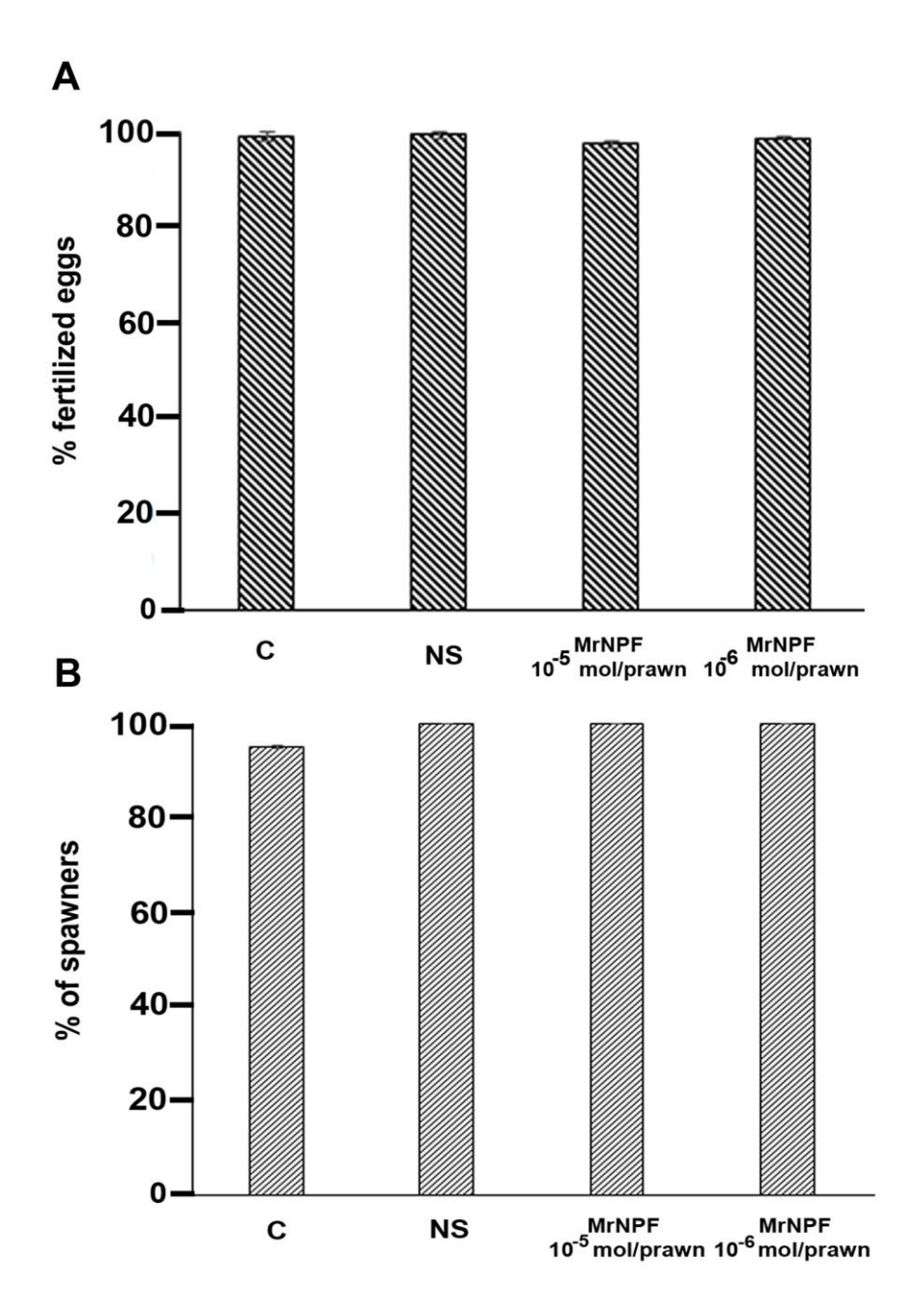


**Fig. 14** Effects of MrNPF on the percentage of fertilized eggs and percentage of spawners of female M. rosenbergii. (A) Percentage of fertilized eggs of all experimental groups after injection with doses of MrNPF at doses of 10-5 and 10-6 mol/prawn compared with the control groups. (B) Percentage of spawners of MrNPF-injected groups at doses of 10-5 and 10-6 mol/prawn, compared with the control groups. The data are presented as mean ± S.E.M.

# **Discussion**

In the present study, we are the first to provide evidence for the stimulatory role of NPF in the female *M. rosenbergii* reproduction. We found that MrNPF significantly shortened the ovarian maturation period and exhibited increases of GSI, OD and hemolymph Vg levels at a shorter time compared with the controls. MrNPF also shortened the spawning duration by about two days compared with that of the control group. Moreover, strong MrNPF-ir and high level of *MrNPF* gene expression were detected in the mid-stage oocytes and ovarian stage III. These results strongly suggest that MrNPF is capable of stimulating ovarian development and early spawning in this crustacean species.

The roles of NPF in controlling feeding and growth in insects and other invertebrates are well known (Schoofs et al., 2001; Nässel and Wegener, 2011; Van Wielendaele et al., 2013). There have been a few reports regarding the role of NPF in regulating the reproduction in several invertebrate species, including insects, mollusks and crustaceans. In the female desert locust, Schistocerca gregaria, injection of NPF increased ovarian-somatic index and stimulated the increase of oocyte diameters (Schoofs et al., 2001; Van Wielendaele et al., 2013). It was shown that the ovaries of NPFtreated females reached vitellogenic stages, while only previtellogenic ovaries were observed in the control groups. NPF also induced higher ovarian and hymolymph ecdysteroid levels, suggesting that NPF may exert its effect through the ovary maturing parsin (OMP) which regulates vitellogenesis indirectly through its ecdysiotropic effect on the ovary (Girardie et al., 1998; Schoofs et al., 2001; Van Wielendaele et al., 2013). It is important to note that the follicle cell of ovary is the major production site for ecdysteroid, which is further incorporated in the growing oocytes (Tawfik et al., 1999; Buszczak et al., 1999; Brown et al., 2009; Parthasarathy et al., 2010). Injecting NPF peptide into L. migratoria, stimulated ovarian maturation, implying that NPF may also be involved in controlling oocyte proliferation during ovarian development (Cerstiaens et al., 1999). In addition, injecting NPF into 6day-old females Leptinotarsa decemlineata, could stimulate oocyte maturation, suggesting a role of NPF in promoting ovarian development (Cerstiaens et al., 1999). NPF also regulates food intake and feeding behaviors in a few crustacean species (Wu et al., 2003; Christie et al., 2011). In L. vannamei, NPF is mixed into packaged food, it stimulated feeding and weight gain of larvae, indicating that NPF can pass through the gastrointestinal tract without being degraded (Christie et al., 2011). In addition, it was suggested that NPF may increase the acquisition of nutrients and energy in order to promote metabolic processes that enabling the gaining of weight, and this may eventually stimulate and increase oocyte size by promoting ovarian maturation (Schoofs et al., 2001; Van Wielendaele et al., 2013). Our present study demonstrates for the first time that injecting MrNPF into female *M. rosenbergii* induced ovarian maturation and significantly increased GSI and OD. It is also possible that MrNPF could be an important signaling neuropeptide that regulates ovarian development of this crustacean species, as reported earlier in the female *S. gregaria*. NPF may serve indirect role in regulating ovarian maturation and oocyte growth in *M. rosenbergii* by acting through ecdysteroid pathways to control ovarian development, as proposed earlier (Schoofs et al., 2001; Van Wielendaele et al., 2013). However, further experiments are necessary to ascertain whether NPF mediates its actions through the ecdysteroid cascade.

Our work showed that MrNPF stimulated early spawning compared with the control groups, thereby suggesting NPF may be required for final egg maturation as well as assisting in the release of eggs from the oviduct in this crustacean species. There have been studies reporting possible role for NPF or NPF-related factors in ovulation and spawning in mollusks. In *Aplysia* spp, NPF and egglaying hormone (ELH) were co-localized in bag cells, suggesting that NPF may be co-released with an ELH to initiate the egg-laying, and both peptides may also control egg laying-associated behaviors (Rajpara et al., 1992; de Jong-Brink et al., 2001). In *Lymnaea stagnalis*, NPF-ir was detected and co-localized with APGWamide in the cerebral ganglia neurons which contact the caudo-dorsal cells, and as such the NPF may control an ovulation (De Lang et al., 1997). In the present study, MrNPF induced early spawning and shorten spawning duration by three times, compared with the control groups. Immunohistochemical data showed that the MrNPF-ir was intense in the epithelium and smooth muscle cells in the oviduct, suggesting that MrNPF stimulates ovulation by controlling the contractile ovarian capsule to squeeze oocytes into the oviduct and broodchamber during spawning (Rajpara et al., 1992; De Lang et al., 1997).

Several studies have reported the presence and distribution of NPF or NPF-related peptides in the ovaries and other reproductive organs of many invertebrates. In the flatworms, NPF-ir was present in gonadal tissues, suggesting this neuropeptide may serve as a reproductive function (Walker et al., 2009). In the red fire ant, *Solenopsis invicta*, the NPF receptor transcript was detected in the ovaries and fat body of the mated queens using RT-PCR, and NPF receptor-ir was also present at periphery of early-, mid-oocyte steps and oocyte membrane, whereas this receptor was not detected in late oocytes. This suggests that NPF may regulate oocyte development processes by promoting early- to mid-oocyte growth during ovarian maturation (Chen and Pietrantonio, 2006; Ling Lu and Pietrantonio,

2011). In female *Drosophila*, sNPF receptor transcripts were detected in the ovaries, indicating that this neuropeptide may be involved in oocyte growth and ovarian development (Mertens et al., 2002). In the present work, we demonstrated that in female *M. rosenbergii*, the levels of *MrNPF* in the ovaries fluctuate during ovarian cycle: MrNPF-ir was most intense in the mid-oocytes (Oc2 and Oc3), while very low intensity was detected in the late oocytes (Oc4). This suggests that NPF may be synthesized and produced locally in Oc2 and Oc3, and thereby stimulating the early to mid-steps of oocyte maturation via an autocrine and/or paracrine pathway, and eventually initiate early spawning. We further confirmed the mRNA transcriptional levels by using RT-PCR which showed that MrNPF levels rose with early to mid stages of ovarian cycle, and suddenly fell in the late ovarian stage. In addition, we found that the levels of MrNPF are about 9, 6 and 15 times higher in the ovaries at stage III than in the ovaries at stages I, II and IV, respectively. Our findings indicate that the changing patterns of NPF levels in the ovaries of *M. rosenbergii* are similar to those reported in *Drosophila* (Mertens et al., 2002), and the fire ant (Chen and Pietrantonio, 2006).

Hemolymph Vg level is an important indicator for ovarian maturation in several decapod crustaceans and in other invertebrates (Okumura, 2004). In adult female desert locusts, NPF stimulates vitellogenesis and oocyte growth, as well as increases ecdysteroid levels in the hemolymph and ovaries (Schoofs et al., 2001; Van Wielendaele et al., 2013). In *L. migratoria, Lom*-OMP induces oocyte differentiation and stimulates the increased level of circulating vitellogenin (Girardie et al., 1998). In *S. gregaria, Scg*-NPF increases vitellogenin concentration in the hemolymph (Schoofs et al., 2001). In the present study, we found that injection of MrNPF increased hemolymph Vg levels in female *M. rosenbergii* as the Vg concentrations of the groups treated with MrNPF were higher at various ovarian stages, especially stages II and III, compared with those of the control groups. These results indicated causal relationships between NPF and ovarian maturation as reflected by the increase of Vg synthesis. However, whether the stimulating effect of the NPFs on vitellogenesis is mediated through ecdysteroids remains to be examined.

Taken together, we provided for the first time and reported a novel, clear and important basic knowledge that NPF is involved in ovarian maturation and spawning in female *M. rosenbergii*. Further research will be needed to study the possible mechanisms of NPF action and to find way to apply this important knowledge for practical application in aquaculture of this female crustacean species.

# PART IV. Examination of the existence, alterations in the levels, and possible relationship of major neurotransmitters and NPF during embryonic development in the female freshwater prawn

In decapod crustaceans, major neurotransmitters that control ovarian maturation are serotonin (5-HT) and dopamine (DA): 5-HT has a stimulating effect on gonadal maturation, perhaps by inhibiting the release of gonad-inhibiting hormone (GIH), and/or by stimulating the release of gonad-stimulating hormone (GSH)/gonadotropins (GnRH), whereas DA plays the opposite role (Sarojini et al., 1995b; Fingerman, 1997). As our previous report (Thongrod et al., 2017; Tinikul et al. 2017), we found that MrNPF immunoreactivity (ir) were detected in neurons of various clusters and in neuropils and fibers in the brain, SEG and thoracic ganglia. In the ovary, NPF immunoreactivity-ir was also detected at high intensity in the cytoplasm of early step oocytes (Oc2) and at high intensity of middle step of oocytes (Oc3). MrNPF stimulates early spawning duration and also has effect on fecundity. In addition to the investigation of the effects of MrNPF on female ovarian maturation and spawning. We are also interested to understand whether this neuropeptide is involved in controlling embryonic development and/or in relation to major neurotransmitters. Therefore, we first examined and provided a novel data in this research grant, the expression and changes in the levels, and possible actions of major neurotransmitters (5-HT and DA), since we believed that 5-HT and DA could be the first hierarchy molecules in regulation of NPF in reproduction and probably embryonic development. Therefore, we have additionally investigated alterations in the levels of 5-HT and DA in several stages of embryos during embryonic development of the female M.rosenbergii by High Performance Liquid Chromatography (HPLC). We also have reported the expression patterns of 5-HT- and DA-ir structures in the various embryonic stages using immunohistochemistry. The implications of data on the opposing roles of the two neurotransmitters are demonstrated. This part of the present study provides us the first, and important basic knowledge regarding the presence and possible relationship of these two neurotransmitters, possible localizations and may interplay with NPF during embryonic development in the female freshwater prawn. Further researches are needed to examine exactly the expression, possible mechanisms and investigation of NPF actions on feeding, growth, ovarian and embryonic development as well as to find way to apply this important knowledge for practical application in larval aquaculture of this female crustacean species.

# Materials and methods

# 4.1. Experimental animals

Mature female freshwater prawns (weighing on average about 32.46 ± 4.17 g) were obtained from commercial farms, in Ayuthaya Province, Thailand. The prawns were kept in outdoor circular concrete tanks, each with 1.50 m diameter with the water depth at 0.80 m, and about 30% water was changed every 2 days. The prawns were fed with commercial pellets (Charoen Pokphand group, Thailand) twice a day. Aeration was given continuously. The plastic cages were added into every tanks (30 pieces per tank) for prawns to hide and to avoid any losses during molting from the cannibalistic behavior of this prawn species. The prawns were acclimatized under a photoperiod of 12:12 h light-dark for two weeks before beginning the experiments. Female prawns were selected and used in all experiments, as soon as they exhibited stage IV of the ovarian cycle. All prawns were cultured until they spawned, and the embryos were allowed to grow following the normal embryonic developmental cycle until reaching the final embryonic stage.

# 4.2. Samples collection and preparation

After they spawned, the mature berried females at various embryonic stages (at least n = 15 prawns) were sampled. The different embryonic stages from abdomen were carefully scraped from the female brood chambers. All spawned eggs were mixed with 3% sodium hypochlorite (NaClO) in distilled water to thoroughly disperse the eggs. At least 300 eggs were observed under a stereo-microscope to determine the morphology and percentage of developing embryos. The embryonic stages were visually evaluated based on the color and morphological characteristics, which are seen through the abdomen in live females, as described by Müller et al. (2003), Manush et al. (2006), Tinikul et al. (2009a), and Habashy et al. (2012). After the dissection, the wet mass of all eggs was weighed, and later used for HPLC analyses and immunohistochemistry.

# 4.3. Chemicals and reagents

All chemicals, including 5-HT and DA, were obtained from Sigma-Aldrich (St. Louis, MO, USA). Standard solutions were made up in freshly prepared ice-cold 0.1 M perchloric acid. Each of the standard solutions were prepared on the day of analysis and stored on ice between injections.

# 4.4. Quantification of 5-HT and DA in the embryos

In the present study, the HPLC methods for quantification of 5-HT and DA concentrations in embryos were based on the method described by Tinikul et al (2011b, 2015), with some modifications. After being dissected out and weighed, a lump of embryos was placed in 100 µl of 0.1 M perchloric acid and homogenized at 4 °C. The 5-HT and DA concentrations were detected electrochemically using a completely isocratic mode. Samples were injected onto a Brownlee C<sub>18</sub>-Aquapore OD-300 HPLC column (250 x 4.6 mm i.d.). A glassy carbon electrode, serving as the working electrode was set with an Aq/AqCl reference electrode. The sensitivity of the detector was maintained at 100 nA with full scale deflection. The potential of the detector was set at a range between +0.7 to +0.8 V. The mobile phase consisted of 75 mM NaH<sub>2</sub>PO<sub>4</sub>, 50 μM EDTA, 0.3 mM sodium octylsulphate, 2.5% acetonitrile, and 4% methanol. The pH was adjusted to 2.75 with orthophosphoric acid. The flow rate was kept constant at 0.7 ml/min. The mixture was sonicated and centrifuged at 14,000 x g at 4 °C. The supernatants were collected, and then filtered through a 0.22 µm spin-x centrifugal filter tube before injection. Samples were injected into a 20 µl injection loop. Each sample was performed in triplicate. The signals from the electrochemical detector were recorded and integrated by using data analysis software (Millennium, Waters). The average concentrations of 5-HT and DA were estimated from three replicates. 5-HT and DA were quantified using the external standard method in which peaks corresponding to 5-HT and DA were detected in the extracts at the same elution times to their corresponding standards. In addition, standard solutions of 5-HT and DA were prepared and dissolved in ice-cold 0.1 M perchloric acid, and then filtered through a 0.45 µm filter and stored on ice during injections into the HPLC system. Furthermore, the identities of the peaks in each sample was verified by spiking known amount of 5-HT and DA standards into the tissue extracts in repeated separations. The Bio-Rad Protein Assay System (Mississauga, Canada) was employed for protein determination according to Bradford (1976). All samples were freshly prepared and analyzed within the same day.

# 4.5. Immunohistochemistry and specificities of antibodies

The dissected embryonic stages were fixed with 4% paraformaldehyde in 0.1 M phosphate-buffered saline (PBS) with 1% sodium meta-bisulfite (SMB) in PBS at 4  $^{\circ}$ C for 12 h. After fixation and paraffin embedding, the tissue sections were cut at 7 to 10  $\mu$ m thicknesses for the investigation of early embryonic stages, whereas the sections were cut at 10 to 20  $\mu$ m thicknesses for late embryonic

stages. The sections were further mounted on slides coated with 3-aminopropyl triethoxy-silane solution (Sigma-Aldrich Co., St. Louis, MO, USA), and then processed for immunohistochemistry.

The immunohistochemical localization of 5-HT immunoreactivity (5-HT-ir) and DA immunoreactivity (DA-ir) during various embryonic stages, was performed based on that described previously (Tinikul et al. 2011a,b). Briefly, the sections were deparaffinized and rehydrated through a graded ethanol series for 10 min each. The sections were incubated with 1% glycine in PBS for 15 min. Subsequently, non-specific binding was blocked by immersing the sections in a blocking solution containing 10% normal goat serum (NGS) and 1% SMB in PBS with 0.4% triton-X (PBST), at room temperature for 2 h, in a moist chamber. The sections were then incubated with the primary antibodies, rabbit anti-5-HT (Chemicon International, USA), diluted 1:50 in the blocking solution, or rabbit anti-DA (Gemacbio, St. Jean d'Illac, France), diluted 1:100 in the blocking solution, at room temperature. The sections were washed three times with PBST, and then incubated in the secondary antibody, Alexa488-conjugated goat anti-rabbit IgG (Molecular Probes, Eugene, OR, USA), diluted 1:200 in the blocking solution, at room temperature for 2 h. In addition, the nuclei of cells in sections of embryos were stained with ToPro-3 (Molecular Probes), diluted at 1:2000 in the blocking solution. The sections were mounted in Vectashield (Vector Laboratory, Burlingame, CA, USA), viewed and images captured by an Olympus FV1000 confocal laser scanning microscope.

The specificities of the polyclonal antibodies against 5-HT and DA were tested by the manufacturer using standard immunohistochemical methods. The manufacturer has demonstrated that anti-5-HT and anti-DA antibodies did not cross-react with other biogenic amines. In the control sections, the specificities of anti-5-HT and anti-DA were ascertained by omitting the primary antibodies from the immunolocalization, or by pre-adsorption of the primary antibodies with 100 µg/ml of synthetic 5-HT or DA (Sigma-Aldrich, St. Louis, MO, USA) at 4 °C for about 20 h, before staining (Tinikul et al., 2011b). In these controls, no immunostaining was observed.

# 4.6. Image analysis

The embryonic sections prepared for immunohistochemistry, were photographed with an Olympus Fluoview 1000 laser-scanning confocal microscope (Olympus America, Center Valley, PA). Subsequently, the tissues were scanned sequentially for each fluorophore to obtain separate images for each label, and an overlayed image of all three channels for each optical section. These projected images were produced using subsets of the z-stacks. Furthermore, the digital images were exported

and converted from the Olympus confocal system, and further transferred into Photoshop CS5 software (Adobe Systems Inc., San Jose, CA, USA), to adjust contrast and brightness to obtain optimal clarity. Images were not modified other than to balance brightness and contrast, as well as to remove irrelevant structures that interfered with visualization of our tissues using Adobe Photoshop CS5 (Adobe Systems, San Jose, USA). In addition, negative controls for each fluorochrome were scanned using the same parameter settings.

# 4.7. Investigation of the specific actions of 5-HT and DA on the development of embryonic stages

The methods and doses of 5-HT and DA used in this study were based on that described previously (Tinikul et al., 2009a; 2014), with some modifications. The experimental groups were divided into three groups and compared with the control group (with all groups having about 40-45 animals each). The first group was untreated control group (C), groups 2, 3 and 4 were injected with 5-HT and DA at doses of 2.5 x10<sup>-5</sup>, 2.5 x 10<sup>-6</sup> and 2.5 x 10<sup>-7</sup> mol/prawn, respectively, which were equivalent to the circulating concentrations of about 5, 0.5, and 0.05 mM, respectively, after dilution by the prawn hemolymph. 5-HT and DA were dissolved in crustacean physiological saline. The injected volumes of 5-HT and DA were 0.1 ml. All injections were performed at 4-day intervals. All prawns tolerated the injected doses of these two neurotransmitters without exhibiting any abnormal behavior. Measurements of total length and weight of the prawns were performed on every treatment day before injection. Prawns were identified in each group by tagging with plastic loops of different colors around the eyestalks. The injections were performed via an intramuscular route at the second abdominal segment using a 1 ml syringe fitted with 26 G × 1/2 (0.45 × 12 mm) thin-wall needles (NIPRO). The experiment was performed in triplicate. The rest of the prawns were allowed to proceed until they spawned. After injections with 5-HT and DA, the quantity and quality of the spawned eggs were evaluated from the number of eggs per spawn and the percentage of fertilized eggs in order to ascertain that the embryonic development is normal. The embryonic developmental days after injections with these two neurotransmitters in comparison with the control group were carefully observed and recorded.

# 4.8. Statistical analyses

Experimental data were analyzed with SPSS program (version 12.0, SPSS Inc., Chicago, IL, USA) using one-way analysis of variance (ANOVA) and Tukey's post hoc test. The probability value less than 0.05 (P<0.05) indicated the significant difference. Experimental data were presented as  $\overline{X}$  ± S.E.M.

# Results

# General morphology of the embryos resulted from fertilized eggs of *M. rosenbergii*

The general morphology of the embryonic stages of M. rosenbergii is demonstrated in Figs. 15A-K. These were used as the basis for the HPLC detection and mapping the distribution of 5-HT and DA during embryonic development. We have classified embryos into various stages based on the criteria described previously (New, 2002; Manush et al., 2006; Tinikul et al., 2009a). Representative micrographs of the ventral views of berried females showed the mid-embryonic stages (orange egg stage; OE) (Fig. 15A), and the late-embryonic stage (grey egg stage; GE) (Fig. 15B). The newly spawned eggs are elliptical in shape, and characterized by a bright yellow, then deep yellow to orange color, which gradually changes to brown, grey and finally black before hatching. The six main embryonic stages included the bright yellow egg stage (BYE), containing mostly high density yolk masses, and a small translucent area (ST) on the egg surface (Fig. 15C-D). A later stage is the deep yellow egg stage (DYE), whose color is a deep yellow with blastocoel (B), clearly visible area in one pole of this embryonic stage (Fig. 15E-F). Later, the orange egg stage (OE), exhibits a clear area that extends to form the body and caudal region of the embryo (Fig. 15F-G). This is followed by the early brown egg stage (BE), which starts to form a pair of eye spots on the yolk area (Fig. 15H-I). At the late BE stage, the heart is firstly observed and starts beating (Fig. 15I). The dark eye spots are oval in shape. In the grey egg stage (GE), rudiments of appendages start to develop and the segmented abdomen is clearly visible (Fig. 15J). Finally, the black egg stage (BLE) is characterized by the presence of a pair of dark-rounded eyes, the abdomen is enlarged and curves forward. The appendages are clearly visible before hatching (Fig. 15K).

# Changes in the concentrations of 5-HT and DA in the embryonic stages

The 5-HT concentrations in the embryonic stages showed a gradual increase from the BYE stage, to reach the highest concentration at BLE stage (Fig. 16A). The concentration of 5-HT at BYE stage was  $0.86 \pm 0.18$  nmol/mg, and then it gradually increased through the DYE stage and OE stage (1.52  $\pm$  0.29 and 2.35  $\pm$  0.37 nmol/mg, respectively), to a higher level at BE and GE stages (3.49  $\pm$  0.68 and 5.38  $\pm$  1.01 nmol/mg, respectively). The highest 5-HT concentration was detected at BLE stage (6.05  $\pm$  1.29 nmol/mg), which showed approximately a 7-fold increase over BYE stage. The differences were statistically significant (P<0.05). In addition to the BLE stage, the 5-HT concentration at the BLE stage appeared to be higher than that of the GE stage, but not significantly different (P>0.05). The 5-HT concentrations were about 2.7, 4, 6.2 times higher in the OE, BE and GE stages, respectively, than at BYE stage (P<0.05) (Fig. 16A).

Very low DA concentrations were detected at the BYE stage  $(0.07 \pm 0.03 \text{ nmol/mg})$ , and DYE stage  $(0.09 \pm 0.01 \text{ nmol/mg})$  (Fig. 16B), whose the difference was not statistically significant (P>0.05). The concentration of DA sharply increased at the OE stage, and it was  $0.81 \pm 0.24 \text{ nmol/mg}$ , and then about two times increased at the BE stage  $(1.54 \pm 0.49 \text{ nmol/mg})$ . DA levels increased steadily at successive stages, and became about a 2-fold increased at the GE stage  $(3.01 \pm 0.75 \text{ nmol/mg})$ . The DA concentration reached a maximal level at BLE stage  $(4.05 \pm 1.16 \text{ nmol/mg})$ , exhibiting approximately a 60- and 48-fold increases over BYE and DYE stages, respectively (P<0.05). Interestingly, when comparing within same embryonic egg stages, the concentrations of DA were about 18.8, 2.9, 2.27 and 1.78 times lower in the DYE, OE, BE, GE and BLE than those of 5-HT, respectively (Fig. 16B).

# The distribution of 5-HT and DA during embryonic developmental stages

The 5-HT-ir was detected in the yolk at the BYE stage (Fig. 17A), and it appeared to be more intense in the yolk and the membrane at the DYE stage (Fig. 17B, C). At the OE stage, 5-HT-ir was present in the yolk and the organ anlage (OA) (Fig. 17D). No positive fluorescence was observed in a control section taken from the DYE stage (Fig. 17E). At the BE stage, little 5-HT-ir was detected in the optic lobe area, including eye anlage (E) (Fig. 18A), but intense 5-HT-ir was detected in the elongated body (EB), and caudal papilla (CP) (Fig. 18B). In addition, 5-HT-ir was first observed in the stomodaeum (ST) and segmented abdomen (SEG) at the GE stage (Fig. 18B). Furthermore, intense

5-HT-ir was detected at the position of heart (H), SEG, and appendages (AP) (Fig. 18C). No 5-HT-ir was detected in a control section of any part of the late embryonic stages (Fig. 18D).

At BYE and DYE stages, DA-ir was detected with a very low intensity and was not clearly visible in the yolk (Fig. 19A-C). At the OE stage, DA-ir was clearly present in the yolk, and in some cases the OA showed moderate staining for DA-ir (Fig. 19D-E). The control sections of the OE stage did not show any positive fluorescence (Fig. 19F). At the BE stage, DA-ir was detected around the E, H, EB and CP structures, and H (Fig. 20A), and strong DA-ir was detected at the periphery of their bodies. Each of the BE, GE, and BLE stages contained DA-ir, which were specifically scattered and intensely stained, compared with those in other early stages of the embryonic eggs (Fig. 20B, C). At the GE and BLE stage, we detected DA-ir in the SEG, CP and H. These DA-irs were continuous from the position of H, thorax regions and passing through the SEG (Fig. 20B, C). No DA-ir was detected in the control section of any part of the GE stage (Fig. 20D).

# The specific actions of 5-HT and DA on the development of embryonic stages

The specific actions of 5-HT and DA on the lengths of development of each embryonic stage are shown in Fig. 21A, B. Generally, there were no differences between the 5-HT- and DA-injected groups, compared with the control group at the period from BYE to DYE (P > 0.05), as this period tends to be short (Fig. 21A). After treatment with 5-HT at doses of  $2.5 \times 10^{-5}$ ,  $2.5 \times 10^{-6}$  and  $2.5 \times 10^{-7}$  mol/prawn, the period from DYE stage to OE stage was shorter than that of the control group and was statistically significant (P < 0.05). 5-HT significantly reduced the time for the OE stage to reach the BE stage, they only took ( $3.85 \pm 0.35$ ,  $3.91 \pm 0.58$ , and  $4.12 \pm 0.54$  days) for  $2.5 \times 10^{-5}$ ,  $2.5 \times 10^{-6}$  and  $2.5 \times 10^{-7}$  mol/prawn, respectively. The time from BE to GE stages was about half as long for the 5-HT at a dose of  $2.5 \times 10^{-5}$  mol/prawn ( $3.54 \pm 0.35$  days), compared with the control group ( $6.87 \pm 0.98$  days) (P < 0.05). A similar effect was observed after injection of 5-HT at a dose of  $2.5 \times 10^{-5}$  mol/prawn, which significantly shortened GE to BLE stages ( $3.29 \pm 0.42$  days), compared with the control group ( $4.65 \pm 0.75$  days) (P < 0.05) (Fig. 21A).

The lengths of BYE to DYE stages from prawns injected with DA at doses of  $2.5 \times 10^{-5}$ ,  $2.5 \times 10^{-6}$  and  $2.5 \times 10^{-7}$  mol/prawn, showed no statistical differences from the control group (P > 0.05) (Fig. 21B). Subsequently, the period from DYE to OE stages was a little longer ( $7.86 \pm 1.61$  and  $7.15 \pm 1.39$  days, respectively), compared with the control group ( $6.14 \pm 0.83$  days), but the difference was not statistically significant (P > 0.05) (Fig. 21B). Interestingly, the period from OE to BE stages (i.e.,

12.44  $\pm$  1.43, 11.32  $\pm$  1.75, and 9.96  $\pm$  1.81 days, respectively) was longer than that of the control group (5.42  $\pm$  1.25 days) (P < 0.05) (Fig. 21B). Similarly, the period from BE to GE stages was considerably longer, compared with the control group (P < 0.05). Finally, the time from GE to BLE stages after treatment with DA at doses of 2.5  $\times$  10<sup>-5</sup> and 2.5  $\times$  10<sup>-6</sup> mol/prawn was about two times longer (9.89  $\pm$  1.59 and 8.88  $\pm$  1.05 days), compared with the control group (P < 0.05) (Fig. 21B).

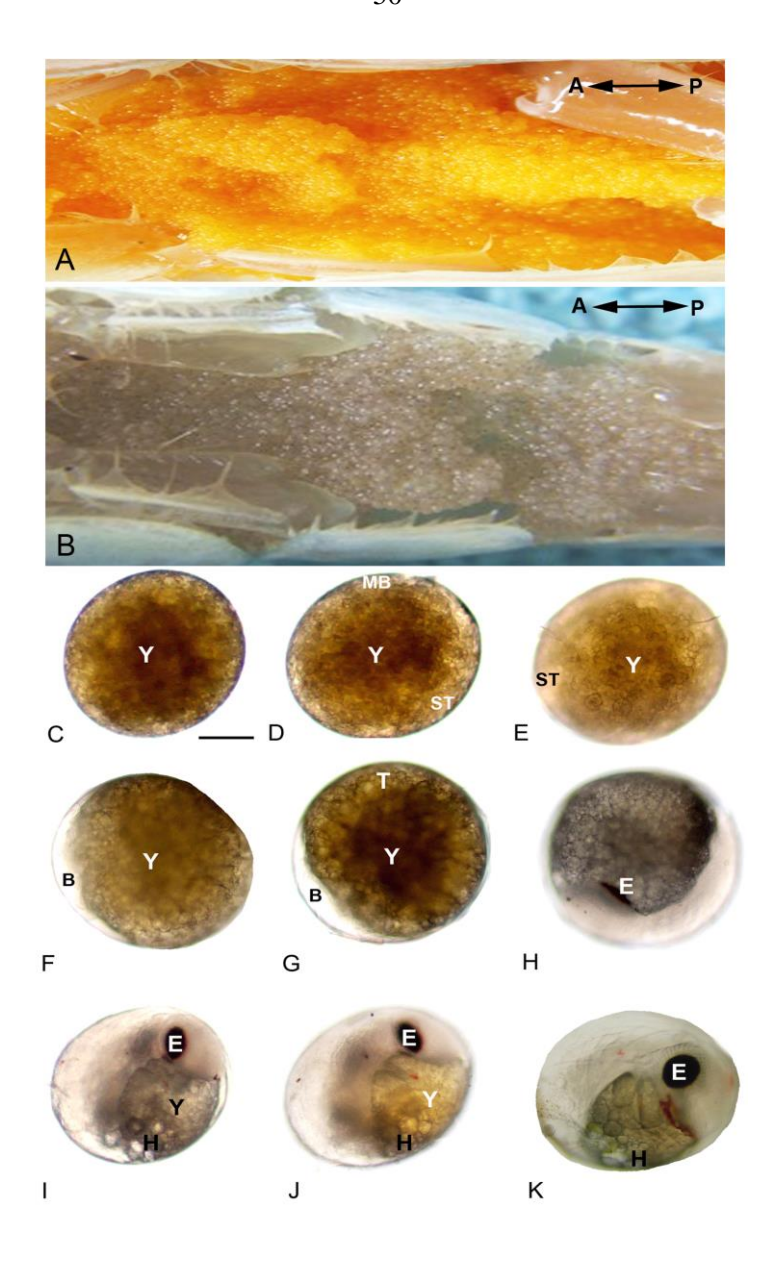


**Fig. 15** Photographs of the ventral views of the brood chambers (A-B) and various stages of developing embryos (C-K) of the mature berried female *M. rosenbergii*. (A-B) The example micrographs of the ventral views of berried females at the mid-embryonic stages (orange egg stage; OE), and the late stage (grey egg stage; GE). The orientation of the prawn is given top right. (C-D) the bright yellow egg (BYE). (E) deep yellow egg stage (DYE). (F-G) orange egg stage (OE). (H-I) brown egg stage (BE). (J) grey egg stage (GE). (K) black egg stage (BLE). A, anterior; B, blastocoel; E, eye; H, heart; MB, egg membrane; P, posterior; ST, small translucent region; T, trunk; Y, yolk. Scale bars: 100 μm.

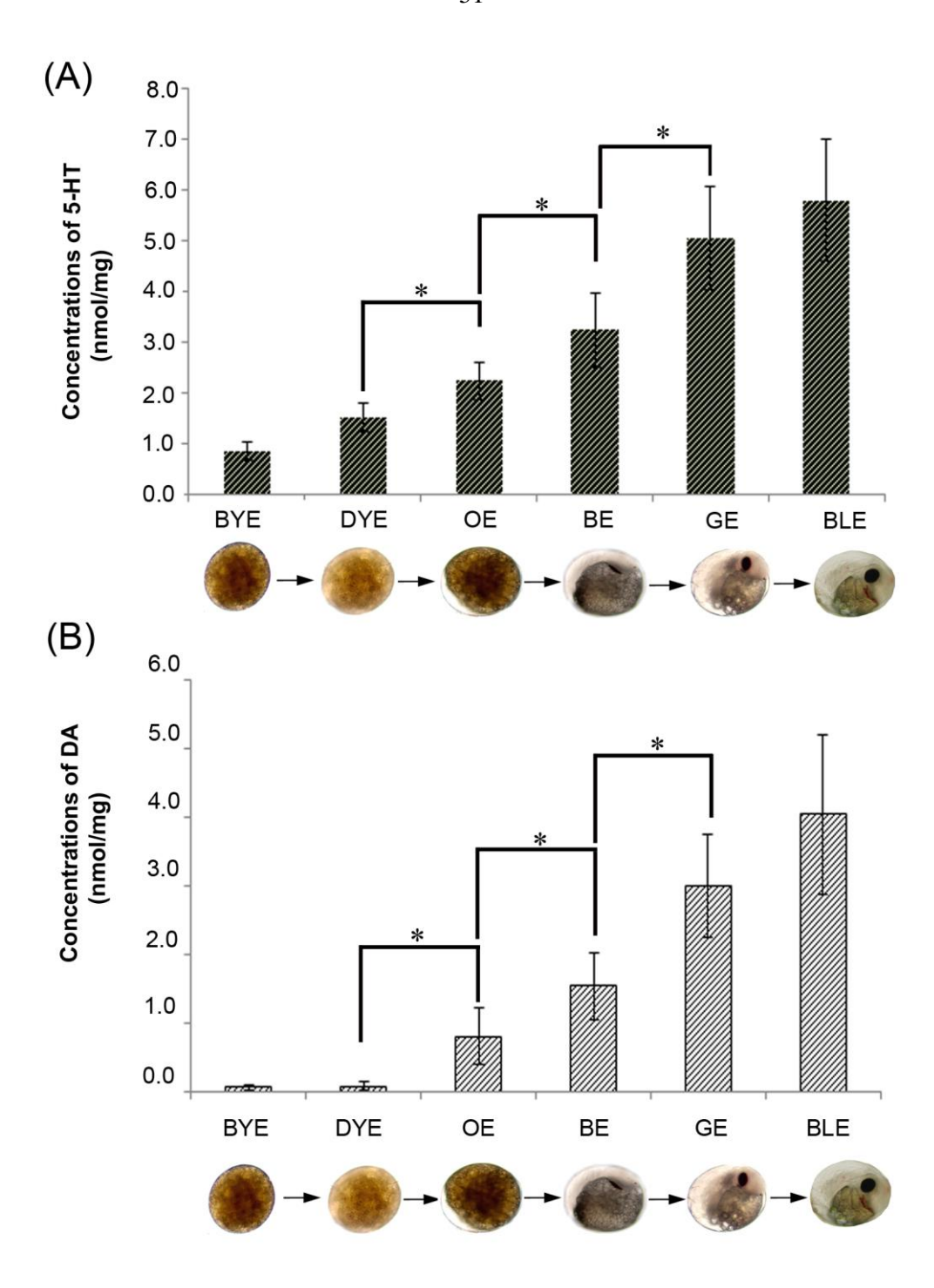


**Fig. 16** (A) The changing concentrations of 5-HT in various embryonic stages, and (B) the concentrations of DA in various embryonic stages, as determined by HPLC. The concentration is expressed as nmol/mg of protein in the tissue extract. Numbers are means ± SEM. Asterisks indicate significant differences at *P*<0.05 in an analysis of variance. BE, brown egg; BLE, black egg; BYE, bright yellow egg; DYE, deep yellow egg; GE, grey egg; OE, orange egg.

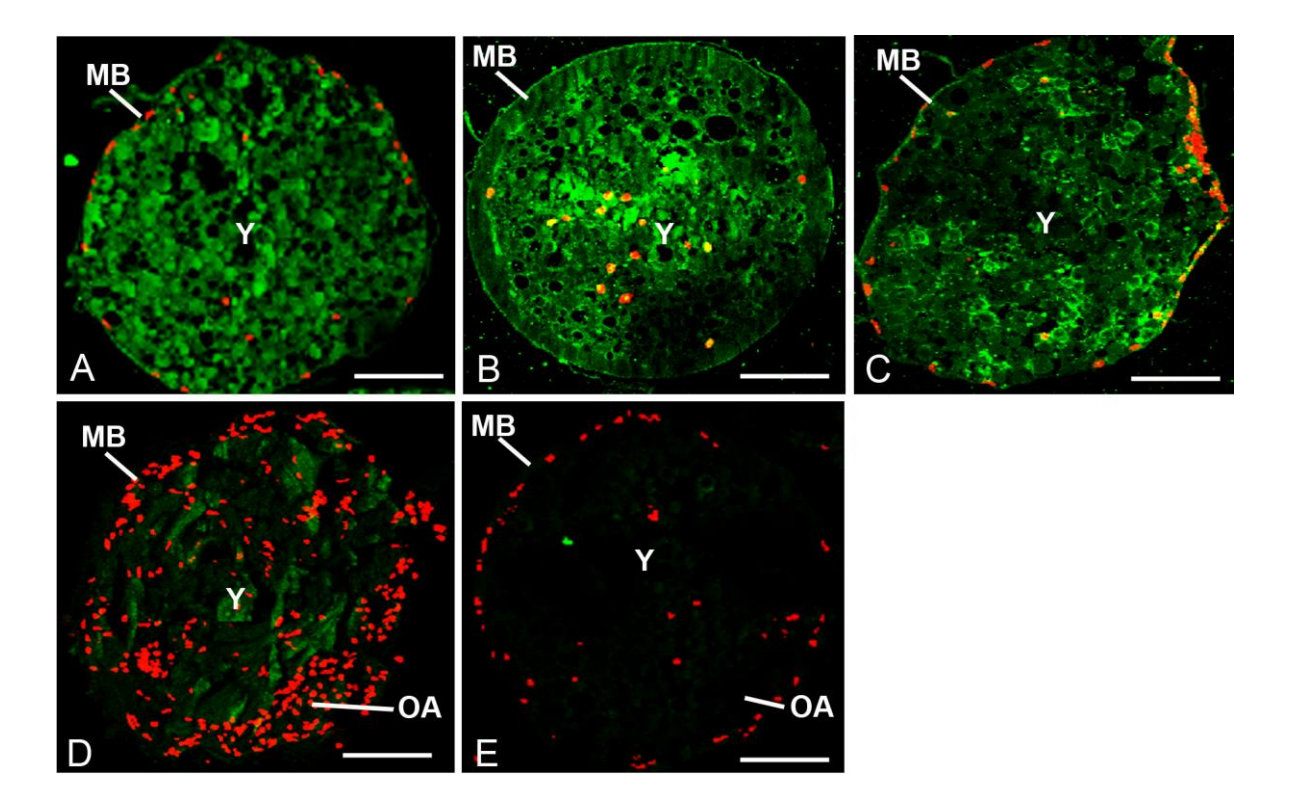


**Fig. 17** Immunofluorescence detection of 5-HT-ir (green) in various embryonic stages, with the nuclei labeled with ToPro-3 (red). (A) 5-HT-ir is detected in the BYE stage (B, C) 5-HT-ir is present in the yolk of the DYE stage. (D) Intense 5-HT-ir is detected in the yolk of OE stages. (E) In the control sections, no immunofluorescence is detected. MB, egg membrane; OA, organ anlage; Y, yolk. Scale bars: 100 μm

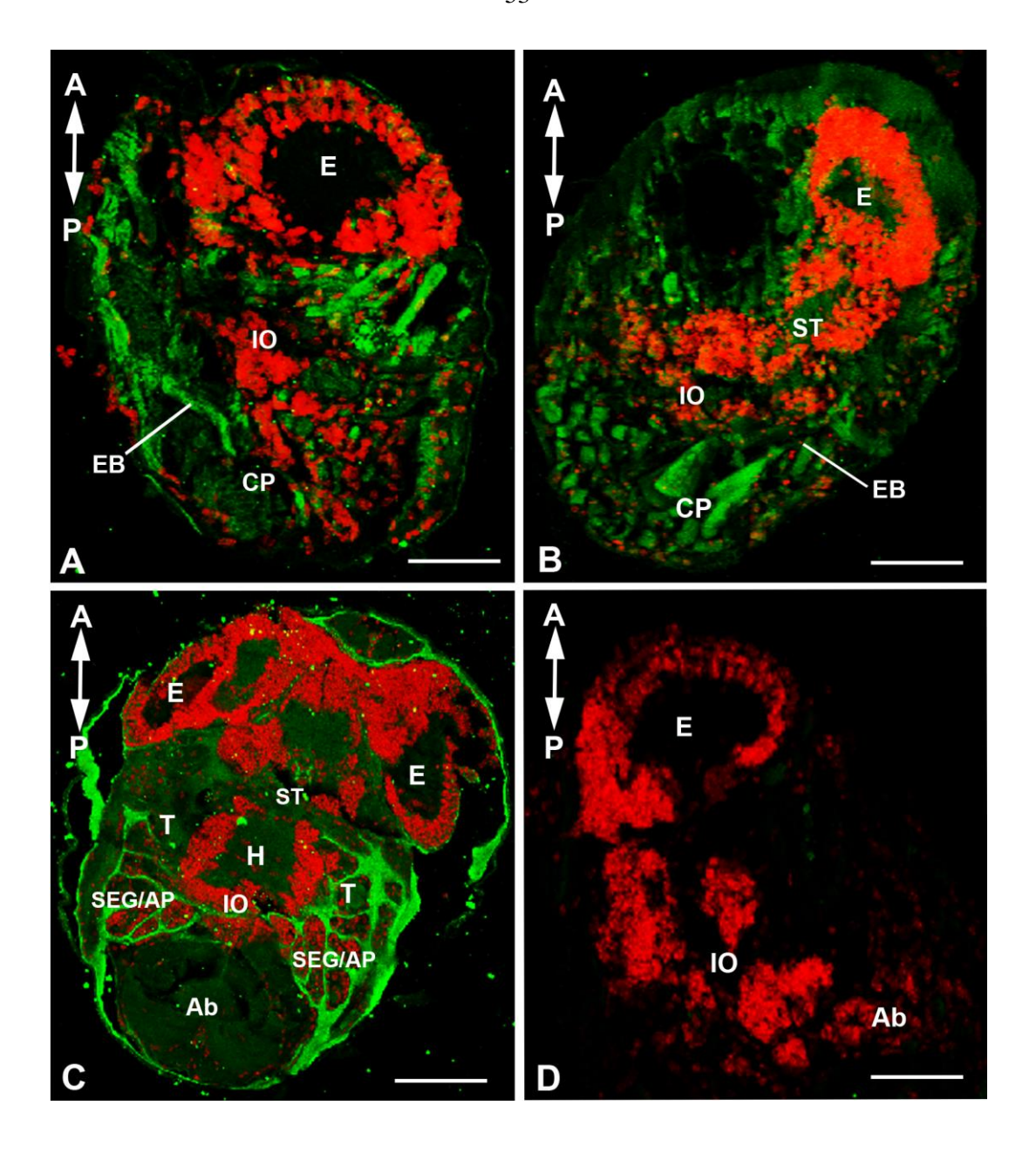


**Fig. 18** Immunofluorescence detection of 5-HT-ir (green) in various embryonic stages, with nuclei labeled with ToPro-3 (red). The orientation of the embryos is given top left. (A) 5-HT-ir is present in the E, H, EB and CP at BE stage. (B-C) 5-HT-ir is detected in the EB, CP, SEG and AP at the GE and BLE stages. (D) In the control sections, no immunofluorescence is observed. A, anterior; Ab; abdomen; AP, appendages; E, eye; EB, elongated body; H, heart; IO, internal organs; P, posterior; SEG, segmented abdomen; ST, stomodaeum; T, trunk; Y, yolk. Scale bars: 100 μm

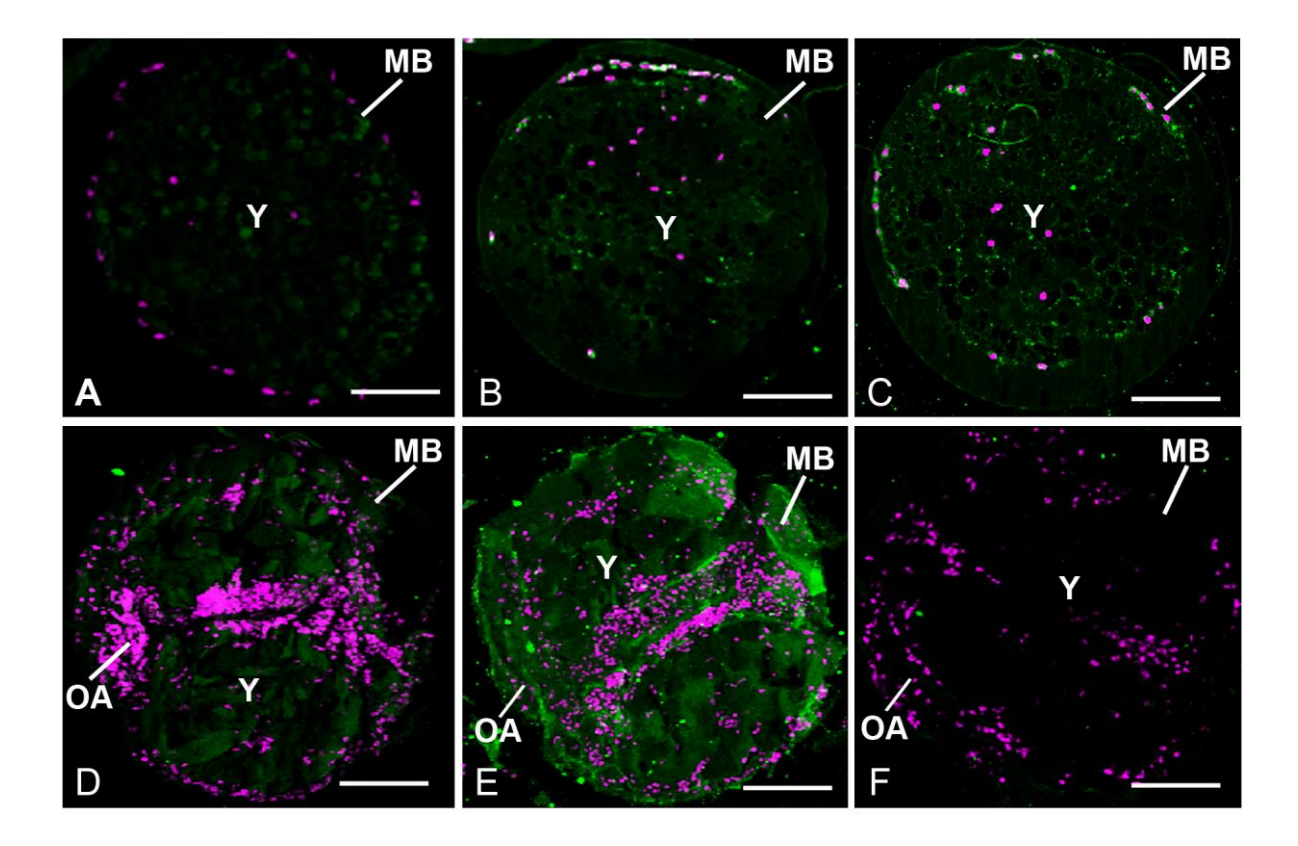


**Fig. 19** Immunofluorescence detection of DA-ir (green) in various embryonic stages, with nuclei labeled with ToPro-3 (magenta). (A) DA-ir is present in the yolk of the BYE stage and (B, C) the DYE stage. (D, E) Intense DA-ir is detected in the yolk of OE stages. (F) In the control sections, no immunostaining is present. MB, egg membrane; OA, organ anlage; Y, yolk. Scale bars: 100 μm

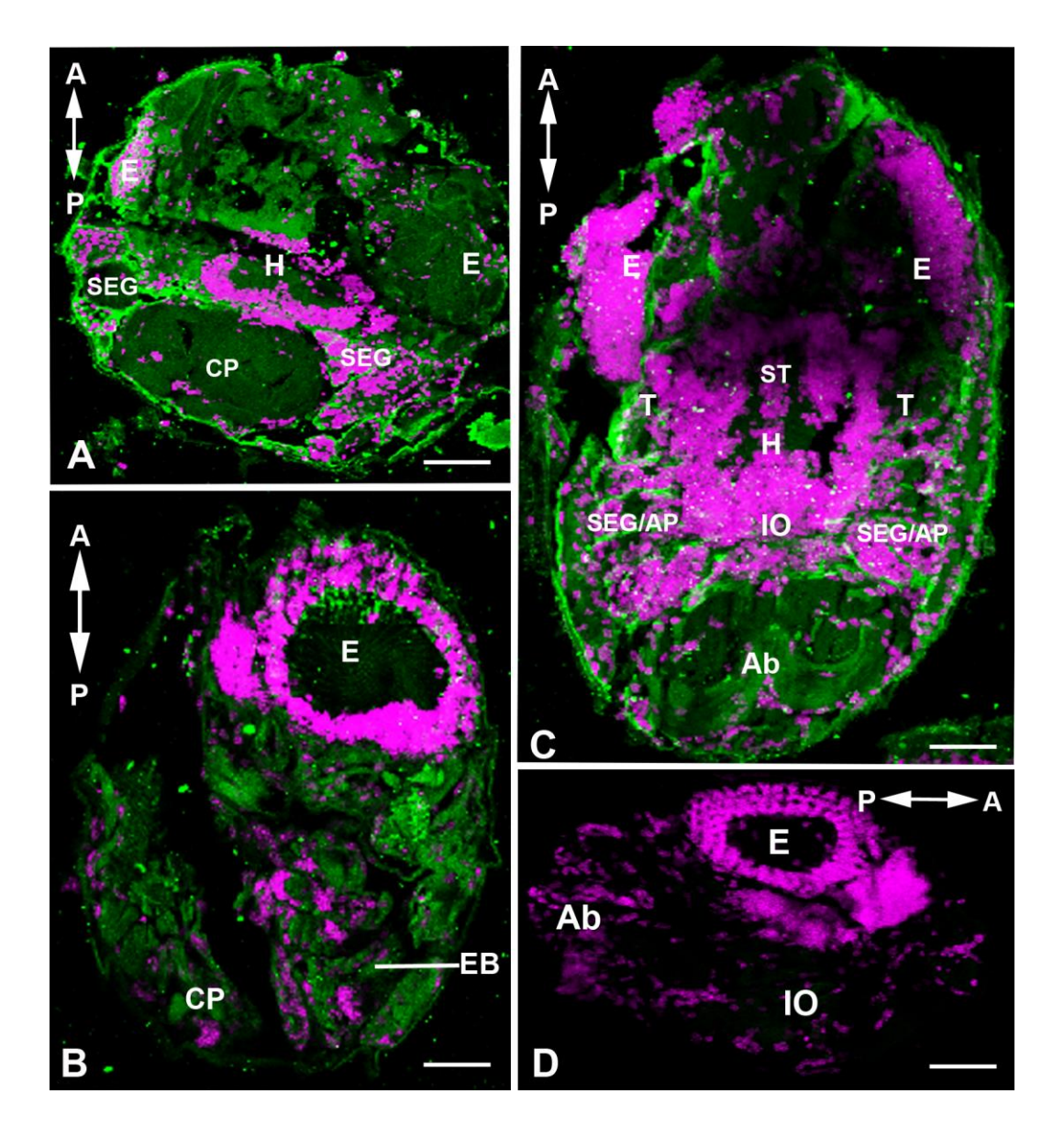


**Fig. 20** Immunofluorescence detection of DA-ir (green) in the BE, GE, and BLE, with nuclei labeled with ToPro-3 (magenta). The orientation of the embryos is given top left (A-C) and top right (D). (A) DA-ir is present in the E, H, and EB at BE stage. (B) DA-ir is detected in the EB and CP at the GE stage, and (C) DA-ir is present in H, SEG, AP and IO at the BLE stage. (D) No immunofluorescence is detected in the control sections. A, anterior; Ab; abdomen; AP, appendages; E, eye; EB, elongated body; H, heart; IO, internal organs; P, posterior; SEG, segmented abdomen; ST, stomodaeum; T, trunk; Y, yolk. Scale bars: 100 μm

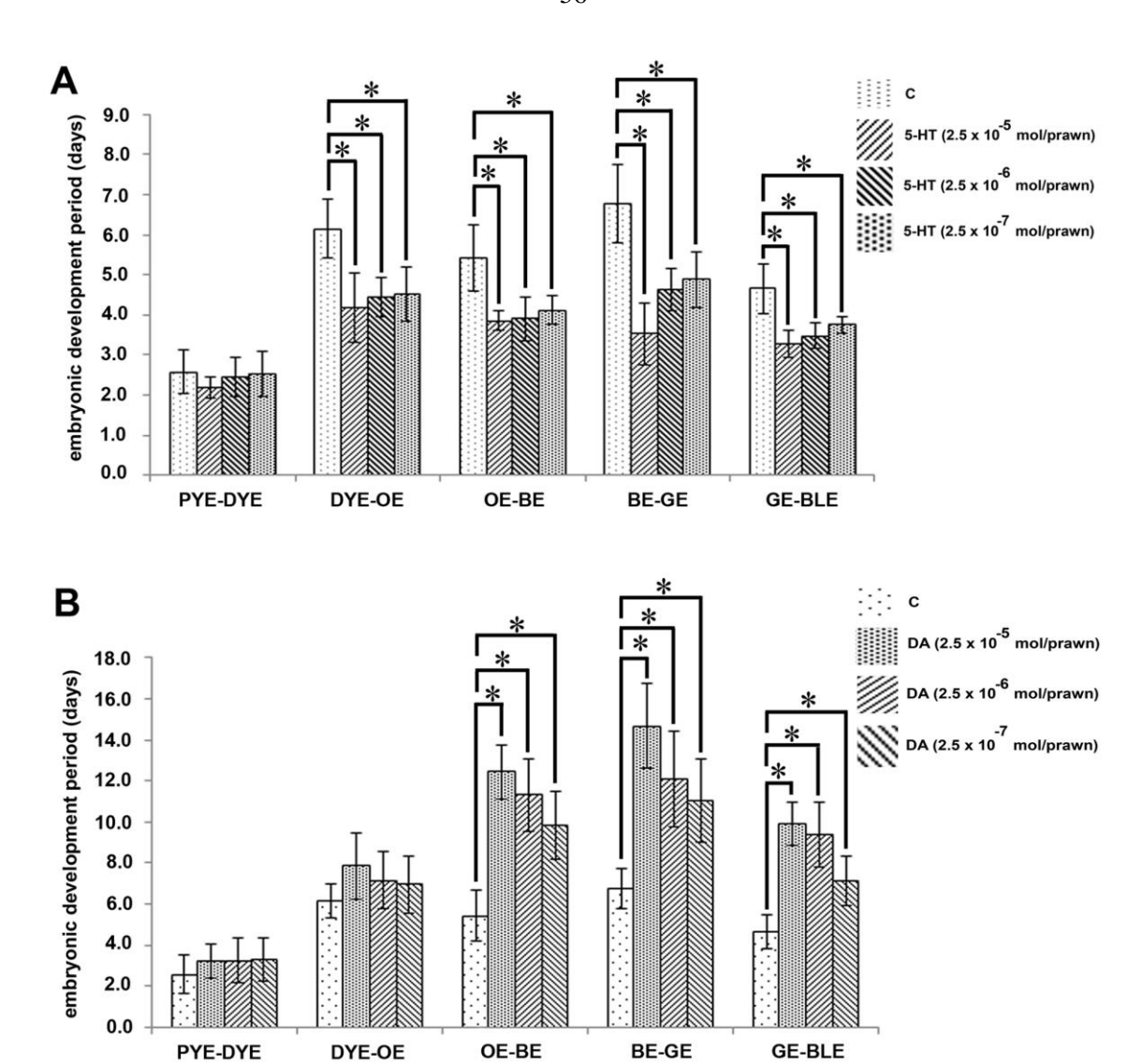


**Fig. 21** The effects of 5-HT and DA on the development of each embryonic stage in *M. rosenbergii*. (A) Histograms showing that female prawns injected with 5-HT at doses of  $2.5 \times 10^{-5}$ ,  $2.5 \times 10^{-6}$  and  $2.5 \times 10^{-7}$  mol/prawn, exhibited significant shortening embryonic developmental period started from DYE to OE stages and onwards, compared with the control group. (B) After injections with DA at doses of  $2.5 \times 10^{-5}$ ,  $2.5 \times 10^{-6}$  and  $2.5 \times 10^{-7}$  mol/prawn, showed significant lengthening embryonic developmental period started from mid-embryonic stage onwards, compared with the control group. Each measurement is expressed as a mean  $\pm$  S.E.M. Asterisks indicate significant differences (P<0.05) with respect to the control groups.

# Discussion

In this study, we reported for the first time in *M. rosenbergii* on the variation in concentrations and distribution of 5-HT and DA during embryogenesis. The 5-HT concentrations increased significantly at the early embryonic stages, while DA levels remained low. DA was clearly detected at about the mid-embryonic stage. 5-HT exerted its action by significantly decreasing durations of nearly all embryonic stages, whereas DA lengthened the durations of the mid-embryonic stages. This demonstrates the opposite actions of 5-HT and DA on embryonic development.

Several studies have reported on the varying concentrations of these two neurotransmitters during developmental processes in invertebrates, including decapod crustaceans. In the hookworm, Nippostrongylus brasiliensis, the fluctuation of 5-HT occurs in the embryonic and larval stages, suggesting that this amine may play important role during embryonic development (Goudey-Perrie et al., 1997). In the crayfish, P. clarkii, 5-HT levels in free larval stages were quantified using HPLC, with the total concentration of 5-HT being higher in the brain than in the eyestalks (Cervantes et al., 1999), which suggests that 5-HT may play an important role in embryonic development (Escamilla-Chimal et al., 1998; Benton et al., 1997). In the sea urchin, DA showed a very low concentration at the blastula stage, and then it gradually increased from the late gastrula to late prism stages, and finally exhibited a sharp increase to reach a maximal concentration at late pluteus larva. This fluctuation in DA levels suggests a regulatory role for DA on the formation and transition of gastrula stage to the late embryonic stages (Anitole-Misleh and Brown, 2004). In addition, tyrosine, which is the precursor for synthesis of DA, exhibited a high concentration in the eyes and internal organs during embryogenesis. implying important roles of DA in accumulation of eye pigments and internal organ formation (Shen and Wang, 1990). Our present work demonstrates for the first time that the levels of 5-HT and DA fluctuate during the embryonic stages of M. rosenbergii, but the timing for the initial appearances of these two transmitters are different with the appearance of 5-HT at early embryonic stage, while DA appears later. The increases in 5-HT and DA to maximum levels by the late embryonic stages in M. rosenbergii, detected with HPLC analyses are in agreement with immunohistochemical data which demonstrated that the 5-HT-ir and DA-ir were more intense in the late embryonic stages. It is also possible that 5-HT and DA are important signaling molecules that regulate embryonic development of this species.

There have been reports regarding the presence and distribution of 5-HT and DA during embryonic development in invertebrates. In the sea urchin, 5-HT regulates cell divisions during

cleavage and blastula stages, and promotes invagination to form the archenteron during gastrulation, suggesting that 5-HT is synthesized in fertilized eggs and early embryos so that it can regulate the processes of early embryogenesis (Buznikov et al., 2001). In addition, 5-HT could be an important molecule at the early embryonic stages that may be involved in expression of zygotic genes during the mid-blastula transition stages (Emanuelsson et al., 1988; Buznikov, 1990; Buznikov, 1991; Colas et al., 1999). In Drosophila, 5-HT also promotes the gastrulation during embryonic development, implying that 5-HT plays important role in the development of early embryos up to gastrulation stage (Colas et al., 1999). In the mollusk, Tritonia diomedea, 5-HT-ir was detected in cleaving embryos, indicating that 5-HT may be involved in the control of cleavage stage (Buznikov and Bezuglov, 2000). There are a few reports regarding the serotonergic system during embryonic development of crustaceans. In the crayfish, Cherax destructor, 5-HT was detected by the second postembryonic stage (Sandeman and Sandeman, 1990; Rieger and Harzsch, 2008). In the American lobster, H. americanus, 5-HT was firstly detected immunohistochemically in early embryonic stages, suggesting that 5-HT was synthesized early during embryogenesis (Beltz, 1999; Beltz et al., 2001). In the present study, we reported for the first time the existence and distribution of 5-HT in several embryonic stages of M. rosenbergii. Specifically, we detected 5-HTir in several regions and structures of different embryonic stages, including the yolk, cell membrane, and organ anlages, including the eye anlage, the elongated body, internal organs, and the heart, suggesting that 5-HT could be synthesized at early embryonic stages, and that it may be involved in regulating the utilization of yolk, and serving in regulating the cleavage stage, as well as in organ formation, for example, the invagination of the archenteron during gastrulation, as reported earlier in the sea urchin (Colas et al., 1999).

DA has been detected during embryonic stages of many invertebrate species, including decapod crustaceans. In the sea urchin and the starfish, DA-ir was detected in the zygotes, cells of cleavage and blastula stages, indicating that DA may be involved in the control of cell divisions during these stages (Buznikov et al., 1996). In *H. americanus*, the DA-ir staining was first detected at about the mid-embryonic stages, indicating that the onset of DA is later than 5-HT (Cournil et al., 1995). DA-ir was detected in the stomatogastric ganglion and other internal organs, suggesting that DA may be involved in the growth of stomach and exerts its activity during the lobster embryogenesis (Pulver et al., 2003). In *Calanus finmarchicus*, DA biosynthetic enzyme-encoding transcripts were present across six developmental stages. This suggests that the synthesis of DA occurs during early naupliar life (Christie et al., 2014). In the present study, we also reported the initial appearance and tissue

distribution of DA at about the mid-embryonic stages of M. rosenbergii embryos. The timing of the first appearance of DA in embryonic stages of M. rosenbergii was similar to those of other crustacean species, though slightly earlier than in H. americanus. Specifically, DA-ir was detected in the yolk and organ anlages, which was similar to those found in the sea urchin, suggesting that DA might be involved in regulating the utilization of yolk and the development of organs during the stages of a rapid growth of the embryos, as reported in *H. americanus*. In *M. rosenbergii*, DA-ir was also detected in the eye anlage and internal organs, implying that DA might be involved in regulating in the development of these organs (Zhao et al., 1998; Yao et al., 2006). There have been reports on the actions of 5-HT and DA during development in invertebrates and in a few decapod crustaceans. In the sea urchin, it was found that 5-HT stimulates cleavage divisions, while DA inhibits cell divisions during these processes, implying their opposite actions during embryonic development (Buznikov and Bezuglov, 2000; Buznikov et al., 2001). Moreover, 5-HT receptors were up-regulated in the midblastula stage, which was correlated with the rapid cell division, resulting in the formation of additional cell layers in the blastula wall in the sea urchin (Buznikov et al., 2001). In H. americanus, the critical role of 5-HT in the embryonic development was demonstrated by pharmacological depletion of 5-HT using 5,7-dihydroxytryptamine, which resulted a long-term reduction of 5-HT that significantly slowed the growth of olfactory and accessory lobes of the brain, suggesting that 5-HT may play a role in the brain development (Benton et al., 1997). In M. rosenbergii, prawn larvae exposed to 5-HT showed significantly reduced lengths of all larval stages and enhanced the transformation to post-larval stage, compared with the control group (Tangvuthipong and Damrongphol, 2006). Previously, we found that injecting 5-HT into adult female M. rosenbergii broodstocks also shortened the whole length of embryonic development, whereas injecting DA showed an opposite effect, suggesting these two neurotransmitters act antagonistically with regard to the embryonic development (Tinikul et al., 2009a,b). However, that study did not detail the specific actions of 5-HT and DA on the lengths of each embryonic developmental stage. In the present study, we further demonstrated that the injection of 5-HT to female broodstocks significantly decreased the lengths of embryonic development from early to late embryonic stages, whereas DA-injected groups significantly lengthened the embryonic development from the mid to late stages, compared with the control group. It is possible that 5-HTmay stimulate the development of early embryonic stages, while DA exercises opposite control as demonstrated in the sea urchin (Buznikov and Bezuglov, 2000; Buznikov et al., 2001). In addition, 5-HT has been reported to stimulate the release of a number of other neurohormones in decapod

crustaceans, particularly crustacean hyperglycemic hormone (CHH) during early development. We postulate that 5-HT may regulate the release of the CHH which stimulates glycogenolysis in muscles and the midgut to promote early development, and supports fast growth during embryonic stages in crustaceans (Kallen et al., 1988). Our results indicate the dynamic balance of these two neurotransmitters acting together during embryonic development, which may be necessary for setting the normal rhythm and pattern of embryonic formation in this prawn species. The precise molecular mechanisms of 5-HT and DA actions with MrNPF and other related neuropeptides in the regulation of embryonic development of this decapod crustacean needed to be clarified by further studies.

# References

- Anitole-Misleh, K.G., Brown, K.M., 2004. Developmental regulation of catecholamine levels during sea urchin embryo morphogenesis. Comp. Biochem. Physiol. Part A 137, 39–50.
- Beltz, B.S., 1999. Distribution and functional anatomy of amine-containing neurons in decapod crustaceans. Microsc. Res. Tech. 44, 105–120.
- Beltz, B.S., Benton, J.L., Sullivan, J.M., 2001. Transient uptake of serotonin by newborn olfactory projection neurons. Proc. Natl. Acad. Sci. U.S.A. 98, 12730–12735.
- Benton, J.L., Huber, R., Ruchhoeft, M., Helluy, S., Beltz, B.S., 1997. Serotonin depletion by 5,7-dihydroxytryptamine alters deutocerebral development in the lobster, *Homarus americanus*. J. Neurobiol. 33, 357–373.
- Bradford, M.M., 1976. A rapid and sensitive method for the quantitation of microgram quantities of protein utilizing the principle of protein-dye binding. Anal. Biochem. 72, 248–254.
- Brown, M.R., Sieglaff, D.H., Rees, H.H., 2009. Gonadal ecdysteroidogenesis in arthropoda: occurrence and regulation. Ann Rev Entomol 54, 105–125.
- Buszczak, M., Freeman, M.R., Carlson, J.R., Bender, M., Cooley, L., Segraves, W.A., 1999. Ecdysone response genes govern egg chamber development during midoogenesis in *Drosophila*. Development 126 (20), 4581-4589.
- Buznikov, G.A., 1991. Neurotransmitters in Embryogenesis. Harwood Academic Press, USA.
- Buznikov, G.A., Bezuglov, V.V., 2000. 5-Hydroxytryptamides and 3- hydroxytyramides of polyenoic fatty acids as a tool for studying the prenervous biogenic monoamines functions. Russ. J. Physiol. 86, 1093–1108.
- Buznikov, G.A., Lambert, H.W., Lauder, J.M., 1996. From oocyte to neuron: do neurotransmitters function in the same way throughout development? Cell. Mol. Neurobiol. 16, 532–559.
- Buznikov, G.A., Lambert, H.W., Lauder, J.M., 2001. Serotonin and serotonin-like substances as regulators of early embryogenesis and morphogenesis. Cell Tissue Res. 305, 177–186.
- Carlsson, M.A., Enell, L.E., Nassel, D.R., 2013. Distribution of short neuropeptide F and its receptor in neuronal circuits related to feeding in larval *Drosophila*. Cell Tissue Res 353:511-523
- Cerstiaens, A., Benfekih, L., Zouiten, H., Verhaert, P., De L.A., Schoofs, L., 1999. Led-NPF-1 stimulates ovarian development in locusts. Peptides 20, 39-44.
- Cervantes, O.C., Battelle, B.A., Moles, M.L.F., 1999. Rhythmic changes in the serotonin content of the brain and eyestalk of crayfish during development. J. Exp. Biol. 202, 2823–2830.

- Chen M-E, Pietrantonio, P.V., 2006. The short neuropeptide F-like receptor from the red imported fire ant, *Solenopsis invicta* Buren (Hymenoptera: Formicidae). Arch Insect Biochem Physiol 61, 195-208.
- Christie, A.E., Chapline, M.C., Jackson, J.M., Dowda, J.K., Hartline, N., Malecha, S.R., Lenz, P.H., 2011. Identification, tissue distribution and orexigenic activity of neuropeptide F (NPF) in penaeid shrimp. J Exp Biology 214, 1386-1396
- Christie, A.E., Fontanilla, T.M., Roncalli, V., Cieslak, M.C., Lenz, P.H., 2014. Identification and developmental expression of the enzymes responsible for dopamine, histamine octopamine and serotonin biosynthesis in the copepod crustacean *Calanus finmarchicus*. Gen. Comp. Endocrinol. 195, 28–39.
- Chung, J.S., Zmora, N., Katayama, H., Tsutsui, N., 2010. Crustacean hyperglycemic hormone (CHH) neuropeptides family: function, titer, and binding to target tissues. Gen Comp Endocrinol 166: 447-454
- Colas, J.F., Launay, J.M., Maroteaux, L., 1999. Maternal and zygotic control of serotonin biosynthesis are both necessary for *Drosophila* germband extension. Mech. Dev. 87, 67–76.
- Cournil, I., Casasnovas, B., Helluy, S.M., Beltz, B.S., 1995. Dopamine in the lobster *Homarus* gammarus: II dopamine-immunoreactive neurons and development of the nervous system. J. Comp. Neurol. 362, 1–16.
- de Jong-Brink, M., ter Maat A., Tensen, C.P., 2001. NPY in invertebrates: molecular answers to altered functions during evolution. Peptides 22, 309-315.
- De Lange, R.P., van Golen, F.A., van Minnen, J., 1997. Diversity in cell specific coexpression of four neuropeptide genes involved in control of male copulation behaviour in *Lymnaea stagnalis*. Neuroscience 78, 289-299.
- Escamilla-Chimal, E.G., García-Rivera, C.C., Aguilar-Morales, M., Romero-Díaz, V., Fanjul-Moles, M.L., 1998. The retina of crayfish *Procambarus clarkii* during development shows serotonin and tryptophan hydroxylase-like immunoreactivity daily changes. Biol. Rhythm Res. 29, 471–479.
- Fingerman, M., 1997. Roles of neurotransmitters in regulating the reproductive hormone release and gonadal maturation in decapod crustaceans. Invertebr. Reprod. Dev. 31, 47–54.
- Girardie, J., Huet, J.C., Atay-Kadiri, Z., Ettaouil, S., Delbecque, J.P., Fournier, B., Pernollet, J.C., Girardie, A., 1998. Isolation, sequence determination, physical and physiological characterization

- of the neuroparsins and ovary maturing parsins of *Schistocerca gregaria*. Insect Biochem Molec 28 (9), 641–650.
- Goudey-Perrie, F., Grosclaude, J.M., Nembo, B., Burreteau, H., Jacquot, F.C., Gayral, P., 1997. Levels of biogenic amines in larvae and adults of the rat hookworm, *Nippostrongylus brasiliensis* (Nematoda). Comp. Biochem. Physiol. Part A 118, 615–623.
- Habashy, M.M., Sharshar, K.M., Hassan, M.M.S., 2012. Morphological and histological studies on the embryonic development of the freshwater prawn, *Macrobrachium rosenbergii* (Crustacea, Decapoda). JOBAZ 65, 157–165.
- Kallen, J.L., Rigiani, N.R., Trompenaars, H.J.A.J., 1988. Aspects of entrainment of CHH cell activity and hemolymph glucose levels in crayfish. Biol. Bull. 175, 137–143.
- Kruangkum, T., Chotwiwatthanakun, C., Vanichviriyakit, R., Tinikul, Y., Anuracpreeda, P., Wanichanon, C., Hanna, P.J., Sobhon, P., 2013. Structure of the olfactory receptor organs, their GABAergic neural pathways, and modulation of mating behavior, in the giant freshwater prawn, *Macrobrachium rosenbergii*. Microsc Res Tech 76:572-587
- Lu, H-L Pietrantonio, P.V., 2011. Immunolocalization of the short neuropeptide F receptor in queen brains and ovaries of the red imported fire ant (*Solenopsis invicta* Buren). BMC Neuroscience 12, 57.
- Manush, S.M., Pal, A.K., Das, T., Mukherjee, S.C., 2006. The influence of temperatures ranging from 25 to 36 C on developmental rates, morphometrics and survival of freshwater prawn (*Macrobrachium rosenbergii*) embryos. Aquaculture 256, 529–536.
- Meeratana, P., Sobhon, P., 2007. Classification of differentiating oocytes during ovarian cycle in the giant freshwater prawn, *Macrobrachium rosenbergii* de man. Aquaculture 270, 249–258.
- Mertens, I., Meeusen, T., Huybrechts, R., De Loof, A., Schoofs, L., 2002. Characterization of the short neuropeptide F receptor from *Drosophila melanogaster*. Biochem Biophys Res Commun 297,1140-1148.
- Müller, Y.M.R., Nazari, E.M., Simões-Costa, M.S., 2003. Embryonic stages of the freshwater prawn, *Macrobrachium olfersii* (Decapoda, Palaemonidae). J. Crustacean. Biol. 23, 869–875.
- Nässel, D.R., Wegener, C., 2011. A comparative review of short and long neuropeptide F signaling in invertebrates: Any similarities to vertebrate neuropeptide Y signaling? Peptides 32, 1335-1355.
- New, M.B., 2002. Farming freshwater prawns: a manual for the culture of the giant river prawn (*Macrobrachium rosenbergii*). FAO Fisheries Technical Paper 428, 1–10.

- Okumura, T., 2004. Perspectives on hormonal manipulation of shrimp reproduction review. JARQ 38, 49-54.
- Parthasarathy, R., Sheng, Z., Sun, Z., Palli, S.R., 2010. Ecdysteroid regulation of ovarian growth and oocyte maturation in the red flour beetle, *Tribolium castaneum*. Insect Biochem Molec 40, 429-439.
- Rajpara, S.M., Garcia, P.D., Roberts, R., Eliassen, J.C., Owens, D.F., Maltby, D., Myers, R.M., Mayeri, E., 1992. Identification and molecular cloning of a neuropeptide Y homolog that produces prolonged inhibition in *Aplysia* neurons. Neuron 9: 505-513.
- Rieger, V., Harzsch, S., 2008. Embryonic development of the histaminergic system in the ventral nerve cord of the marbled crayfish (Marmorkrebs). Tissue Cell 40, 113–126.
- Sandeman, R., Sandeman, D.C., 1990. Development and identified neural systems in the crayfish brain. In: Wiese, K., Krenz, W.D., Tautz, J., Reichert, H., Mulloney, B. (Eds.), Frontiers in Crustacean Neurobiology. Birkhaüser, Basel, pp. 498–508.
- Sarojini, R., Nagabhushanam, R., Fingerman, M., 1995. Mode of action of the neurotransmitter 5-hydroxytryptamine in stimulating ovarian maturation in the red swamp crayfish, Procambarus clarkii: an in vivo and in vitro study. J. Exp. Zool. 271, 395–400.
- Schoofs, L., Clynen, E., Cerstiaens, A., Baggerman, G., Wei, Z., Vercammen, T., Nachman, R., De Loof, A., Tanaka, S., 2001. Newly discovered functions for some myotropic neuropeptides in locusts. Peptides 22, 219–227.
- Shen, T., Wang, J.Y., 1990. Biochemistry [M]. Higher Education Publisher, pp. 67–86.
- Soonklang, N., Wanichanon, C., Stewart, M.J., Stewart, P., Meeratana, P., Hanna, P.J., Sobhon, P., 2012. Ultrastructure of differentiating oocytes and vitellogenesis in the giant freshwater prawn, *Macrobrachium rosenbergii* (De Man). Microsc Res Tech 75, 1402–1415.
- Suwansa-Ard, S., Thongbuakaew, T., Wang, T., Zhao, M., Elizur, A., Hanna, P.J., Sretarugsa, P., Cummins, S.F., Sobhon, P., 2015. In silico neuropeptidome of female *Macrobrachium rosenbergii* based on transcriptome and peptide mining of eyestalk, central nervous system and ovary. PLoS One 10:e0123848.
- Tangvuthipong, P., Damrongphol, P., 2006. 5-Hydroxytryptamine enhances larval development of the giant freshwater prawn, *Macrobrachium rosenbergii*. Aquaculture 251, 567–572.

- Tawfik, A.I., Vedrova, A., Sehnal, F., 1999. Ecdysteroids during ovarian development and embryogenesis in solitary and gregarious Schistocerca gregaria. Arch Insect Biochem Physiol 41 (3), 134-143.
- Tinikul, Y., Mercier, A.J., Soonklang, N., Sobhon, P., 2008. Changes in the levels of serotonin and dopamine in the central nervous system and ovary, and their possible roles in the ovarian development in the giant freshwater prawn, *Macrobrachium rosenbergii*. Gen. Comp. Endocrinol. 158, 250-258.
- Tinikul, Y., Soonthornsumrith, B., Phoungpetchara, I., Poljareon, J., Meeratana, P., Duangsuwan, P., Soonklang, N., Mercier, A.J., Sobhon, P., 2009a. Effects of serotonin, dopamine, octopamine, and spiperone on ovarian maturation and embryonic development in the giant freshwater prawn, *Macrobrachium rosenbergii* (De Man, 1879). Crustaceana 82, 1007–1022.
- Tinikul, Y., Mercier, A.J., Sobhon, P., 2009b. Distribution of dopamine and octopamine in the central nervous system and ovary during the ovarian maturation cycle in the giant freshwater prawn, *Macrobrachium rosenbergii*. Tissue Cell 41, 430–442.
- Tinikul, Y., Poljaroen, J., Nuurai, P., Anuracpreeda, P., Chotwiwatthanakun, C., Phoungpetchara, I., Kornthong, N., Poomtong, T., Hanna, P.J., Sobhon, P., 2011a. Existence and distribution of gonadotropin-releasing hormone-like peptides in the central nervous system and ovary in the Pacific white shrimp, *Litopenaeus vannamei*. Cell Tissue Res. 343, 579–593.
- Tinikul, Y., Poljaroen, J., Kornthong, N., Chotwiwatthanakun, C., Anuracpreeda, P., Poomtong, T., Hanna, P.J., Sobhon, P., 2011b. Distribution and changes of serotonin and dopamine levels in the central nervous system and ovary of the Pacific white shrimp, *Litopenaeus vannamei*, during ovarian maturation cycle. Cell Tissue Res. 345, 103–124.
- Tinikul, Y., Poljaroen, J., Tinikul, R., Anuracpreeda, P., Chotwiwatthanakun, C., Senin, N., Poomtong, T., Hanna, P.J., Sobhon, P., 2014. Effects of gonadotropin-releasing hormones and dopamine on ovarian maturation and their presence in the ovary during ovarian development of the Pacific white shrimp, *Litopenaeus vannamei*. Aquaculture 420–421, 79–88.
- Tinikul, Y., Poljaroen, J., Tinikul, R., Chotwiwatthanakun, C., Anuracpreeda, P., Hanna, P.J., Sobhon, P., 2015. Alterations in the levels and distribution of octopamine in the central nervous system and ovary of the Pacific white shrimp, *Litopenaeus vannamei*, and its possible role in ovarian development.

- Tinikul, Y., Poljaroen, J., Tinikul, R., Sobhon, P., 2016. Changes in the levels, expression, and their possible roles of serotonin and dopamine during embryonic development in the giant freshwater prawn, *Macrobrachium rosenbergii*. Gen. Comp. Endocrinol. 225, 71-80.
- Tinikul, Y., Engsusophon, A., Kruangkum, T., Thongrod, S., Tinikul, R., Sobhon, P., 2017. Neuropeptide F stimulates ovarian development and spawning in the female giant freshwater prawn, *Macrobrachium rosenbergii*, and its expression in the ovary during ovarian maturation cycle. Aguaculture 469: 128-136.
- Thongrod, S., Changklungmoa, N., Chansela, P., Siangcham, T., Kruangkum, T., Suwansa-ard, S., Saetan, J., Sroyraya, M., Tinikul, Y., Wanichanon, C., Sobhon, P., 2017. Characterization and tissue distribution of neuropeptide F in the eyestalk and brain of the male giant freshwater prawns, *Macrobrachium rosenbergii*. Cell Tissue Res. 367, 181-195.
- Van Wielendaele, P., Wynant, N., Dillen, S., Badisco, L., Marchal, E., Vanden Broeck, J., 2013. *In vivo* effect of Neuropeptide F on ecdysteroidogenesis in adult female desert locusts (*Schistocerca gregaria*). J Insect Physiol 59, 624-630.
- Walker, R.J., Papaioannou, S., Holden-Dye, L., 2009. A review of FMRFamide- and RFamide-like peptides in metazoa. Invert Neurosci 9, 111-153.
- Wu, Q, Wen, T., Lee, G., Park, J.H., Cai, H.N., Shen, P., 2003. Developmental Control of Foraging and Social Behavior by the *Drosophila* Neuropeptide Y-like System. Neuron 39, 147-161.
- Yao, J.J., Zhao, Y.L., Wang, Q., Zhou, Z.L., Hu, X.C., Duan, X.W., An, C.G., 2006. Biochemical compositions and digestive enzyme activities during the embryonic development of prawn, *Macrobrachium rosenbergii*. Aquaculture 253, 573–582.
- Zhao, Y.L., Wang, Q., Du, N.S.H., Lai, W., 1998. Embryonic development of the giant freshwater prawn, *Macrobrachium rosenbergii* (Crustacea: Decapoda): I. Morphogenesis of external structures of embryo (Chinese). Acta Zool. Sin. 44, 249–256.

# Outputs จากโครงการวิจัยที่ได้รับทุนจาก สกว.

Outputs, conferences, and awards that were supported by this TRF Research Career Development Grant to Assoc. Prof. Dr. Yotsawan Tinikul (grant no. RSA5780011, jointly funded by the Thailand Research Fund and Mahidol University) are shown below and please also see the appendix.

# **International publications:**

- 1. <u>Tinikul Y</u>, Engsusophon, A, Kruangkum T, Thongrod S, Tinikul, R, Sobhon P (2017) Neuropeptide F stimulates ovarian development and spawning in the female giant freshwater prawn, *Macrobrachium rosenbergii*, and its expression in the ovary during ovarian maturation cycle. Aquaculture 469: 128-136
  (โปรดดูเอกสารแนบ)
- 2 . <u>Tinikul Y</u>, Poljaroen J, Tinikul R, Sobhon P. (2016) Changes in the levels, expression, and their possible roles of serotonin and dopamine during embryonic development in the giant freshwater prawn, *Macrobrachium rosenbergii*. General and Comparative Endocrinology 225: 71-80. (โปรดดูเอกสารแนบ)
- 3. Thongrod S, Changklungmoa N, Chansela P, Siangcham T, Kruangkum T, Suwansa-ard S, Saetan J, Sroyraya M, <u>Tinikul Y</u>, Wanichanon C, Sobhon P. (2017) Characterization and tissue distribution of neuropeptide F in the eyestalk and brain of the male giant freshwater prawns, *Macrobrachium rosenbergii*. Cell and Tissue Research 367: 181-195. (โปรดดเอกสารแนบ)

# การนำผลงานวิจัยไปใช้ประโยชน์

ในโครงการวิจัยนี้ จากการได้รับองค์ความรู้พื้นฐานใหม่ที่สำคัญและการวิจัยต่อยอดถึงการศึกษาคุณลักษณะ การปรากฏ การกระจาย หน้าที่ของนิวโรเปปไทด์เอฟ (NPF) และความสัมพันธ์เกี่ยวข้องของสารสื่อประสาทเหล่านี้ต่อ วงจรของการพัฒนารังไข่ การสืบพันธุ์ การตกไข่ และการเจริญของตัวอ่อน จะมีการนำผลงานวิจัยไปใช้ประโยชน์ใน เชิงวิชาการเป็นหลัก ดังที่รายงานในโครงการวิจัยมาแล้วนั้น โดยทำการฉีดกระตุ้นแม่พันธุ์กุ้งด้วย NPF ในกุ้ง ก้ามกรามเพศเมีย เมื่อพิจารณาระดับปริมาณของสาร (dose) ที่ใช้ต่อน้ำหนักตัวของแม่พันธุ์เพื่อให้เกิดผลตอบสนอง ทางบวก พบว่า NPF น่าจะเป็นนิวโรฮอร์โมนตัวสำคัญตัวหนึ่งที่มีประสิทธิภาพสูงในระดับหนึ่งในการออกฤทธิ์ โดย อาจออกฤทธิโดยตรงที่อวัยวะสืบพันธุ์และรังไข่ ซึ่งการใช้ NPF ร่วมกับสารสื่อประสาทตัวหลัก อาทิ 5-HT และ/หรือ ตัวห้าม (antagonist) ต่อ DA ในอัตราส่วนที่เหมาะสมอาจจะสามารถช่วยในกระตุ้นการพัฒนาของรังไข่ การตกไข่ และการเจริญของตัวอ่อนได้ดีมากยิ่งขึ้น โดยเฉพาะในแม่พันธุ์กุ้งที่ถูกเลี้ยงในสภาพกักขังให้มีความสมบูรณ์เพศของแม่ พันธุ์กุ้ง การพัฒนาของรังไข่ และเซลล์ไข่ให้ได้ผลดีโดยไม่ต้องตัดตา ซึ่งการตัดตาซึ่งใช้อยู่ในปัจจุบันนั้น นอกจากจะ ทำให้สามารถใช้แม่พันธุ์กุ้งได้เพียงไม่กี่ครั้ง ก็ทำให้ประสิทธิภาพของแม่พันธุ์ลงลง หรือหมดประสิทธิภาพลง และยังทำ ให้แม่พันธุ์กุ้งมีอายุสั้นลงจากการที่ตาถูกตัดด้วย นอกจากนั้นแล้ว การผลิตลูกกุ้งโดยการตัดตาอาจได้ชื่อว่าเป็นการ ทรมานสัตว์และเป็นการปฏิบัติที่ผิดจริยธรรมในการผลิตสัตว์ ซึ่งประเทศคู่ค้าโดยเฉพาะประเทศในกลุ่ม EC, USA และ ญี่ปุ่น อาจถือเป็นข้อห้ามหรือกีดกันที่ไม่ใช่กำแพงภาษีก็ได้ในอนาคตอันใกล้ ดังนั้น การใช้ฮอร์โมน NPF และ สารสื่อ ประสาทเพื่อกระตุ้นให้แม่พันธุ์กุ้งพัฒนารังไข่ เซลล์ไข่ และเจริญของตัวอ่อน ซึ่งน่าจะเป็นทางเลือกที่สำคัญทางหนึ่งที่ อาจจะนำไปปฏิบัติที่ทำให้การใช้แม่พันธุ์กุ้งได้มีประสิทธิภาพและใช้ได้ยาวนานนานขึ้นซึ่งจะไม่ได้รับการต่อต้านจาก ประเทศนำเข้ากุ้งจากประเทศไทยของเรา นอกจากนี้ยังคาดว่า อาจจะสามารถนำไปปรับเพื่อประยุกต์ใช้ในการกระตุ้น ประสิทธิภาพการสืบพันธุ์ของแม่กุ้งก้ามกรามเพื่อเพิ่มผลผลิตในระดับเกษตรกรรายย่อยและระดับการเพาะเลี้ยงในเชิง พาณิชย์ต่อไปได้ในอนาคต นอกจากนั้น งานวิจัยนี้สามารถสร้างองค์ความรู้พื้นฐานใหม่ที่สำคัญ สำหรับนักวิจัยที่ทำ วิจัยเกี่ยวข้องทางวิทยาศาสตร์การเกษตรและชีววิทยา วิทยาศาสตร์ชีวภาพ รวมถึงสาขาที่เกี่ยวข้องในวงกว้าง ตลอดจนนักเรียน นักศึกษา และประชาชนทั่วไปได้มีความรู้ ความเข้าใจ ความตระหนัก ถึงโครงสร้าง หน้าที่ ความสำคัญ ตลอดจนความสัมพันธ์ของฮอร์โมน ระบบประสาท ระบบเอ็นโดครายน์ และระบบสืบพันธุ์ โดยเฉพาะกุ้ง และสามารถนำองค์ความรู้พื้นฐานใหม่ที่สำคัญที่ได้ค้นพบนี้นำไปประยุกต์ใช้ต่อได้ในการกระตุ้นประสิทธิภาพการ สืบพันธุ์ของแม่พันธุ์กุ้งก้ามกราม สัตว์กลุ่มคลัสเตเชียนอื่นๆ และสัตว์ไม่มีกระดูกสันหลังกลุ่มอื่นๆต่อไปได้ รวมทั้ง ในทางปฏิบัติ องค์ความรู้พื้นฐานที่สำคัญดังกล่าวอาจนำไปสู่การประยุกต์ใช้ฮอร์โมนสำหรับกระตุ้นแม่พันธุ์กุ้งที่ถูก เลี้ยงในสภาพกักขังให้มีการพัฒนาของรังไข่และเซลล์ไข่โดยไม่ต้องตัดตา ตามที่กล่าวมาแล้วข้างต้น อย่างไรก็ตาม งานวิจัยถึงการใช้ฮอร์โมนประสาทต่อการควมคุมการพัฒนาของระบบสืบพันธุ์ของกุ้งก้ามกรามเพศเมีย ยังคง ้จำเป็นต้องมีการศึกษาเพิ่มเติมและใช้เวลาระยะหนึ่ง ประกอบกับงานวิจัยนี้ยังคงเป็นงานวิจัยเพื่อมุ่งสร้างองค์ความรู้ พื้นฐานใหม่ที่สำคัญที่เป็นพื้นฐานต่อการพัฒนาประเทศ และสำหรับการวิจัยต่อยอดในมิติต่างๆ ให้ครอบคลุมก่อน เพื่อ นำไปสู่การใช้ในทางปฏิบัติได้จริงในอนาคต

# Other outputs/conferences:

- นำเสนอผลงานแบบ Oral Presentation ที่งานประชุมวิชาการประจำปี " นักวิจัยรุ่นใหม่พบเมธีวิจัยอาวุโส สกว." ครั้งที่ 15 ระหว่างวันที่ 6-8 มกราคม 2559 ณ โรงแรมเดอะรีเจนท์ ชะอำบีชรีสอร์ท หัวหิน ชะอำ จ. เพชรบุรี
- 2. นำเสนอผลงานแบบ <u>Poster Presentation</u> ที่งานประชุมวิชาการประจำปี " นักวิจัยรุ่นใหม่พบเมธีวิจัย อาวุโส สกว." ครั้งที่ 16 ระหว่างวันที่ 11-13 มกราคม 2560 ณ โรงแรมเดอะรีเจนท์ ชะอำบีชรีสอร์ท หัวหิน ชะอำ จ.เพชรบุรี

# Awards:

1. ได้ รับ รางวัล "2015 TRF-OHEC-SCOPUS Young Researcher Awards in Life Sciences & Agricultural Sciences (นักวิจัยรุ่นใหม่ดีเด่น สกว.)" ณ งานประชุมวิชาการประจำปี "นักวิจัยรุ่นใหม่พบเมธี วิจัยอาวุโส สกว." ครั้งที่ 15 ระหว่างวันที่ 6-8 มกราคม 2559 ณ โรงแรมเดอะรีเจนท์ ชะอำบีชรีสอร์ท หัวหิน ชะอำ จ.เพชรบุรี

# **APPENDIX**

ELSEVIER

Contents lists available at ScienceDirect

# Aquaculture

journal homepage: www.elsevier.com/locate/aquaculture



# Neuropeptide F stimulates ovarian development and spawning in the female giant freshwater prawn, *Macrobrachium rosenbergii*, and its expression in the ovary during ovarian maturation cycle



Yotsawan Tinikul <sup>a,b,\*</sup>, Attakorn Engsusophon <sup>b</sup>, Thanapong Kruangkum <sup>b,c</sup>, Sirorat Thongrod <sup>b</sup>, Ruchanok Tinikul <sup>a</sup>, Prasert Sobhon <sup>b,d</sup>

- <sup>a</sup> Mahidol University, Nakhonsawan Campus, Phayuhakiri District, Nakhonsawan 60130, Thailand
- <sup>b</sup> Department of Anatomy, Faculty of Science, Mahidol University, Bangkok 10400, Thailand
- <sup>c</sup> Center of Excellence for Shrimp Molecular Biology and Biotechnology (CENTEX Shrimp), Faculty of Science, Mahidol University, 272 Rama VI Rd, Bangkok 10400, Thailand
- d Faculty of Allied Health Sciences, Burapha University, Long-Hard Bangsaen Rd, Mueang District, Chonburi 20131, Thailand

#### ARTICLE INFO

# Article history: Received 26 August 2016 Received in revised form 14 November 2016 Accepted 15 November 2016 Available online 18 November 2016

Keywords:
Neuropeptide F
Macrobrachium rosenbergii
Ovarian development
Spawning
Vitellogenin
Freshwater prawn
Aquaculture

#### ABSTRACT

Neuropeptide F (NPF) plays important roles in the regulation of a variety of physiological processes, including stimulation of food intake. At present, there is a current lack of basic knowledge regarding the effect of NPF in the control of female crustacean reproduction. In this study, we investigated expression of NPF in ovaries of female Macrobrachium rosenbergii (Mr) during ovarian development cycle, and its effects on ovarian maturation and spawning. MrNPF-immunoreactivity (-ir) was detected in the ovaries and its levels fluctuated during the ovarian maturation cycle: MrNPF-ir was more intense in the early- and mid-stages of ovarian development, and suddenly decreased in the mature stages. By RT-PCR, MrNPF transcript levels also increased during the early- and middle stages of ovarian development, and suddenly fell at late stage. The prawns were treated with varied doses of MrNPF and the effects were investigated by assessing the ovarian maturation period, oocyte diameter (OD), gonado-somatic index (GSI), and hemolymph vitellogenin (Vg) concentration. MrNPF-treated prawns showed significantly decreased ovarian maturation periods, and increased GSI, OD, and Vg levels compared with those of control groups. MrNPF also caused significantly earlier spawning compared with the control groups, while the mean fecundity between MrNPF-treated prawns and controls did not differ significantly. However, the numbers of eggs per spawn among experimental groups were higher compared with those of the controls. This work provides a novel and useful basic knowledge of NPF on female reproduction in crustaceans, and its possible use in aquaculture for accelerating and enhancing reproduction of the female prawns.

Statement of relevance: Alternative techniques to eyestalk ablation to stimulate ovarian maturation in captive prawn broodstock are needed in order to avoid cruel practice on cultured prawns. Attempts have been made in using neurohormones, including neuropeptides to prime female broodstocks to stimulate growth and reproduction to replace the eyestalk ablation. NPF is a neuropeptide known for its control of feeding; however, there is currently no report on the role of NPF in female *M. rosenbergii* reproduction. We are the first to report the effects of NPF on ovarian maturation and spawning, and its expression and fluctuation in ovaries during the ovarian cycle in the female decapod crustacean. Our findings are novel and the data obtained could be useful for accelerating and enhancing reproduction of the female freshwater prawns.

© 2016 Elsevier B.V. All rights reserved.

## 1. Introduction

The giant freshwater prawn, *Macrobrachium rosenbergii*, is an important food source worldwide. It is extensively distributed and is one of the most popular species being cultured in Asian countries, including Thailand, Vietnam, Malaysia, China and India (Sandifer and Smith,

E-mail addresses: anatch2002@gmail.com, yotsawan.tin@mahidol.ac.th (Y. Tinikul).

1985). It is favored by consumers primarily due to its large size, particularly males, and relative ease of culture (Suwansa-Ard et al., 2015). In decapod crustaceans, the physiological processes of molting and reproduction are under the regulation of various neurohormones (Fingerman, 1997). The X-organ-sinus gland complex (XO-SG) in the eyestalk is a major neuroendocrine organ which secretes various types of neurohormones, including neurotransmitters and neuropeptides, to regulate growth and reproduction (Nagaraju, 2011). Gonad-inhibiting hormone (GIH) from XO-SG plays a key role in inhibiting the ovarian maturation in unfavorable environment conditions. Female broodstocks

<sup>\*</sup> Correspondence author at: Mahidol University, Nakhonsawan Campus, Phayuhakiri District. Nakhonsawan Province 60130. Thailand.

often have their eyestalk ablated to initiate ovarian maturation and spawning, a practice that has its limitations and requires alternative techniques (Benzie, 1998; Nagaraju, 2011). Attempts have been made in using neurohormones, including neuropeptides to prime female broodstocks for stimulating growth and reproduction to replace the eyestalk ablation (Benzie, 1998; Vanden Broeck, 2001; Nässel and Wegener, 2011).

Neuropeptide F (NPF) is a homolog of neuropeptide Y (NPY) included within the same group of FMRFamide-like peptides (FLPs), and it has an important role in the regulation of feeding behavior in invertebrates to enhance growth and reproduction (Barb et al., 2006; Larhammar et al., 2009). In crustaceans, neuropeptide F has at least two isoforms having typically 36 amino acids in overall length, and possess the C-terminal motif-GRPRFamide (Christie et al., 2011; Nässel and Wegener, 2011; Suwansa-Ard et al., 2015). NPF/NPF-related peptides have also been found in a number of arthropod and mollusk species and it plays a role in controlling feeding and reproduction in insects and mollusks (Nässel and Wegener, 2011). In addition, NPF-ir was present in endocrine cells of the forgut and midgut in several insects, implying that NPF may play important roles in hunger-driven motivation, feeding, and aggressive behaviors (Gonzalez and Orchard, 2008). In the female desert locust, Schistocerca gregaria, NPF stimulates ovarian maturation and oocyte growth. This study suggests that in addition to feeding, NPF is involved in regulating ovarian maturation (Schoofs et al., 2001; Van Wielendaele et al., 2013). Furthermore, FMRFamide-like peptide plays a role in ovulation in Rhodnius. In Locust, NPF increased hemolymph Vg levels during the vitellogenic cycle, while the levels drops after oviposition (Sevala et al., 1992). In Lymnaea, NPF-ir neurons was present in the cerebral ganglia contacting the processes of the caudodorsal cells, implying that it regulates ovulation and egg-laying by controlling the release of ovulation hormone (CDCH) (de Jong-Brink et al., 2001).

There have been few reports on the characterization and immunolocaliation of NPF in crustacean species. In Marsupenaeus japonicus, NPF contains 32 amino acid, and has a C-terminal with SRPRFa, whereas NPF sequences of Daphnia magna and D. pulex contained 38 amino acids, ending at a C-terminal with ARRFa (Christie et al., 2008; Gard et al., 2009). In Litopenaeus vannamei and M. marginatus, NPFs were detected in neural tissues using RT-PCR, and it was suggested that NPF may play a role as autocrine or paracrine function in both shrimp species. In addition, when mixing NPF into packaged food, it stimulated feeding and increased larval weight, indicating that NPF significantly involves in regulation of feeding and food intake (Christie, et al., 2011). Furthermore, there are reports regarding the characterization and expression of short NPF (sNPF) in decapod crustaceans, include the crab, Carcinus maenas (Ma et al., 2009), lobster Homarus americanus, white shrimp L. vannamei (Ma et al., 2010), and tiger shrimp Penaeus monodon (Sithigorngul et al., 2002).

Up to now, there is no report on the role and regulation of NPF in female *M. rosenbergii* reproduction. Therefore, we examined whether NPF exists in the ovaries, and its dynamic alterations during ovarian maturation cycle, and subsequently we investigated the effects of NPF on ovarian maturation and early spawning. This study provides an important basic knowledge in determining the existence and effects of NPF on reproduction of the female *M. rosenbergii*, and may be useful in using this neuropeptide to improve female reproduction and fecundity of this important crustacean species.

### 2. Materials and methods

# 2.1. Experimental animals and acclimatization

Mature female freshwater prawns (weighing 30–45 g) were obtained from a local market (Phran Nok market, Bangkok, Thailand). The prawns were kept in indoor circular plastic tanks, each 1.50 m in diameter with water depth at 0.80 m, and about 30% of water changed every

2 days. The prawns were fed commercial food pellets (Charoen Pokphand Group, Thailand) twice per day. Aeration was given all day. Small plastic cages were added in every tank for molting animals to hide and to avoid being killed due to the cannibalistic behavior of this species. Male and female prawns were stocked at a ratio of 1:5, respectively, in the same tank. The prawns were acclimatized under a photoperiod of 12:12 h light-dark for a week before starting the experiments.

# 2.2. Histological examination and determination of ovarian stages

The maturation stages of ovaries during the ovarian cycle were examined directly, and classified based on the criteria described previously (Meeratana and Sobhon, 2007; Tinikul et al., 2008). Ovaries were fixed in Bouin's fixative and processed for paraffin embedding, as described previously (Tinikul et al., 2015), in order to evaluate the histology. The sections were cut at  $5-6~\mu m$  thicknesses from each ovary, after which they were deparaffinized and stained with hematoxylin and eosin (H&E). The sections were mounted with Permount (Bio-Optica, Milan, Italy), and viewed under a Nikon ECLIPSE E600 light microscope. Then images were photographed using a Nikon digital DXM1200 camera.

### 2.3. Peptides and antibodies

The MrNPF used in this study was MrNPF (KPDPTQLAAMADALKYLQE LDKYYSQVSRPRFamide) peptide identified and characterized from the eyestalks and CNS transcriptomes by our research group (Suwansa-Ard et al., 2015). This peptide was custom synthesized (GenScript, Piscataway, NJ, USA). In addition, a polyclonal antibody against MrNPF was produced and its specificity was also tested rigorously (Thongrod et al., in press). Briefly, female New Zealand white rabbits (8 week-old) were obtained from the Animal Care Unit, Faculty of Science, Mahidol University, and used for production of anti-MrNPF with the approval of Animal Ethics Committee, Faculty of Science, Mahidol University.

# 2.4. In vivo effects of MrNPF on ovarian maturation and spawning

The doses of MrNPF used in this work were based on the stimulatory effects of L. vannamei NPF (Christie et al., 2011; Tinikul et al., 2014, 2015), with some modifications. In this study, in order to investigate the effects of MrNPF on ovarian maturation and early spawning, we employed two doses,  $10^{-6}$  and  $10^{-5}$  mol/prawn of MrNPF. All injections were given at 4-day intervals. The injections were performed via an intramuscular site at the second abdominal segment using 1 ml syringes fitted with a 26 G  $\times$  1/2 (0.45  $\times$  12 mm) thin-wall needle. The measurement of total length and weight of the prawns were performed on every treatment day prior to injections. MrNPF synthetic peptide was dissolved in 0.9% normal saline. For ovarian maturation assay, the prawns were divided into 4 groups of about 45 animals each, and treated as follows: (1) the non-injected control group (C); (2) the sham control; (3 and 4) the groups injected with MrNPF at doses of  $10^{-6}$  and 10<sup>-5</sup> mol/prawn, respectively. For spawning assay, we divided prawns into four groups: (1) the non-injected control group (C); (2) the sham control; (3 and 4) the groups injected with MrNPF at doses of  $10^{-6}$ and  $10^{-5}$  mol/prawn. Prawns in each group were identified by tying plastic loops of different colors around one eyestalk. At least, five prawns in each group were randomly selected and sacrificed at 4-day intervals to examine a gonado-somatic index (GSI = [ovarian weight (g)/body weight (g)]  $\times$  100), and oocyte diameters (OD) were carefully measured as described previously (Tinikul et al., 2015). One hundred oocytes were randomly selected at each ovarian stage in each prawn in at least three separate ovarian regions, were examined under the light microscope. Diameters of the one hundred oocytes with full nuclear profiles were measured, and the data expressed as a mean  $\pm$  SD for each treatment group. The experiment was performed in duplicate. GSI and OD values of the MrNPF-injected groups and the control groups

**Table 1** Specific primers used for semi-quantitative RT-PCR.

Primer	Direction	Nucleotide sequence
MrNPF-F	Forward	5' CCAAGTGTGGGCGGCTATTT 3'
MrNPF-R	Reverse	5' TCACCAGGAGGAACGGCATA 3'
Actin-F	Forward	5' AAGTAGCCGCGTTGGTTGTA 3'
Actin-R	Reverse	5' CCAGAGTCGAGCACGATACC 3'

were then analyzed and compared by statistical analyses. The rest of the prawns were allowed to proceed until they spawned in order to determine the spawning duration. Pieces of ovary were subsequently fixed in Bouin's solution, paraffin-embedded, sectioned, stained with H&E, and examined under the light microscope, in order to determine the stages of ovarian maturation and oocyte diameters.

#### 2.5. Hemolymph vitellogenin (vg) levels after treatment with MrNPF

An anti-vitellin antibody was produced from female M. rosenbergii, and the tests of its specificity and cross reactivity were rigorously performed by Western blot analysis as reported earlier (Soonklang et al., 2012), and the protocol for quantification of hemolymph Vg levels in M. rosenbergii was based on the report of Tinikul et al., (2015) with some modifications. The hemolymph of MrNPF-injected groups and the control groups was collected from the hemolymph sinus at 4-day intervals. The hemolymph vitellogenin (Vg) levels was evaluated by an indirect ELISA technique. Briefly, a 100 µl of hemolymph was centrifuged, and the supernatants collected and stored at -20 °C until used. Microtiter plates were coated with 100 µl of hemolymph supernatant diluted in coating buffer for 2 h at 37 °C. Non-specific bindings were blocked with a blocking buffer containing 0.25% bovine serum albumin (BSA) in 0.01 M PBS, at 37 °C for 2 h. After washing three times, the plates were incubated in anti-vitellin diluted 1:2000 in a diluent containing 0.25% BSA in 0.01 M PBS. Aliquots of 100 µl of primary antibody were added to the wells and the plates incubated at 37 °C for 2 h, and then incubated with goat-anti rabbit-HRP (Southern Biotech, Birmingham, USA), diluted 1:4000, at 37 °C, for 1 h. Further, the plates were washed and the color was developed by adding TMB substrate for 15 min, and the reaction was stopped by adding 1 M HCl. The Vg concentrations were calculated from a standard curve established from measurements using purified vitellin. Determinations of hemolymph Vg levels were performed in duplicate. The OD's were read at 450 nm using an automatic spectrophotometer. A negative control sample was prepared in parallel using rabbit pre-immune serum in place of primary antibody.

### 2.6. Immunohistochemistry in various ovarian stages

The female prawns (n=5 each) of the four stages of the ovarian maturation cycle were anesthetized on ice for 15–20 min and the ovaries were dissected out and immediately fixed with 4% paraformaldehyde in 0.1 M PBS for MrNPFs for 12–16 h at 4 °C. The ovaries were cut at a 6  $\mu$ m thickness and mounted on coated slides. The sections were deparaffinized and rehydrated through a graded series of ethyl alcohol, and then processed for immunohistochemistry.

The method for immunohistochemical detections was based on that described previously (Tinikul et al., 2015, 2016) with some

modifications. For the immunolocalization of MrNPF, rehydrated ovarian sections were incubated with 1% glycine in PBS, and non-specific binding was blocked by the blocking solution containing 10% NGS in PBST. The sections were then incubated with rabbit anti-MrNPF diluted 1:100 in the blocking solution, and then incubated in secondary antibody, Alexa488-conjugated goat anti-rabbit IgG (Molecular Probes, Eugene, OR, USA), diluted 1:200. In addition, the nuclei in ovarian sections were counterstained with ToPro-3 (Molecular Probes) diluted 1:4000 in blocking solution. The sections were mounted in Vectashield (Vector Laboratory, Burlingame, CA, USA). They were then viewed and images captured using an Olympus FV1000 confocal laser scanning microscope. Negative controls were performed by replacing the primary antibody with the pre-immune rabbit serum, or pre-absorption of the primary antibody with excess of synthetic MrNPF.

#### 2.7. Expression of MrNPF gene in various ovarian stages by RT-PCR

Mature female prawns were anesthetized in ice for 10–15 min. The different stages of ovaries were carefully collected. The protocol for examination of expression of MrNPF gene was based on previous reports (Phoungpetchara et al., 2012; Kornthong et al., 2013). All tissues were immediately immersed in liquid nitrogen and store at -80 °C until used. Each sample was homogenized and the total RNA was isolated using Trizol® reagent (Invitrogen, CA, USA), following the manufacturer's protocol. The purity and quantity of total RNA were determined by spectrophotometer at 260 and 280 nm. The total RNA was treated by DNase I enzyme (Invitrogen, Carlsbad, CA, USA) to remove genomic DNA following the manufacturer's protocol. First stranded cDNA was synthesized by reverse transcription using SuperScript™ III Reverse Transcriptase (Invitrogen, CA, USA) with random hexamer primers. The cDNA was then amplified using Platinum® Taq Polymerase (Invitrogen, CA, USA) with MrNPF specific primers (Table 1). RT-PCR products were then separated by 1.5% agarose gel electrophoresis. Beta-actin gene was used as the normalization control and the expression levels of MrNPF were normalized against beta-actin.

#### 2.8. Statistical analyses

Data were presented as means  $\pm$  SEM. The data were then analyzed for statistical differences with a SPSS program, using one-way analysis of variance (ANOVA) and Duncan's multiple range test. A probability value <0.05 (P<0.05) indicated a significant difference.

# 3. Results

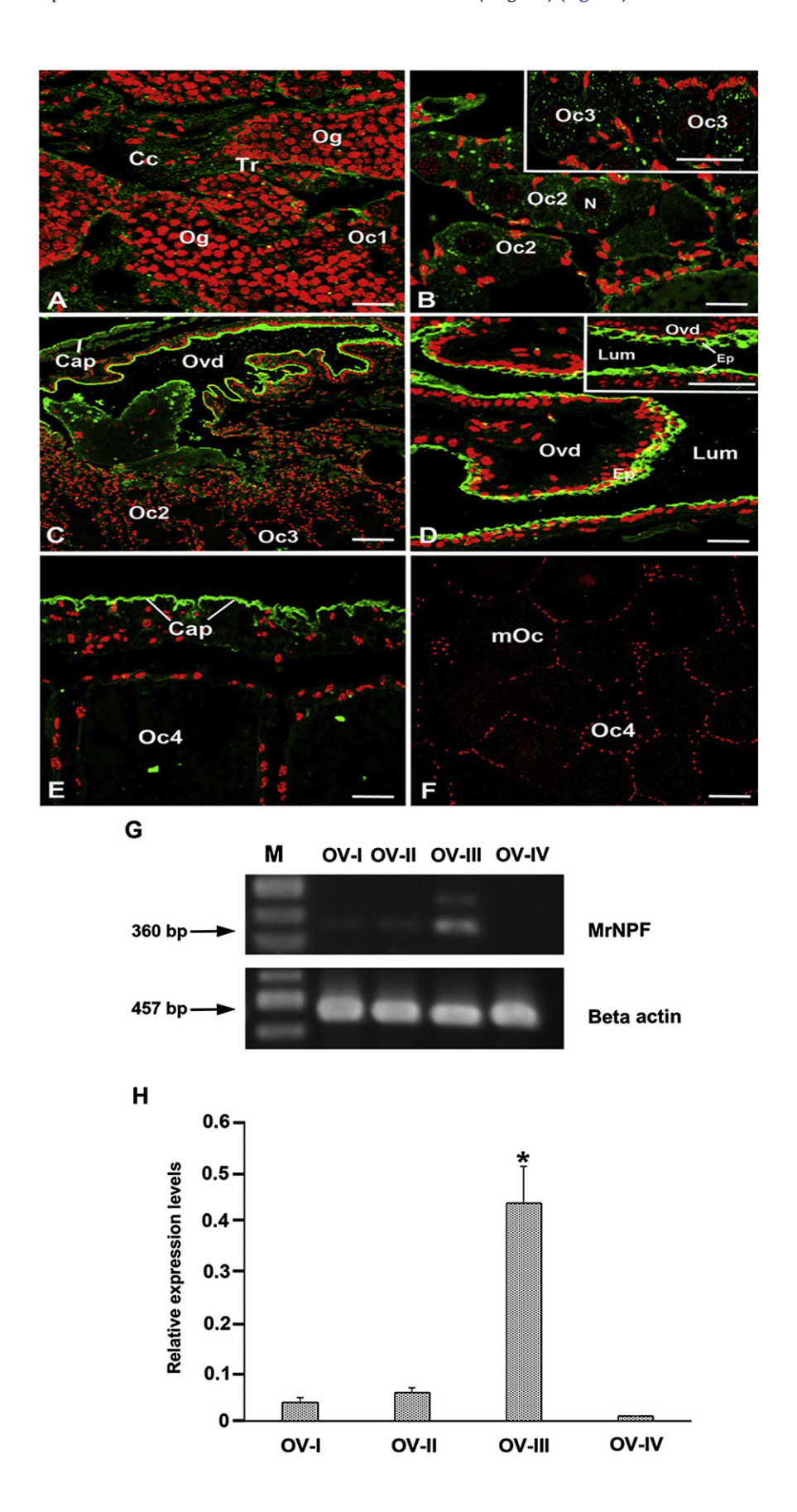
#### 3.1. The expression of MrNPF in various stages of ovaries

In the ovaries, the oogonia and early previtellogenic oocytes (Oc1) were not immunoreactive when detected with anti-MrNPF as a probe (Fig. 1A). Intense MrNPF-ir was observed in the cytoplasm of late previtellogenic and early vitellogenic oocytes (Oc2 and Oc3) (Fig. 1B), the epithelium and smooth muscle cells of the oviduct (Fig. 1C–D) and the capsule of ovaries (Fig. 1D–E). In contrast, MrNPF-ir appeared much weaker in late vitellogenic oocytes (Oc4 and mOc) (Fig. 1E). The control sections of oocytes and follicular cells showed no positive staining (Fig. 1F). Using RT-PCR, *MrNPF* transcript was detected in the total extract of various stages of ovaries (Fig. 1G–H). The detection of beta-

**Fig. 1.** Expression of MrNPF-immunoreactivities (-ir) and relative mRNA levels of *MrNPF* gene expression against beta-actin gene in the four ovarian stages of female *M. rosenbergii*. (A) Control section of the early oocytes (Oc1) showing no immunoreactivity. (B) MrNPF-ir appeared more intense in early to mid-oocyte steps (Oc2 and Oc3) in ovarian stages II and III. (C–D) Intense MrNPF-ir is also present in the Ep of oviduct, smooth muscle and the capsule (E). (F) No immunoreactivity was observed in the late oocytes (Oc4) in ovarian stage IV of the control section. (G) Upper row showed the expression of *MrNPF* gene, which was strongly detected by RT-PCR in the ovarian stage III containing mostly Oc2 and Oc3. Bottom row indicates beta-actin gene expression in corresponding tissues. (H) Histograms indicate relative expression of *MrNPF* normalized by beta-actin gene in different ovarian stage, with ovarian stage III showing highest levels, while ovarian stage IV having the lowest levels. Each bar is mean  $\pm$  SD of three replicates. Bars with superscript '\*' differ significantly from other stages of ovaries at *P* < 0.05. M = marker. Cap, capsule; Cc, central core of oocyte pouch; Ep, epithelium; Lum, lumen; mOc, mature oocyte; Ovd, oviduct; Tr, trabecular; Oc1, early previtellogenic oocyte; Oc2, late previtellogenic oocyte; Oc3, early vitellogenic oocyte; Oc4, late vitellogenic oocyte; OV-I, ovarian stage II; OV-II, ovarian stage II; OV-II, ovarian stage IV. Scale bars = 100 μm.

actin gene expression (used as a positive control and as for normalization of the *MrNPF* expression), was identified in all tissues with equal intensity in all samples. The expression of the mRNA of *MrNPF* was most

intense in the ovarian stage III (Fig. 1G, lane 3), and less intense in the early stages of ovaries (stages I and II), while almost absent in mature ovaries (stage IV) (Fig. 1H).



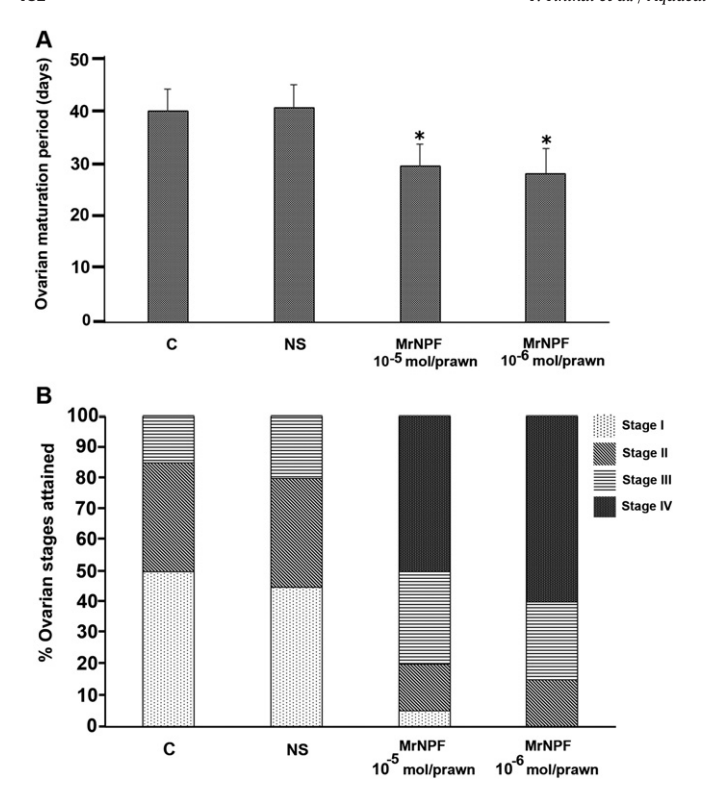
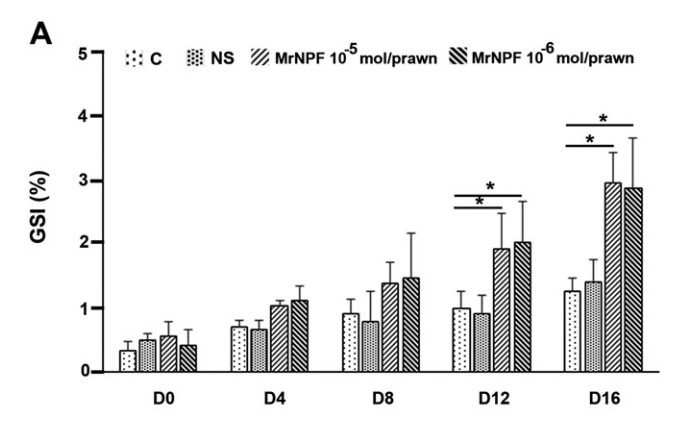


**Fig. 2.** Effects of MrNPF on the ovarian maturation period of female *M. rosenbergii.* (A) Histograms demonstrating that prawns treated with MrNPF at doses of  $10^{-5}$  and  $10^{-6}$  mol/prawn showed significant shortening ovarian maturation period, compared with the control group. (B) The example of percentages of ovarian stages that the female prawns attained at 16 days after the first injection. After injections with MrNPF at doses of  $10^{-5}$  and  $10^{-6}$  mol/prawn, the prawns ovaries showed significant progress of maturation to reach from stage III to stage IV, faster when compared with the control groups. Each measurement is expressed as a mean  $\pm$  S.E.M. Asterisks indicate significant differences (P < 0.05) with respect to the control groups. Stage I, ovarian stage I; Stage II, ovarian stage II; Stage IIV, ovarian stage IV.

#### 3.2. Effect of MrNPF on ovarian development

In this study, the ovarian maturation period of the prawns treated with MrNPF at both doses of  $10^{-6}$  or  $10^{-5}$  mol/prawn were 28.6  $\pm$ 4.28 and 29.76  $\pm$  5.7 days, respectively, which were significantly shorter (P < 0.05) than that of the controls (i.e., 39.2  $\pm$  4.66 days) (Fig.2A). Moreover, the percentage of prawns that attained various ovarian stages at 16 days after the first MrNPF injections showed that in non-injected and sham control groups, most female prawns developed to ovarian stage II (30% and 35%, respectively) and stage III (15% and 20%, respectively), whereas the rest remained at stage I (Fig. 2B). By contrast, 30% of prawns injected with a dose of  $10^{-5}$  mol/prawn, and 25% of prawns injected with a dose of 10<sup>-6</sup> mol/prawn, showed the ovaries at stage III. In addition, the prawns injected with doses of  $10^{-5}$  and  $10^{-6}$  mol/prawn exhibited 50% and 60% ovarian stage IV (Fig. 2B). These data indicated that MrNPF at doses of  $10^{-6}$  or  $10^{-5}$ mol/prawn shortened ovarian maturation period by nearly 10-12 days or about 30%, particularly at the lower dose of  $10^{-6}$  mol/prawn.

At days 1 and 4 after treatment, the GSI values of the controls and MrNPF-injected groups at both doses were all low and not significantly different (P < 0.05) (Fig. 3A). At day 8 post-injection, the GSI values of both groups of MrNPF-injected prawns trended to have slightly higher GSI values, but still with no significant difference from the control groups (P > 0.05). On days 12 and 16, both groups of injected prawns exhibited significantly higher GSI values compared with the control group (P < 0.05) (Fig. 3A). During the experiments, female prawns also exhibited the increase of weight (30.14  $\pm$  4.62 g), but were not statistically significant compared with the control (30.53  $\pm$  3.39 g). In addition, mean oocyte diameters (OD) of vitellogenic oocytes (Oc3) and



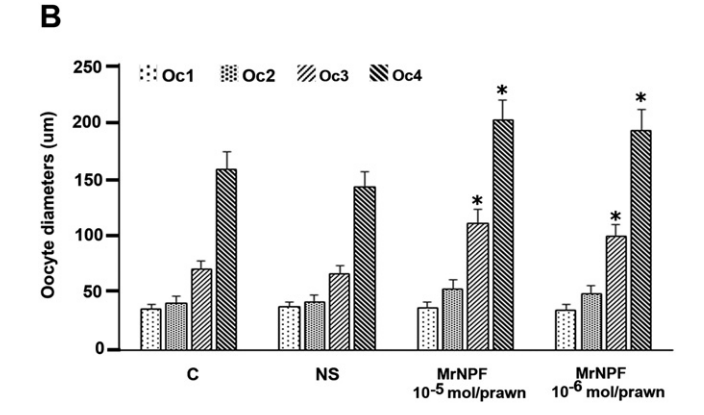


**Fig. 3.** Effects of MrNPF on gonado-somatic index and oocyte diameter values of female M. rosenbergii. (A) Mean gonado-somatic index (GSI) values after the MrNPF injections, evaluated at 0, 4, 8, 12 and 16 days. The MrNPF-injected groups (with  $10^{-5}$  and  $10^{-6}$  mol/prawn), showed significant increases of GSI by days 12 and 16, compared with the control groups. (B) Histograms showing the oocyte diameters after injections with MrNPF compared with the control groups. Asterisks indicate significant differences, compared with the control group (P < 0.05).

mature oocytes (Oc4) in both groups of treated prawns increased significantly when compared with the control groups (P < 0.05) (Fig. 3B). MrNPF-injected prawns, whose ovaries were determined to be at stage IV by external observations, underwent spawning on the following night. All prawns tolerated the injected doses of MrNPF without showing any abnormal behavior.

## 3.3. Assessment of ovarian histology

Examination of ovarian histology of the MrNPF-injected and control groups was conducted to ascertain the degree of the ovarian maturation. On days 1 and 4, there were no difference in the ovarian histology in the control groups (Fig. 4A), and the MrNPF-treated groups as the ovaries contained mostly early previtellogenic oocytes (Oc1) and few late previtellogenic oocytes (Oc2) (Fig. 4B). Distinct differences were observed at day 12 and 16 when the ovaries of the control group contained mostly previtellogenic oocytes (Oc2) (Fig. 4C), while the ovaries of the MrNPF-treated groups with doses of  $10^{-5}$  or  $10^{-6}$  mol/prawn contained mostly early vitellogenic oocytes (Oc3) and late vitellogenic oocytes (Oc4) with numerous lipid droplets. In addition, the diameters of oocytes in the MrNPF-injected groups were larger than those of the control groups (Fig. 4D).

## 3.4. Hemolymph vg concentrations after treatment with MrNPF

Vg concentrations in the non-injected control group, gradually increased from day 0 to about days 36–40 which were from 26.33  $\pm$  4.77 to 266.7  $\pm$  14.38 µg/ml, respectively (Fig. 4E). The Vg concentrations

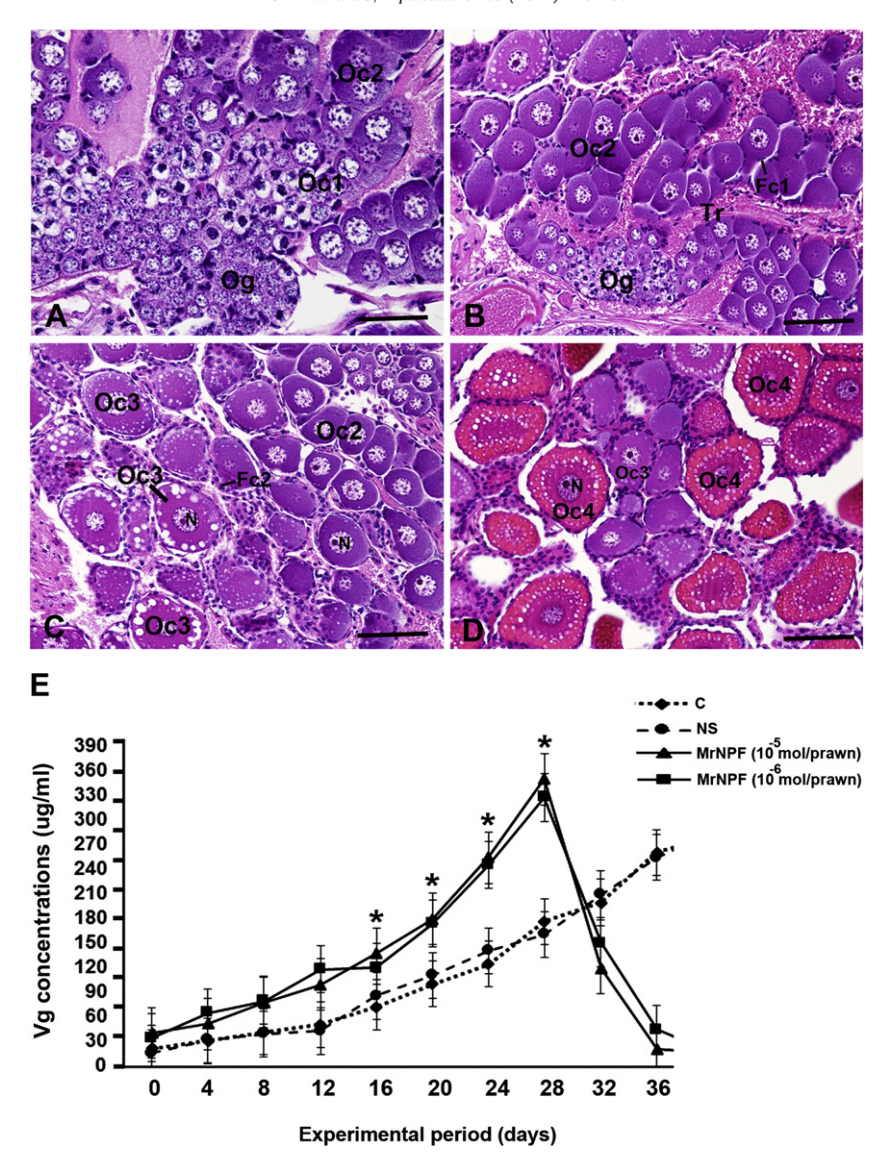


**Fig. 4.** Effects of MrNPF on ovarian histology and hemolymph Vg concentrations of female M. rosenbergii. A, B) The examples of ovaries of the control group at day 4 (A), and of MrNPF-injected group at a dose of  $10^{-6}$  mol/prawn (B), showing there is no histological difference in both groups. C–D) Ovaries of MrNPF-injected groups at  $10^{-6}$  mol/prawn contained mostly the late stage oocytes (Oc4) at day 16 (D), while they were only early stage oocytes (Oc1, Oc2) in the control groups (C). (E) A graph showing hemolymph Vg concentrations during the experimental period following treatments with both doses of MrNPF and control groups. The concentrations are expressed as  $\mu$ g/ml. Each measurement is expressed as mean  $\pm$  S.E.M. Asterisks indicate significant differences (P < 0.05), comparing the experimental groups and the control groups. Fc1 and Fc2, follicular cell types 1 and 2; Og, oogonia; Oc1, early previtellogenic oocyte; Oc2, late previtellogenic oocyte; Oc3, early vitellogenic oocyte; Oc4, late vitellogenic oocyte; moc, mature oocyte; n, nucleus; Tr, trabeculae. Scale bars  $= 100 \, \mu$ m.

in the MrNPF-treated prawns with  $10^{-5}$  and  $10^{-6}$  mol/prawn showed significant increases from ovarian stage I ( $19.8\pm4.1$  and  $23.75\pm4.83~\mu\text{g/ml}$ ) to peak at stage IV ( $348.5\pm13.1$  and  $327.2\pm14.9~\mu\text{g/ml}$ ), respectively, compared with the control group ( $266.7\pm14.38~\mu\text{g/ml}$ ) (P<0.05). The Vg concentrations after injection with  $10^{-5}$  or  $10^{-6}$  mol/prawn of MrNPF were approximately 1.3 and 1.2 times higher than that of the control group at ovarian stage IV (P<0.05) (Fig. 4E).

# 3.5. Effects of MrNPF on spawning

The durations of spawning, the quality of spawned eggs and the percentage of fertilized eggs from MrNPF-treated groups and control groups were also investigated (Figs. 5, 6). Interestingly, the durations of spawning of MrNPF-injected groups at doses of  $10^{-5}$  or  $10^{-6}$  mol/prawn were much shorter ( $1.01 \pm 0.32$  and  $1.25 \pm 0.58$  days, respectively), than the control group ( $2.79 \pm 0.74$  days) (P < 0.05) (Fig. 5A). Our data strongly indicated that both doses of MrNPF could shorten the duration of early spawning by nearly three times.

The number of eggs per spawn from both groups of MrNPF-treated groups were about  $12\times 10^4$  and  $14\times 10^4$  eggs per prawn, respectively, and these values were not significantly different from the both control groups  $(12\times 10^4$  and  $16\times 10^4$  eggs per prawn, respectively) (P>0.05) (Fig. 5B). The percentages of fertilized eggs were about 97.5% and 98.7% for prawns treated with  $10^{-5}$  and  $10^{-6}$  mol/prawn of MrNPF (Fig. 6A), which were not statistically different from the controls (98.4% and 99.1%, respectively). The sizes of eggs from female prawns that received both doses of MrNPF were not statistically different, compared with those of the control groups (P>0.05). In addition, the percentages of spawners was about 95% in the non-injected group and 100% for the sham group, compared with 100% for prawns receiving both doses of MrNPF (Fig. 6B).

# 4. Discussion

In the present study, we are the first to provide evidence for the stimulatory role of NPF in the female *M. rosenbergii* reproduction. We

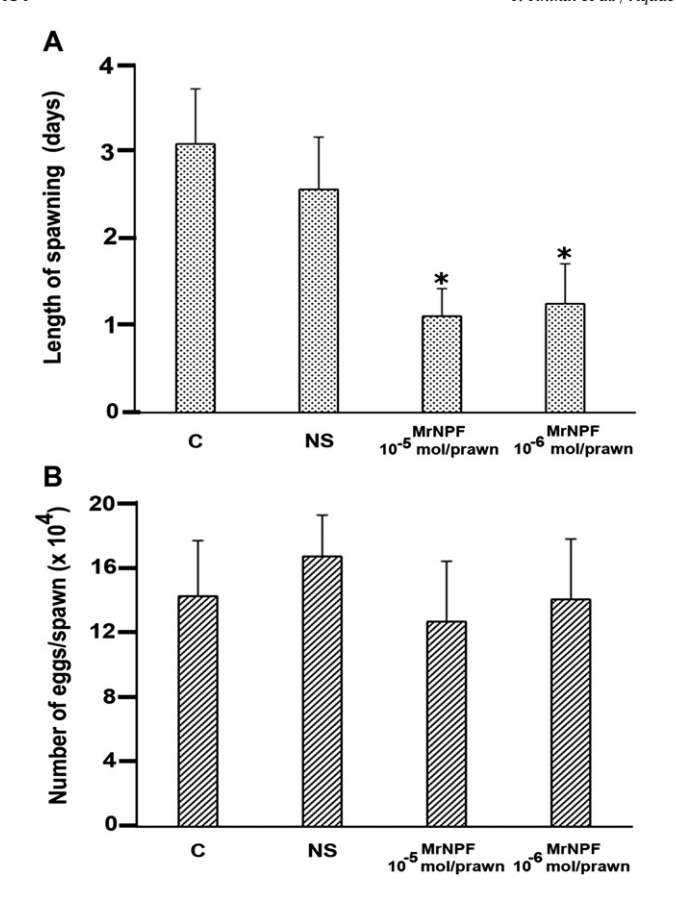


**Fig. 5.** Effects of MrNPF on the spawning period and the numbers of eggs per spawn of female M. rosenbergii. (A) Histograms demonstrating that prawns injected with MrNPF at doses of  $10^{-5}$  and  $10^{-6}$  mol/prawn showed significantly shorter spawning time, compared with the control group. (B) Numbers of eggs per spawned after injection with doses of MrNPF at doses of  $10^{-5}$  and  $10^{-6}$  mol/prawn compared with the controls. The data are presented as mean  $\pm$  S.E.M. Asterisks indicate significant differences (P < 0.05).

found that MrNPF significantly shortened the ovarian maturation period and exhibited increases of GSI, OD and hemolymph Vg levels at a shorter time compared with the controls. MrNPF also shortened the spawning duration by about two days compared with that of the control group. Moreover, strong MrNPF-ir and high level of *MrNPF* gene expression were detected in the mid-stage oocytes and ovarian stage III. These results strongly suggest that MrNPF is capable of stimulating ovarian development and early spawning in this crustacean species.

The roles of NPF in controlling feeding and growth in insects and other invertebrates are well known (Schoofs et al., 2001; Nässel and Wegener, 2011; Van Wielendaele et al., 2013). There have been a few reports regarding the role of NPF in regulating the reproduction in several invertebrate species, including insects, mollusks and crustaceans. In the female desert locust, Schistocerca gregaria, injection of NPF increased ovarian-somatic index and stimulated the increase of oocyte diameters (Schoofs et al., 2001; Van Wielendaele et al., 2013). It was shown that the ovaries of NPF-treated females reached vitellogenic stages, while only previtellogenic ovaries were observed in the control groups. NPF also induced higher ovarian and hymolymph ecdysteroid levels, suggesting that NPF may exert its effect through the ovary maturing parsin (OMP) which regulates vitellogenesis indirectly through its ecdysiotropic effect on the ovary (Girardie et al., 1998; Schoofs et al., 2001; Van Wielendaele et al., 2013). It is important to note that the follicle cell of ovary is the major production site for ecdysteroid, which is further incorporated in the growing oocytes (Tawfik et al., 1999; Buszczak et al., 1999; Brown et al., 2009; Parthasarathy et al., 2010). Injecting NPF peptide into *L. migratoria*, stimulated ovarian maturation,

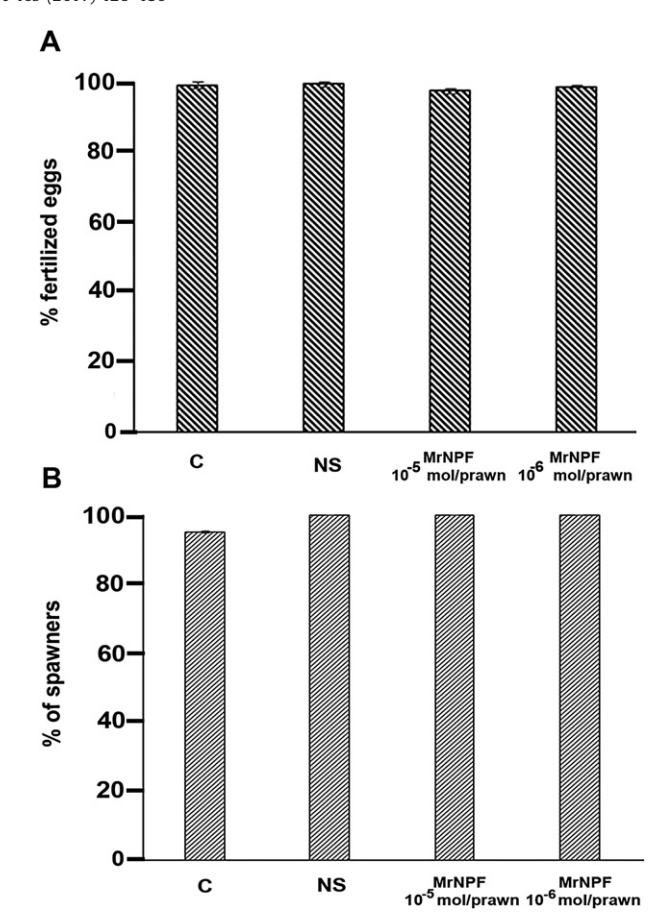


**Fig. 6.** Effects of MrNPF on the percentage of fertilized eggs and percentage of spawners of female *M. rosenbergii*. (A) Percentage of fertilized eggs of all experimental groups after injection with doses of MrNPF at doses of  $10^{-5}$  and  $10^{-6}$  mol/prawn compared with the control groups. (B) Percentage of spawners of MrNPF-injected groups at doses of  $10^{-5}$  and  $10^{-6}$  mol/prawn, compared with the control groups. The data are presented as mean  $\pm$  S.E.M.

implying that NPF may also be involved in controlling oocyte proliferation during ovarian development (Cerstiaens et al., 1999). In addition, injecting NPF into 6-day-old females Leptinotarsa decemlineata, could stimulate oocyte maturation, suggesting a role of NPF in promoting ovarian development (Cerstiaens et al., 1999). NPF also regulates food intake and feeding behaviors in a few crustacean species (Wu et al., 2003; Christie et al., 2011). In L. vannamei, NPF is mixed into packaged food, it stimulated feeding and weight gain of larvae, indicating that NPF can pass through the gastrointestinal tract without being degraded (Christie et al., 2011). In addition, it was suggested that NPF may increase the acquisition of nutrients and energy in order to promote metabolic processes that enabling the gaining of weight, and this may eventually stimulate and increase oocyte size by promoting ovarian maturation (Schoofs et al., 2001; Van Wielendaele et al., 2013). Our present study demonstrates for the first time that injecting MrNPF into female M. rosenbergii induced ovarian maturation and significantly increased GSI and OD. It is also possible that MrNPF could be an important signaling neuropeptide that regulates ovarian development of this crustacean species, as reported earlier in the female S. gregaria. NPF may serve indirect role in regulating ovarian maturation and oocyte growth in M. rosenbergii by acting through ecdysteroid pathways to control ovarian development, as proposed earlier (Schoofs et al., 2001; Van Wielendaele et al., 2013). However, further experiments are necessary to ascertain whether NPF mediates its actions through the ecdysteroid cascade.

Our work showed that MrNPF stimulated early spawning compared with the control groups, thereby suggesting NPF may be required for

final egg maturation as well as assisting in the release of eggs from the oviduct in this crustacean species. There have been studies reporting possible role for NPF or NPF-related factors in ovulation and spawning in mollusks. In Aplysia spp., NPF and egg-laying hormone (ELH) were co-localized in bag cells, suggesting that NPF may be co-released with an ELH to initiate the egg-laying, and both peptides may also control egg laying-associated behaviors (Rajpara et al., 1992; de Jong-Brink et al., 2001). In Lymnaea stagnalis, NPF-ir was detected and co-localized with APGWamide in the cerebral ganglia neurons which contact the caudo-dorsal cells, and as such the NPF may control an ovulation (De Lange et al., 1997). In the present study, MrNPF induced early spawning and shorten spawning duration by three times, compared with the control groups. Immunohistochemical data showed that the MrNPF-ir was intense in the epithelium and smooth muscle cells in the oviduct, suggesting that MrNPF stimulates ovulation by controlling the contractile ovarian capsule to squeeze oocytes into the oviduct and broodchamber during spawning (Rajpara et al., 1992; De Lange et al., 1997).

Several studies have reported the presence and distribution of NPF or NPF-related peptides in the ovaries and other reproductive organs of many invertebrates. In the flatworms, NPF-ir was present in gonadal tissues, suggesting this neuropeptide may serve as a reproductive function (Walker et al., 2009). In the red fire ant, Solenopsis invicta, the NPF receptor transcript was detected in the ovaries and fat body of the mated gueens using RT-PCR, and NPF receptor-ir was also present at periphery of early-, mid-oocyte steps and oocyte membrane, whereas this receptor was not detected in late oocytes. This suggests that NPF may regulate oocyte development processes by promoting early- to mid-oocyte growth during ovarian maturation (Chen and Pietrantonio, 2006; Lu and Pietrantonio, 2011). In female Drosophila, sNPF receptor transcripts were detected in the ovaries, indicating that this neuropeptide may be involved in oocyte growth and ovarian development (Mertens et al., 2002). In the present work, we demonstrated that in female M. rosenbergii, the levels of MrNPF in the ovaries fluctuate during ovarian cycle: MrNPF-ir was most intense in the mid-oocytes (Oc2 and Oc3), while very low intensity was detected in the late oocytes (Oc4). This suggests that NPF may be synthesized and produced locally in Oc2 and Oc3, and thereby stimulating the early to mid-steps of oocyte maturation via an autocrine and/or paracrine pathway, and eventually initiate early spawning. We further confirmed the mRNA transcriptional levels by using RT-PCR which showed that MrNPF levels rose with early to mid stages of ovarian cycle, and suddenly fell in the late ovarian stage. In addition, we found that the levels of MrNPF are about 9, 6 and 15 times higher in the ovaries at stage III than in the ovaries at stages I, II and IV, respectively. Our findings indicate that the changing patterns of NPF levels in the ovaries of M. rosenbergii are similar to those reported in Drosophila (Mertens et al., 2002), and the fire ant (Chen and Pietrantonio, 2006).

Hemolymph Vg level is an important indicator for ovarian maturation in several decapod crustaceans and in other invertebrates (Okumura, 2004). In adult female desert locusts, NPF stimulates vitellogenesis and oocyte growth, as well as increases ecdysteroid levels in the hemolymph and ovaries (Schoofs et al., 2001; Van Wielendaele et al., 2013). In L. migratoria, Lom-OMP induces oocyte differentiation and stimulates the increased level of circulating vitellogenin (Girardie et al., 1998). In S. gregaria, Scg-NPF increases vitellogenin concentration in the hemolymph (Schoofs et al., 2001). In the present study, we found that injection of MrNPF increased hemolymph Vg levels in female M. rosenbergii as the Vg concentrations of the groups treated with MrNPF were higher at various ovarian stages, especially stages II and III, compared with those of the control groups. These results indicated causal relationships between NPF and ovarian maturation as reflected by the increase of Vg synthesis. However, whether the stimulating effect of the NPFs on vitellogenesis is mediated through ecdysteroids remains to be examined.

Taken together, we provided for the first time and reported a novel, clear and important basic knowledge that NPF is involved in ovarian

maturation and spawning in female *M. rosenbergii*. Further research will be needed to study the possible mechanisms of NPF action and to find way to apply this important knowledge for practical application in aquaculture of this female crustacean species.

#### Acknowledgements

This research was financially supported by the Thailand Research Fund and Mahidol University (TRF Research Career Development Grant, Grant No. RSA5780011) to Yotsawan Tinikul. This work was also supported by a grant from the Office of the Higher Education Commission (OHEC), and Mahidol University through the National Research Universities Initiatives to Prasert Sobhon. We are grateful to Dr. Jaruwan Poljaroen for suggestions and comments, and to Dr. Saowaros Suwansa-Ard for kindly providing MrNPF primers. We thank the Center of Nanoimaging (CNI), Faculty of Science, Mahidol University, for the use of a confocal microscope and technical assistance. This study is dedicated to the memory of Prof. Dr. Peter J. Hanna, Deakin University, Geelong, Australia.

#### References

- Barb, C.R., Kraeling, R.R., Rampacek, G.B., Hausman, G.J., 2006. The role of neuropeptide Y and interaction with leptin in regulating feed intake and luteinizing hormone and growth hormone secretion in the pig. Reproduction 131, 1127–1135.
- Benzie, J.A.H., 1998. Penaeid genetics and biotechnology. Aquaculture 164, 23-47.
- Brown, M.R., Sieglaff, D.H., Rees, H.H., 2009. Gonadal ecdysteroidogenesis in arthropoda: occurrence and regulation. Annu. Rev. Entomol. 54, 105–125.
- Buszczak, M., Freeman, M.R., Carlson, J.R., Bender, M., Cooley, L., Segraves, W.A., 1999. Ecdysone response genes govern egg chamber development during midoogenesis in *Drosophila*. Development 126 (20), 4581–4589.
- Cerstiaens, A., Benfekih, L., Zouiten, H., Verhaert, P., De, L.A., Schoofs, L., 1999. Led-NPF-1 stimulates ovarian development in locusts. Peptides 20, 39–44.
- Chen, M.-E., Pietrantonio, P.V., 2006. The short neuropeptide F-like receptor from the red imported fire ant, *Solenopsis invicta* Buren (Hymenoptera: Formicidae). Arch. Insect Biochem. Physiol. 61, 195–208.
- Christie, A.E., Cashman, C.R., Brennan, H.R., Ma, M., Sousa, G.L., Li, L., Stemmler, E.A., Dickinson, P.S., 2008. Identification of putative crustacean neuropeptides using in silico analyses of publicly accessible expressed sequence tags. Gen. Comp. Endocrinol. 156, 246–264.
- Christie, A.E., Chapline, M.C., Jackson, J.M., Dowda, J.K., Hartline, N., Malecha, S.R., Lenz, P.H., 2011. Identification, tissue distribution and orexigenic activity of neuropeptide F (NPF) in penaeid shrimp. J. Exp. Biol. 214, 1386–1396.
- de Jong-Brink, M., ter Maat, A., Tensen, C.P., 2001. NPY in invertebrates: molecular answers to altered functions during evolution. Peptides 22, 309–315.
- De Lange, R.P., van Golen, F.A., van Minnen, J., 1997. Diversity in cell specific coexpression of four neuropeptide genes involved in control of male copulation behaviour in *Lymnaea stagnalis*. Neuroscience 78, 289–299.
- Fingerman, M., 1997. Roles of neurotransmitters in regulating the reproductive hormone release and gonadal maturation in decapod crustaceans. Invertebr. Reprod. Dev. 31, 47–54
- Gard, A.L., Lenz, P.H., Shaw, J.R., Christie, A.E., 2009. Identification of putative peptide paracrines/hormones in the water flea *Daphnia pulex* (Crustacea; Branchiopoda; Cladocera) using transcriptomics and immunohistochemistry. Gen. Comp. Endocrinol. 160, 271–287
- Girardie, J., Huet, J.C., Atay-Kadiri, Z., Ettaouil, S., Delbecque, J.P., Fournier, B., Pernollet, J.C., Girardie, A., 1998. Isolation, sequence determination, physical and physiological characterization of the neuroparsins and ovary maturing parsins of Schistocerca gregaria. Insect Biochem Molec 28 (9), 641–650.
- Gonzalez, R., Orchard, I., 2008. Characterization of neuropeptide F-like immunoreactivity in the blood-feeding hemipteran, *Rhodnius prolixus*. Peptides 29, 545–558.
- Kornthong, N., Chotwiwatthanakun, C., Chansela, P., Tinikul, Y., Cummins, S.F., Hanna, P.J., Sobhon, P., 2013. Characterization of red pigment concentrating hormone (RPCH) in the female mud crab (*Scylla olivacea*) and the effect of 5-HT on its expression. Gen. Comp. Endocrinol. 185, 28–36.
- Larhammar, D., Sundström, G., Dreborg, S., Daza, D.O., Larsson, T.A., 2009. Major genomic events and their consequences for vertebrate evolution and endocrinology. Ann. N. Y. Acad. Sci. 1163, 201–208.
- Lu, H.-L., Pietrantonio, P.V., 2011. Immunolocalization of the short neuropeptide F receptor in queen brains and ovaries of the red imported fire ant (Solenopsis invicta Buren). BMC Neurosci. 12, 57.
- Ma, M.M., Bors, E.K., Dickinson, E.S., Kwiatkowski, M.A., Sousa, G.L., Henry, R.P., Smith, C.M., Towle, D.W., Christie, A.E., Li, L., 2009. Characterization of the *Carcinus maenas* neuropeptidome by mass spectrometry and functional genomics. Gen. Comp. Endocrinol. 161, 320–334.
- Ma, M.M., Gard, A.L., Xiang, F., Wang, J., Davoodian, N., Lenz, P.H., Malecha, S.R., Christie, A.E., Li, L., 2010. Combining in silico transcriptome mining and biological mass spectrometry for neuropeptide discovery in the Pacific white shrimp *Litopenaeus* vannamei. Peptides 31, 27–43.

- Meeratana, P., Sobhon, P., 2007. Classification of differentiating oocytes during ovarian cycle in the giant freshwater prawn, *Macrobrachium rosenbergii* de man. Aquaculture 270, 249–258.
- Mertens, I., Meeusen, T., Huybrechts, R., De Loof, A., Schoofs, L., 2002. Characterization of the short neuropeptide F receptor from *Drosophila melanogaster*. Biochem. Biophys. Res. Commun. 297, 1140–1148.
- Nagaraju, G.P., 2011. Reproductive regulators in decapod crustaceans: an overview. J. Exp. Biol. 214. 3–16.
- Nässel, D.R., Wegener, C., 2011. A comparative review of short and long neuropeptide F signaling in invertebrates: any similarities to vertebrate neuropeptide Y signaling? Pentides 32, 1335–1355.
- Okumura, T., 2004. Perspectives on hormonal manipulation of shrimp reproduction review. JARQ 38, 49–54.
- Parthasarathy, R., Sheng, Z., Sun, Z., Palli, S.R., 2010. Ecdysteroid regulation of ovarian growth and oocyte maturation in the red flour beetle, *Tribolium castaneum*. Insect Biochem Moley 40, 429–439
- Phoungpetchara, I., Tinikul, Y., Poljaroen, J., Changklungmoa, N., Siangcham, T., Sroyraya, M., Chotwiwatthanakun, C., Vanichviriyakit, R., Hanna, P.J., Sobhon, P., 2012. Expression of the male reproduction-related gene (Mar-Mrr) in the spermatic duct of the giant freshwater prawn, *Macrobrachium rosenbergii*. Cell Tissue Res. 348, 609–623.
- Rajpara, S.M., Garcia, P.D., Roberts, R., Eliassen, J.C., Owens, D.F., Maltby, D., Myers, R.M., Mayeri, E., 1992. Identification and molecular cloning of a neuropeptide Y homolog that produces prolonged inhibition in *Aplysia* neurons. Neuron 9, 505–513.
- Sandifer, P.A., Smith, T.J., 1985. Freshwater Prawn: Crustacean and Mollusk Aquaculture in the United States. AVI Publishing Company, Inc., West port, USA, pp. 1–15.
- Schoofs, L., Clynen, E., Cerstiaens, A., Baggerman, G., Wei, Z., Vercammen, T., Nachman, R., De Loof, A., Tanaka, S., 2001. Newly discovered functions for some myotropic neuropeptides in locusts. Peptides 22, 219–227.
- Sevala, V.L., Sevala, V.M., Davey, K.G., Loughton, B.G., 1992. A FMRFamide-like peptide is associated with the myotropic ovulation hormone in *Rhodnius prolixus*. Arch. Insect Biochem. Physiol. 20, 193–203.
- Sithigorngul, P., Pupuem, J., Krungkasem, C., Longyant, S., Panchan, N., Chaivisuthangkura, P., Sithigorngul, W., Petsom, A., 2002. Four novel PYFs: membersof NPY/PP peptide superfamily from the eyestalk of the giant tiger prawn *Penaeus monodon*. Peptides 23, 1895–1906.
- Soonklang, N., Wanichanon, C., Stewart, M.J., Stewart, P., Meeratana, P., Hanna, P.J., Sobhon, P., 2012. Ultrastructure of differentiating oocytes and vitellogenesis in the giant freshwater prawn, *Macrobrachium rosenbergii* (De Man). Microsc. Res. Tech. 75. 1402–1415.

- Suwansa-Ard, S., Thongbuakaew, T., Wang, T., Zhao, M., Elizur, A., Hanna, P.J., Sretarugsa, P., Cummins, S.F., Sobhon, P., 2015. In silico neuropeptidome of female *Macrobrachium rosenbergii* based on transcriptome and peptide mining of eyestalk, central nervous system and ovary. PLoS One 10. e0123848.
- Tawfik, A.I., Vedrova, A., Sehnal, F., 1999. Ecdysteroids during ovarian development and embryogenesis in solitary and gregarious Schistocerca gregaria. Arch. Insect Biochem. Physiol. 41 (3), 134–143.
- Thongrod, S., Changklungmoa, N., Chansela, P., Siangcham, T., Kruangkum, T., Suwansa-ard, S., Saetan, J., Sroyraya, M., Tinikul, Y., Wanichanon, C., Sobhon, P., 2016. Characterization and tissue distribution of neuropeptide F in the eyestalk and brain of the male giant freshwater prawns, *Macrobrachium rosenbergii*. Cell Tissue Res. (in press).
- Tinikul, Y., Mercier, A.J., Soonklang, N., Sobhon, P., 2008. Changes in the levels of serotonin and dopamine in the central nervous system and ovary, and their possible roles in the ovarian development in the giant freshwater prawn, *Macrobrachium rosenbergii*. Gen. Comp. Endocrinol. 158. 250–258.
- Tinikul, Y., Poljaroen, J., Tinikul, R., Anuracpreeda, P., Chotwiwatthanakun, C., Senin, N., Poomtong, T., Hanna, P.J., Sobhon, P., 2014. Effects of gonadotropin-releasing hormones and dopamine on ovarian maturation and their presence in the ovary during ovarian development of the Pacific white shrimp, *Litopenaeus vannamei*. Aquaculture 420-421, 79-88.
- Tinikul, Y., Poljaroen, J., Tinikul, R., Chotwiwatthanakun, C., Anuracpreeda, P., Hanna, P.J., Sobhon, P., 2015. Alterations in the levels and distribution of octopamine in the central nervous system and ovary of the Pacific white shrimp, *Litopenaeus vannamei*, and its possible role in ovarian development. Gen. Comp. Endocrinol. 210, 12–22.
- Tinikul, Y., Poljaroen, J., Tinikul, R., Sobhon, P., 2016. Changes in the levels, expression, and their possible roles of serotonin and dopamine during embryonic development in the giant freshwater prawn, *Macrobrachium rosenbergii*. Gen. Comp. Endocrinol. 225, 71–80.
- Van Wielendaele, P., Wynant, N., Dillen, S., Badisco, L., Marchal, E., Vanden Broeck, J., 2013. In vivo effect of Neuropeptide F on ecdysteroidogenesis in adult female desert locusts (*Schistocerca gregaria*). J. Insect Physiol. 59, 624–630.
- Vanden Broeck, J., 2001. Neuropeptides and their precursors in the fruit fly, *Drosophila melanogaster*. Peptides 22, 241–254.
- Walker, R.J., Papaioannou, S., Holden-Dye, L., 2009. A review of FMRFamide- and RFamide-like peptides in metazoa. Invertebr. Neurosci. 9, 111–153.
- Wu, Q., Wen, T., Lee, G., Park, J.H., Cai, H.N., Shen, P., 2003. Developmental control of foraging and social behavior by the *Drosophila* neuropeptide Y-like system. Neuron 39, 147–161.

## REGULAR ARTICLE



# Characterization and tissue distribution of neuropeptide F in the eyestalk and brain of the male giant freshwater prawn, *Macrobrachium rosenbergii*

Sirorat Thongrod 1 · Narin Changklungmoa 2 · Piyachat Chansela 3 · Tanapan Siangcham 2 · Thanapong Kruangkum 1,4 · Saowaros Suwansa-Ard 1,5 · Jirawat Saetan 6 · Morakot Sroyraya 1,7 · Yotsawan Tinikul 1,7 · Chaitip Wanichanon 1 · Prasert Sobhon 1,2

Received: 30 May 2016 / Accepted: 16 November 2016 / Published online: 12 December 2016 © Springer-Verlag Berlin Heidelberg 2016

Abstract We previously analyzed the central nervous system (CNS) transcriptome and found three isotypes of long neuropeptide F (MrNPF-I, –II, –III) and four isoforms of short NPF (sMrNPF) in the giant freshwater prawn, *Macrobrachium rosenbergii*. We now validate the complete sequences of the MrNPF-I and –II precursor proteins, which show high similarity (91–95 %) to NPFs of the penaeus shrimp (PsNPF). MrNPF-I and -II precursors share 71 % amino acid identity, whereas the mature 32-amino-acid MrNPF-I and 69-amino-acid MrNPF-II are identical, except for a 37-amino-acid insert within the middle part of the latter. Both mature MrNPFs are almost identical to PsNPF-I and –II except for four amino acids at the mid-region of the peptides. Reverse transcription plus the polymerase chain reaction revealed that transripts of

MrNPF-I and -II were expressed in various parts of CNS including the eyestalk, brain and thoracic and abdominal ganglia, with the highest expression occurring in the brain and thoracic ganglia and with MrNPF-I showing five- to sevenfold higher expression than MrNPF-II. These peptides were also expressed in the midgut hindgut, and hepatopancreas, with MrNPF-I expression in the former two organs being at the same level as that in the brain and thoracic ganglia and about 4-fold higher than NPF-II. The expression of NPFs was also detected in the testes and spermatic duct but appeared much weaker in the latter. Other tissues that also expressed a considerable amount of NPF-I included the hematopoeitic tissue, heart and muscle. By immunohistochemistry, we detected MrNPFs in neurons of clusters 2, 3 and 4 and neuropils ME, MT and SG of the optic ganglia, neurons in cluster 6 and neuropils AMPN, PMPN, PT, PB and CB of the medial protocerebrum, neurons in clusters 9 and 11 and neurophils ON and OGTN of the deutocerebrum and neurons in clusters 14, 15 and 16 and neuropils TN and AnN of the tritocerebrum. Because of their high degree of conservation and strong and wide-spread expression in tissues other than CNS, we believe that, in addition to being a neuromodulator in controlling feeding, MrNPFs also play critical roles in tissue homeostasis. This should be further explored.

- Prasert Sobhon prasert.sob@mahidol.ac.th
- Department of Anatomy, Faculty of Science, Mahidol University, 272 Rama VI Road, Ratchathewi, Bangkok 10400, Thailand
- Faculty of Allied Health Sciences, Burapha University, Long-Hard Bangsaen Road, Mueang District, Chonburi 20131, Thailand
- Department of Anatomy, Phramongkutklao College of Medicine, 315 Rajvithi Road, Bangkok 10400, Thailand
- Center of Excellence for Shrimp Molecular Biology and Biotechnology (CENTEX Shrimp), Faculty of Science, Mahidol University, 272 Rama VI Road, Bangkok 10400, Thailand
- Faculty of Science, Health, Education and Engineering, University of the Sunshine Coast, Maroochydore, Queensland QLD 4558, Australia
- Department of Anatomy, Faculty of Science, Prince of Songkla University, Hat Yai, Songkhla 90112, Thailand
- Mahidol University, Nakhonsawan Campus, Phayuhakiri District, Nakhonsawan 60130, Thailand

**Keywords** Neuropeptide F · Male prawn · Eyestalk · Characterization · Tissue distribution

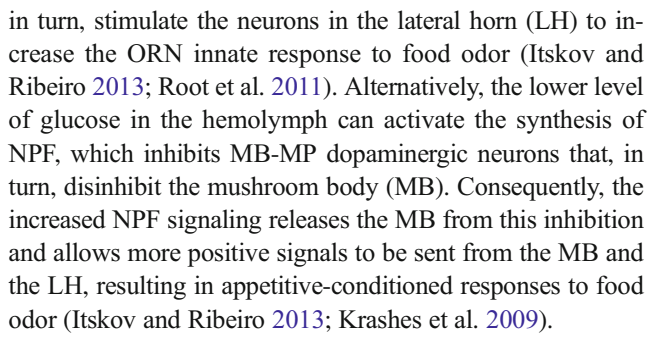
## Introduction

In vertebrates, several studies have shown that the circulating peptides released from the gut, pancreas and adipose cells



control energy homeostasis via hypothalamic neuronal networks employing several neuropeptides. Many peptides from the gut and pancreas, such as peptide YY (PYY), oxyntomodulin (OXM), cholecystokinin (CCK), pancreatic polypeptide (PP) and glucagon-like peptide 1 (GLP-1), exert negative effects on food intake and energy balance by influencing the central circuits in the hypothalamus and brainstem (Chaudhri et al. 2006; Field et al. 2010). Moreover, the signals from adipose tissue including leptin, insulin, and adiponectin also have negative effects on food intake (Stanley et al. 2005). Only ghrelin from the gut, through its stimulation of neuropeptide Y (NPY) neurons, sends a positive signal regarding food intake and energy balance (Sobrino Crespo et al. 2014). Within the arcuate nucleus (ARC) of the hypothalamus, two major groups of neurons control energy homeostasis: the neurons that co-express NPY and agouti-related protein (AgRP) and the proopiomelanocortin (POMC) neurons. The NPY and AgRP neurons stimulate appetite and food intake, whereas POMC neurons inhibit them (Cansell et al. 2012; Loh et al. 2015). The ARC-NPY neurons integrate peripheral signals including ghrelin, PYY, insulin and leptin. Leptin and insulin inhibit NPY/AgRP neurons but stimulate POMC neurons leading to the inhibition of food intake. In contrast, ghrelin stimulates NPY/AgRP neurons to increase the food intake (Stanley et al. 2005). Furthermore, NPY directly inhibits POMC neurons via its Y receptors (Acuna-Goycolea et al. 2005) and it also activates dopaminergic neurons in the paraventricular nucleus (PVN), which concurrently inhibits POMC neurons.

In invertebrates, neuropeptide F (NPF) is a homolog of NPY and is a subgroup of the FMRFamide peptides. NPF is known to play a crucial role in the regulation of foraging, feeding-related behaviors, circadian rhythm, stress responses and aggression (Karl and Herzog 2007; Nassel and Wegener 2011). In Arthropods, represented by the most studied Drosophila, we find two types of NPFs, the so-called long NPFs, which consist of two isoforms, NPF-I and -II, arising from a gene duplication and a short NPF (sNPF) comprising four isoforms arising from a duplication within a single gene (Carlsson et al. 2013; Lee et al. 2004; Nassel and Wegener 2011). Both NPFs and sNPF can activate feeding and associated behaviors (Broeck 2001; Krashes et al. 2009; Nassel and Wegener 2011; Wu et al. 2003, 2005). Furthermore, both types of NPFs have been localized in the brain, subesophageal ganglion and ventral nerve cord of larval and adult stages (Carlsson et al. 2013). To motivate feeding, starved insects employ NPF signaling in response to food odor via two pathways. First, the signaling of decreased insulin-like peptide (ILP) and its receptor (InR) in the olfactory receptor neurons (ORNs) stimulates the synthesis and insertion of sNPFR1 into the membrane of these neurons. Then, sNPF binds to sNPFR1 to facilitate the presynaptic transmission and stimulation of projection neurons (PNs) in the antennal lobe; these neurons,



In crustaceans, NPFs were first identified in the penaeid shrimp, Litopenaeus vannamei (Christie et al. 2008,) and in Daphnia pulex (Gard et al. 2009) by transcriptomic analyses. Later, the full sequences of the two isoforms, NPF-I and NPF-II, were cloned by reverse transcription plus the polymerase chain reaction (RT-PCR) for L. vannamei and Mericertus marginatus and determined to be identical in both species. Moreover, the shorter isoform, NPF-I, was demonstrated to be able to stimulate food intake and growth in juveniles of L. vannamei (Christie et al. 2011). Recently, our transcriptomic analysis revealed three isoforms of NPFs and four isoforms of sNPF in the central nervous system (CNS) of M. rosenbergii (MrNPF-I, NPF-II, NPF-III and four short MrNPF [sMrNPF], respectively; Suwansa-Ard et al. 2015). Moreover, a precursor of the sNPF transcript has also been identified from the eyestalk and CNS transcriptomes; this sNPF precursor is predicted to be cleaved at multiple sites to give rise to four active short peptides. At present, the distribution and physiological roles of these peptides remain uninvestigated. In this report, we validate the sequences of the MrNPF-I and II peptides and investigate their tissue distributions by RT-PCR and immunohistochemistry.

### Materials and methods

# **Experimental animals**

Mature blue claw male giant freshwater prawns, M. rosenbergii, with a body weight of  $100 \pm 5.0$  g, were purchased from Phrannok market, Bangkok, Thailand. They were maintained in rectangular plastic tanks at Department of Anatomy, Faculty of Science, Mahidol University. The prawns were kept under a photoperiod of 12:12 h light–dark with continuous aeration and fed with commercial pellets (Sunshine, Bangkok, Thailand) once a day for 1 week before being killed.

### RNA preparation and molecular cloning of MrNPFs

Brains were collected from the male prawns (n = 6), immediately frozen in liquid nitrogen and then stored at -80 °C until used. Total RNA was extracted by using TriPure isolation



reagent (Roche, Ind., USA) following the manufacturer's protocol. The RNA concentration was measured in a spectrophotometer (NanoDrop2000, Thermo Fisher Scientific, Del., USA). Total RNA (1 µg) was used for cDNA synthesis by RevertAid Reverse Transcriptase (Fermentas, Lithuania) and all steps were performed following the manufacturer's protocol. Specific primers used for PCR amplification of NPF cDNA were designed based on the conserved parts of NPFs from S. gregaria and L. vannamai (forward primer: 5' CACCCGTCGCCAGTCCGCTTT 3'; reverse primer: OligodT). PCR was performed following a routine protocol under optimized conditions by using the previously described cDNA and the specific primers. The PCR products were separated by gel electrophoresis, purified with a QIAquick gel extraction kit (Qiagen, Germany) and used for further sequencing. To increase the amount of purified PCR product, a purified PCR fragment was ligated into a plasmid vector (pGEM-T Easy Vector, Promega, Calif., USA). A recombinant plasmid containing the gene insert was transformed into competent bacterial cells (DH5-α) that were then cultured overnight followed by plasmid extraction with the GeneJET Plasmid Miniprep kit (Fermentas, Lithuania). The purified plasmid with the gene insert was subsequently analyzed for nucleotide sequences by Macrogen, Korea.

#### Analysis of tissue distribution by RT-PCR

Total RNAs were extracted from various tissues of the male prawns (n = 6) by using TriPure isolation reagent (Roche). Total RNAs of the eyestalk, brain, thoracic ganglion, abdominal ganglion, hepatopancreas, midgut, hindgut, testis, proximal spermatic duct, middle spermatic duct, hematopoietic tissue, heart and muscle were used for cDNA synthesis. The synthesized cDNAs were used as templates for RT-PCR with specific primers able to amplify both MrNPF-I and MrNPF-II (forward primer: 5' CACCCGTCGCCAGTCCGCTTT 3'; reverse primer: 5' TCTGTGAAGTCGCTACGACGC 3'). RT-PCR was performed under optimized conditions following a routine protocol. The negative control was performed by omitting the cDNA and the  $\beta$ -actin (forward primer: 5' AAGTAGCCGCGTTGGTTGTA 3'; reverse primer: 5' CCAGAGTCGAGCACGATACC 3') gene was used as an internal control and for the normalization of MrNPF gene expression. The experiment was carried out in triplicate. The intensity of the PCR bands was measured by using ImageJ software (Kornthong et al. 2014).

# Preparation of rabbit polyclonal antibody against MrNPF-I

The *M. rosenbergii* (Mr) NPF-I (KPDPTQLAAMA DALKYLQELDKYYSQVSRPRFamide) peptide (Suwansa-Ard et al. 2015), *L. vannamai* (Lv) NPF-I (KPDPSQLAN

MAEALKYLQELDKYYSQVSRPRFamide) peptide (Christie et al. 2011), FMRFamide, KISS1 and KISS2 were synthesized by Genscript (Piscataway, N.J., USA). The antibody against MrNPF-I was produced and tested for its specificity and cross -reactivities against the above-mentioned peptides. Briefly, the synthetic MrNPF-I peptide was cross-linked by being mixed with 1-ethyl-3-dimethylaminopropyl carbodiimide (Sigma-Aldrich, USA). Two female white New Zealand rabbits were immunized subcutaneously with 250 µg cross-linked peptide mixed with an equal volume of Freund's complete adjuvant. Blood was collected before the first immunization and was used as preimmune serum. Four additional injections of the peptide were performed with Freund's incomplete adjuvant at 14-day intervals and the blood was collected every 10 days after the first injection, centrifuged at 6,000 rpm for 20 min at 4 °C and kept at -20 °C until the antibody titers were estimated by indirect enzyme-linked immunosorbent assay. The antibody titer was found to be highest at 30 days after the first injection, even at a dilution of 1:1,000 and thus, the serum collected at this time was used for the immunohistochemical detection of NPFs.

#### Specificity of anti-MrNPF-I for MrNPF-I and LvNPF-I

The specificity and cross -reactivity of anti-MrNPF-I for MrNPF-I LvNPF-I, and MrNPFs in CNS extract were rigorously tested by dot blot analysis. Both synthetic NPFs and crude extract of prawn CNS, at concentrations of 0.1, 0.5, 1.0 and 2.0 µg/ml, were dotted onto 0.45-µm nitrocellulose membranes (Amersham Pharmacia Biotech, Buckinghamshire, UK), which were then dried for 45 min at room temperature and kept overnight at -20 °C for further testing by dot blot analysis. In addition, a test of crossreactivities of anti-MrNPF-I and anti-FMRFamide (Palasoon et al. 2011) for MrNPF-I, FMRFamide, KISS1 and KISS2 was performed by using 1 µg of each synthetic peptide dotted onto 0.45-µm nitrocellulose membranes, which were then dried for 45 min at room temperature and kept at -20 °C overnight. The membranes were subsequently washed three times with phosphate-buffered saline (PBS), pH 7.4, for 5 min each, incubated in PBST1 blocking solution (PBS plus 0.2 % Tween-20 containing 5 % skimmed milk), for 2 h at room temperature and then incubated in the primary antisera, i.e., anti-MrNPF-I or anti-FMRFamide diluted at 1:1000 in the blocking solution overnight at 4 °C. They were then washed three times with PBS for 5 min each and incubated in horseradish peroxidase (HRP)-conjugated goat anti-rabbit IgG (SouthernBiotech, USA), diluted 1:15,000 in the blocking solution, for 1 h at room temperature and washed again with PBS. Immunoreactivity signals were revealed by using a chemiluminescence detection kit (Thermo Fisher Scientific, Ill., USA) and the membranes were exposed to X-ray films (Amersham Pharmacia Biotech, Buckinghamshire, UK).



Positive dots on the exposed films were observed and analyzed. Negative controls were performed by substituting primary antisera with pre-immune rabbit serum or pre-absorbed antisera.

# Immunoperoxidase detection of MrNPFs in eyestalk and brain sections

The method for immunoperoxidase detection used in the present study was based on that described previously (Tinikul et al. 2015). Eyestalks and brains were collected and fixed with Davidson's fixative (Saetan et al. 2013) for 24 h at room temperature. The fixed tissues were dehydrated in a series of ethanol (70 %, 80 %, 90 %, 95 % and 100 % for 1 h each). The tissues were immersed in xylene, infiltrated with paraffin and embedded in paraffin blocks. The embedded tissues were cut at a thickness of 5 µm on a rotary microtome (Leica RM2235, Germany) and the sections were mounted on slides coated with 3-aminopropyl triethoxy-silane solution (Sigma, St. Louis, Mo., USA) at 37 °C overnight. Rehydrated sections were immersed in 10 mM citrate buffer, pH 6.0 and then endogenous peroxidase and free aldehyde groups were blocked by immersing the sections in 3 % H<sub>2</sub>O<sub>2</sub> in methanol and in 1 % glycine in 0.1 M PBS. Subsequently, the sections were incubated in a blocking solution of 5 % normal goat serum (NGS) in PBST1 to block nonspecific binding. The sections were subsequently incubated with anti-MrNPF-I diluted at 1:1000 at 4 °C overnight, followed by the secondary antibody, namely HRP-conjugated goat anti-rabbit IgG (SouthernBiotech, Birmingham, USA), at a 1:2000 dilution for 2 h. Immunoreactivity was detected by immersing the sections in NovaRed substrate (Vector Laboratory, Burlingame, Calif., USA) until a red color was observed. Finally, the sections were counterstained with Meyer's hematoxylin for nuclear staining, mounted in 90 % glycerol in PBS, observed under a Nikon E600 light microscope and photographed by a Nikon DXM 12000E digital camera (Japan).

# Immunofluorescence detection of MrNPFs in whole-mount of brain

Immunofluorescence was performed in whole brains taken from male prawns and fixed with 4 % paraformaldehyde according to the method described previously (Antonsen and Paul 2001; Tinikul et al. 2015, 2016). Briefly, brains were washed with PBS and then the surrounding fibrous tissue was carefully desheathed under a stereomicroscope. The brains were incubated in 0.4 % Triton X-100 in PBST2 (0.25 % Tween-20 in PBS, containing 0.1 % sodium azide) at 4 °C for 2 days. Subsequently, they were washed three times with 0.1 % Triton X-100 in PBST2 at 4 °C for 15 min and permeabilized in Dent's solution (20 % dimethylsufoxide in

methanol) at -20 °C for 6 h. The brains were washed twice with PBS and incubated in anti-MrNPF-I at a dilution of 1:500 in a blocking solution containing 10 % NGS in PBST2 at 4 °C for 1 week. After thorough washes with cold PBST2 and PBS for several hours, the specimens were immersed in the secondary antibody, namely Alexa-488-conjugated goat antirabbit IgG (Molecular Probe, Eugene, Ore., USA) at a dilution of 1:500 followed by nuclear staining with TO-PRO-3 (Invitrogen, Eugene, Ore., USA) at a dilution of 1:2000 in the blocking solution at 4 °C for 4 days. The specimens were washed twice for 1 h each in PBST2, followed by two washes for 30 min each in PBS. The whole brains were dehydrated by being immersed in increasing concentrations of ethanol (50 %, 70 %, 80 %, 90 %, 95 % and twice in 100 % for 30 min each) on ice. Finally, the clear brains were infused with methyl salicylate overnight. They were then examined and photographed under an Olympus FV 1000 laser-scanning confocal microscope.

## **Results**

# Molecular cloning, sequencing and characterization of cDNA encoding MrNPFs

We were able to clone cDNA of the two isoforms of MrNPFs in M. rosenbergii, namely MrNPF-I and -II (GenBank accession numbers KX219729 and KX219730, respectively). The full-length transcript of MrNPF-I is 867 base-pair (bp) in length and comprises a 45-bp 5' untranslated region (UTR), a 273-bp open reading frame (ORF) encoding the MrNPF-I precursor and a 549-bp 3' UTR. Its 3'UTR contains two polyadenylation signal sequences (at positions 801 and 810) located upstream of a 19-bp poly (A)<sup>+</sup> tail (Fig. 1). The encoded MrNPF-I precursor has 90 amino acid residues and includes a 29-amino-acid signal peptide and a 61-amino-acid MrNPF-I immature peptide that contains a dibasic cleavage site  $(K_{63}R)$ , which is probably cleaved to release a 33-aminoacid MrNPF-I and a 26-amino-acid MrNPF-I precursor-related peptide. The 33-amino-acid MrNPF-I immature peptide is post-translationally modified by amidation at the C-terminal glycine residue ( $G_{62}$ ) and gives rise to a 32-amino-acid active MrNPF-I (KPDPTQLAAMADALKYLQELDKYYSQVS RPRFamide).

*MrNPF-II* is a partial cDNA missing a part of its 3' UTR. The sequence is 471 bp in length and comprises a 45-bp 5' UTR, a 384-bp ORF encoding the MrNPF-II precursor and a 42-bp 3' UTR (Fig. 2). The translated MrNPF-II precursor consists of 127 amino acid residues, which are divided into a 29-amino-acid signal peptide and a 98-amino-acid immature MrNPF-II. Like MrNPF-I, immature MrNPF-II contains a dibasic cleavage site ( $K_{100}R$ ) and a glycine residue ( $G_{99}$ ) responsible for C-terminal amidation; it is cleaved and modified



Α Ι L VG VV  $\nabla$ V S VМ ggagttgagggcaaacccgacccaacgcagctggcggccatggctgatgccctcaagtac K P D P T Q  $\mathbf{L}$ Α Α M A D A Y ctqcaqqaqctcqacaaatattactcccaqqtqtcacqacccaqattcqqaaaacqcaqc D K Y Y S R Q V S P F gagtatgccqttcctcctggtgatgttctgatggaagccagcgagagactcatggagact Р G Р D  $\bigvee$  $\mathbf{L}$ М Ε A S Ε R  $\mathbf{L}$ M Ε Τ ttggcacgcaggaggtgaattcccatacatcaccactactctgtgaagtcgctacgacgc R R ctccqcaaattttcatccaatcaqctaccqccaaaqatqqcttaqaqccaatcatcc gagetgeceaettatettetteagecaatetgegtetttgtttaeattttaeatttttt tctctctctgtctcactttcctaaaatggcacaaatatcgatgtatgaaatgacgtggtg acqcaccaqctqqtaqqaqqtttcacatttaaaaaaatataqatqatatttaqacctataq tatacaagacagacagatccagcccttcgtaccagctagggcgtcatctatgaagtcaa aattcaqaatttttctcctttcqcqattcttcaqccttcatataatttcccccccactca ctaaaactttqtaqtqtcctaataatqaaaataaaaatqcacqttqtqtattaaatqtqq

Fig. 1 Nucleotide and amino acid sequences of *Macrobrachium rosenbergii* neuropeptide F (NPF)-I. The encoded amino acid sequence is shown as *single letters* underneath the nucleotide sequence. *Bold letters* 

tacaqcacaaaaaaaaaaaaaaaaaaaaaa

indicate the NPF-I mature peptide consisting of 32 amino acids. The *underlined* sequence indicates the RPRF conserved site of NPF. The *hyphen* indicates the stop codon

to release a 69-amino-acid MrNPF-II active peptide (KPDPTQLAAMADALKYLQELDKYYSQVSRPSPRLAP GPASQIQALEKTLKFLQLQELGKLYSLRARPRFamide) and a MrNPF-II precursor-related peptide.

The alignment of MrNPF precursors with other crustacean NPF precursors shows a high degree of conservation of amino acid sequences throughout the length of the precursor proteins. The similarity of MrNPF-I and -II precursors to

others ranges from 91 % to 95 %, whereas MrNPF-I and -II precursors share 71 % amino acid identity. MrNPF-I and -II active peptides share identical amino acids except for a 37-amino-acid insert within the middle part of MrNPF-II (Fig. 3). Overall, the MrNPF-I precursor shows 91 % and 93 % similarities to NPF-I of *M. marginatus* and *L. vannamei*, respectively, whereas the MrNPF-II precursor shares 94 % and 95 % similarities to the NPF-II precursors of

Fig. 2 Nucleotide and amino acid sequences of *M. rosenbergii* NPF-II. The encoded amino acid sequence is shown as *single letters* underlying the nucleotide sequence. *Bold letters* indicate the NPF-II mature peptide, which consists of 69 amino acids. The *underlined* sequence indicates the RPRF conserved site of NPF. The *hyphen* indicates the stop codon

Y ggccaagtgtgggcggctattttggtgggcgtggtcgtcgtcagcgtcatgcagatgggc VWAAIL V G V V V V S V M qqaqttqaqqqcaaacccqacccaacqcaqctqqcqqccatqqctqatqcctcaaqtac G V E G K P D P TQLAAMADAL ctgcaggagctcgacaaatattactcccaggtgtcacgacccagcccccgttcggcgcca Q E L D K Y Y S Q V S R P S P R S ggcccggcctcgcagattcaggctttggaaaagactttaaagttcctacaactacaagag G P A S Q I Q A L E K T L K F L Q L Q E ctcqqcaaattqtactcacttaqqqctcqqccqcqattcqqaaaacqcaqcqaqtatqcc K L Y S L R A R P R F G K R gttcctcctggtgatgttctgatggaagccagcgagagactcatggagactttggcacgc V L M E A S E R L M E  $aggaggtgaattcccatacatcaccactac {\color{blue}tctgtgaagtcgctacgacgc}$ R



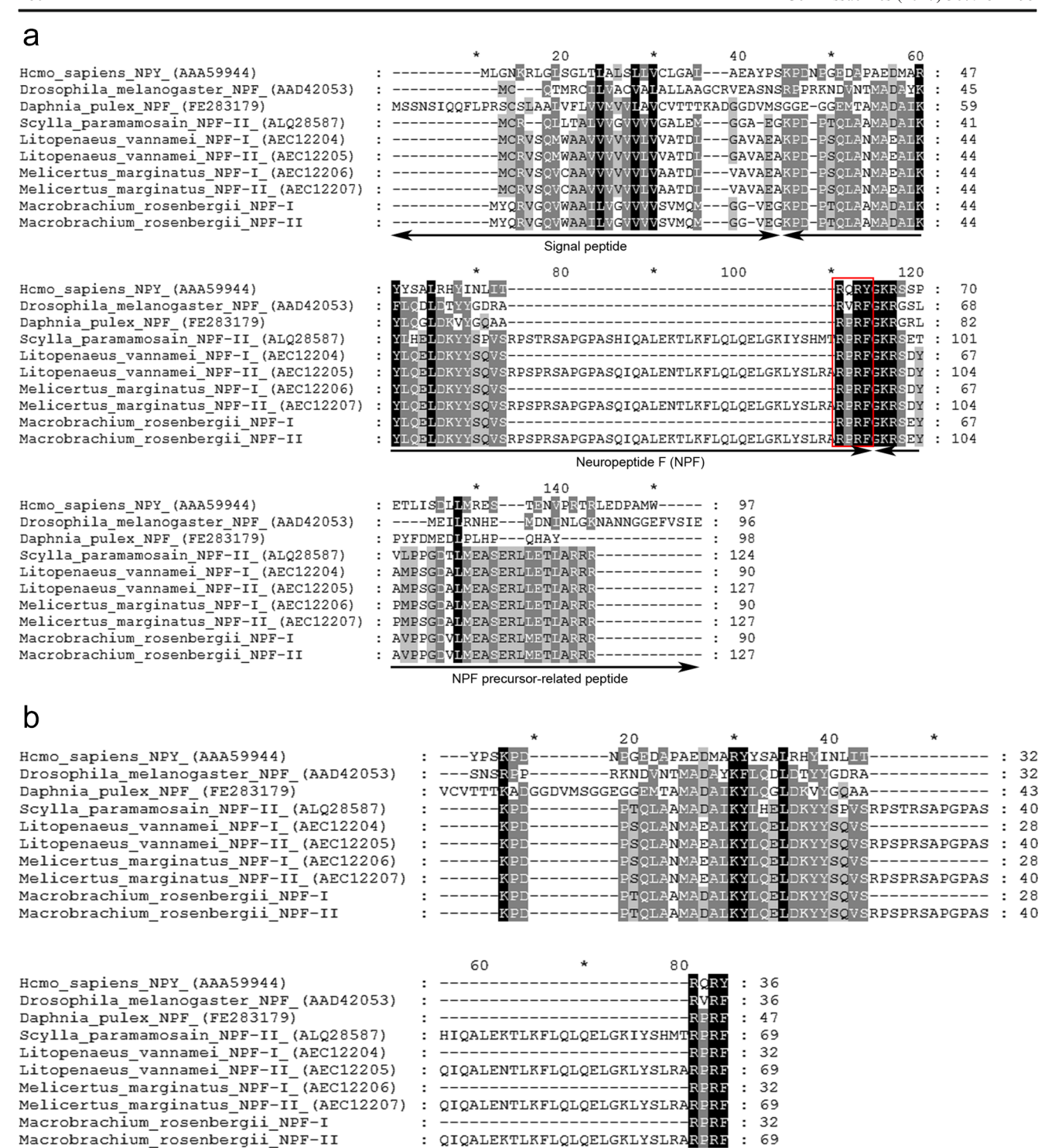


**Fig. 3** a Amino acid sequence alignment of *M. rosenbergii* neuropeptide F (NPF)-I and –II precursors with NPF precursors from other crustaceans and *Drosophila*. Parts of the signal peptide, NPF peptide and NPF precursor-related peptide are indicated by *double-headed arrows* underneath the aligned sequences. *Black shading* indicates identical amino acid

residues, whereas *gray shading* indicates similar amino acid residues. *Red box* shows the conserved NPF motif, which is followed by a glycine residue and a dibasic cleavage site, respectively. **b** Amino acid sequence alignment of *M. rosenbergii* active NPF-I and –II with those of penaeus shrimp, *Daphnia* and *Drosophila* 

*M. marginatus* and *L. vannamei*, respectively. The insert of a 37-amino-acid sequence within MrNPF-II is typical for the second isoform of giant fresh water prawns and those of the penaeus shrimp.

#### Phylogenetic analysis of MrNPFs

The analysis of the evolutionary relationship of MrNPFs with other invertebrate NPFs showed that NPFs of the



freshwater prawn, penaeus shrimp and the crab *Scylla* paramamosain formed a monophyletic clade with a 99 % bootstrap value (Fig. 4), whereas NPFs of a member of another class of crustaceans, namely *Amphibalanus* amphitrite, belonged to a different clade whose NPF-I showed more similarity to NPY of two mollusc species, *Lymnea stagnalis* and *Aplysia californica*. Moreover,

NPF-I of *Daphnia pulex*, a primitive crustacean, shared the same root with NPF-I of *Drosophila melanogaster*. The remaining major clades that shared the same root were NPFs of other insect species. Interestingly, the NPFs of parasitic tremotode worms including *Schistosoma japonicum* and *Schistosoma mansoni* shared the same original root with insect and crustacean NPFs (Fig. 4).

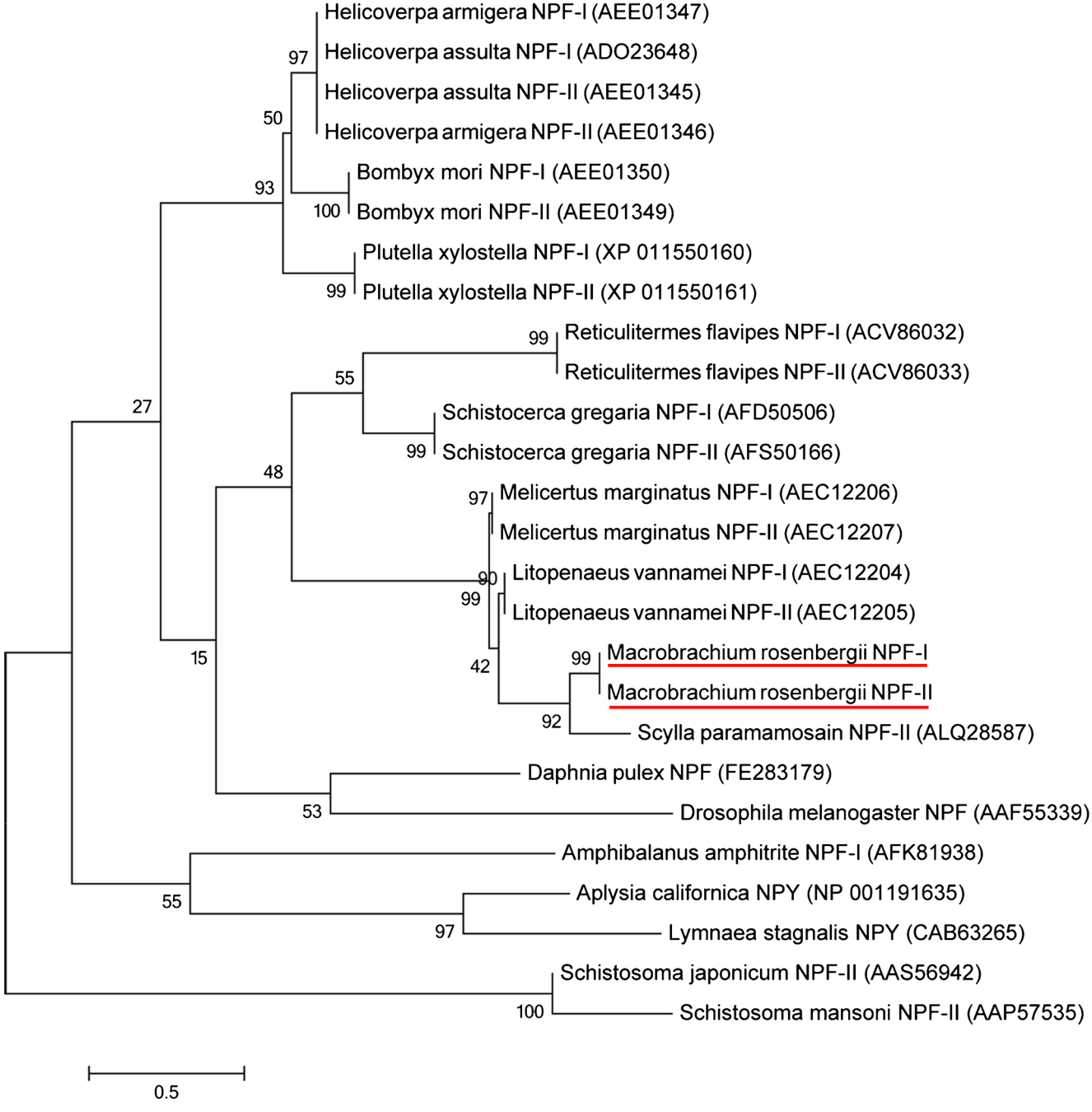


**Fig. 4** Phylogenetic tree analysis of NPFI and –II precursors with NPFs in other invertebrate species. The *numbers below* the node indicate the bootstrap value. The *scale bar* indicates the rate of amino acid

substitution per site. *M. rosenbergii* NPF-I and –II are *underlined*. Maximum-likelihood estimation with LG model; 1000 replications



### Tissue expression of NPFs detected by RT-PCR

Analysis by RT-PCR indicated that the MrNPF-I and -II were expressed widely in various tissues of the male prawn (Fig. 5), with MrNPF-I exhibiting a higher level of expression than MrNPF-II in all examined tissues. MrNPF-I was highly expressed within the neural tissues including eyestalk, brain, thoracic and abdominal ganglia with a significantly higher expression in the brain and thoracic ganglia than in the eyestalk and abdominal ganglia. In comparison, NPF-II was expressed at a much lower level than NPF-I in these tissues. For the digestive tissues, the expression of NPF-I was higher in the midgut and hindgut than in the hepatopancreas, whereas the expression of NPF-II was barely discernible. In the reproductive tissues, MrNPF-I expression was very high in the testis but low in the proximal and absent in middle spermatic ducts. NPF-II was also expressed at a low but discernible level in the testis, whereas it was not expressed in the spermatic duct. The expression of NPF-I was also detected at a relatively lower level in the hematopoietic tissue, heart and muscle, whereas NPF-II expression was not detectable. No positive

ative control (Fig. 5).

**Antibody specificity** 

The specificity of the anti-MrNPF-I antibody was rigorously tested against synthetic NPF-Is, FMRFamide, KISS1 and KISS2 peptides. The anti-MrNPF-I showed no cross-reaction with the synthetic FMRFamide, KISS1 and KISS2 peptides, whereas anti-FMRFamide showed very low reactivity against MrNPF-I. Preabsorption of anti-MrNPF-I with MrNPF-I reduced the intensity of the MrNPF-I dot appreciably, whereas preabsorption with FMRFamide did not. Preabsorption of anti-FMRFamide with MrNPF-I totally abolished the reactivity of the antibody against MrNPF-I (Fig. 6a). Anti-MrNPF-I showed strong reactivity to both LvNPF-I and MrNPF-I peptides and also to protein extract from the CNS (Fig. 6b). For immunohistochemical testing, anti-MrNPF-I showed intense staining in the olfactory neuropil (ON; Fig. 6c) but no reactivity was detected when anti-MrNPF-I was preabsorbed with MrNPF-I peptide (Fig. 6c'). These results confirmed that anti-MrNPF-I was strictly

signal for the expression of MrNPFs was detected in the neg-

Fig. 5 Distribution of MrNPF-I and -II in various tissues of the male prawn by reverse transcription plus the polymerase chain reaction. a Expression of MrNPF-I and -II was detected in the nervous tissues, digestive organs, reproductive organs and other tissues. The expression of  $\beta$ actin was used as an internal control. b Histogram of the intensities of MrNPF-I and -II normalized against that of actin (M marker, Es eyestalk, Br brain, Tg thoracic ganglion, Ab abdominal ganglion, Hp hepatopancreas, Mg midgut, Hg hindgut, Tt testis, Psd proximal spermatic duct, Msd middle spermatic duct, Ht hematopoietic tissue, Hr heart, Ms muscle, N negative control)

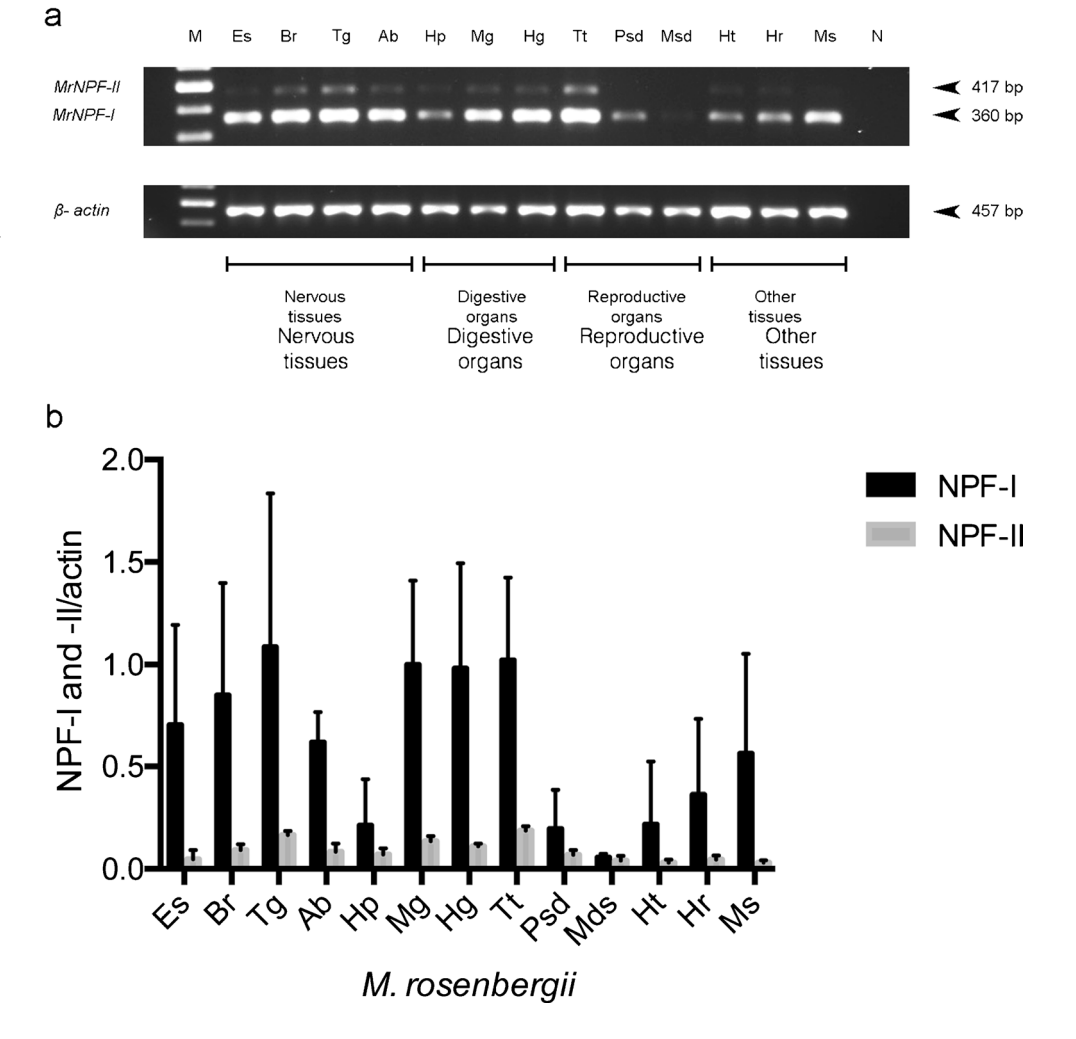




Fig. 6 Specificity test of anti-MrNPF-I antibody. a Cross-reactivity tests of anti-MrNPF-I and anti-FMRFamide with synthetic MrNPF-I, FMRFamide, KISSI and KISSII peptides. The anti-MrNPF-I shows no cross-reaction with synthetic FMRFamide, KISSI and KISSII peptides and the preabsorption with MrNPF-I largely abolishes its reactivity to MrNPF-I. b Anti-MrNPF-I shows strong immunoreactivity for NPF-I of *L. vannamei*, as intensely as for NPF-I of *M. rosenbergii* and also for a presumptive NPF protein in the CNS extract. c Intense immunoreactivity of anti-MrNPF-I in the olfactory neuropil. c' No reactivity was seen when using anti-MrNPF-I preabsorbed with the peptide. These results show that anti-MrNPF-I is specific to NPFs

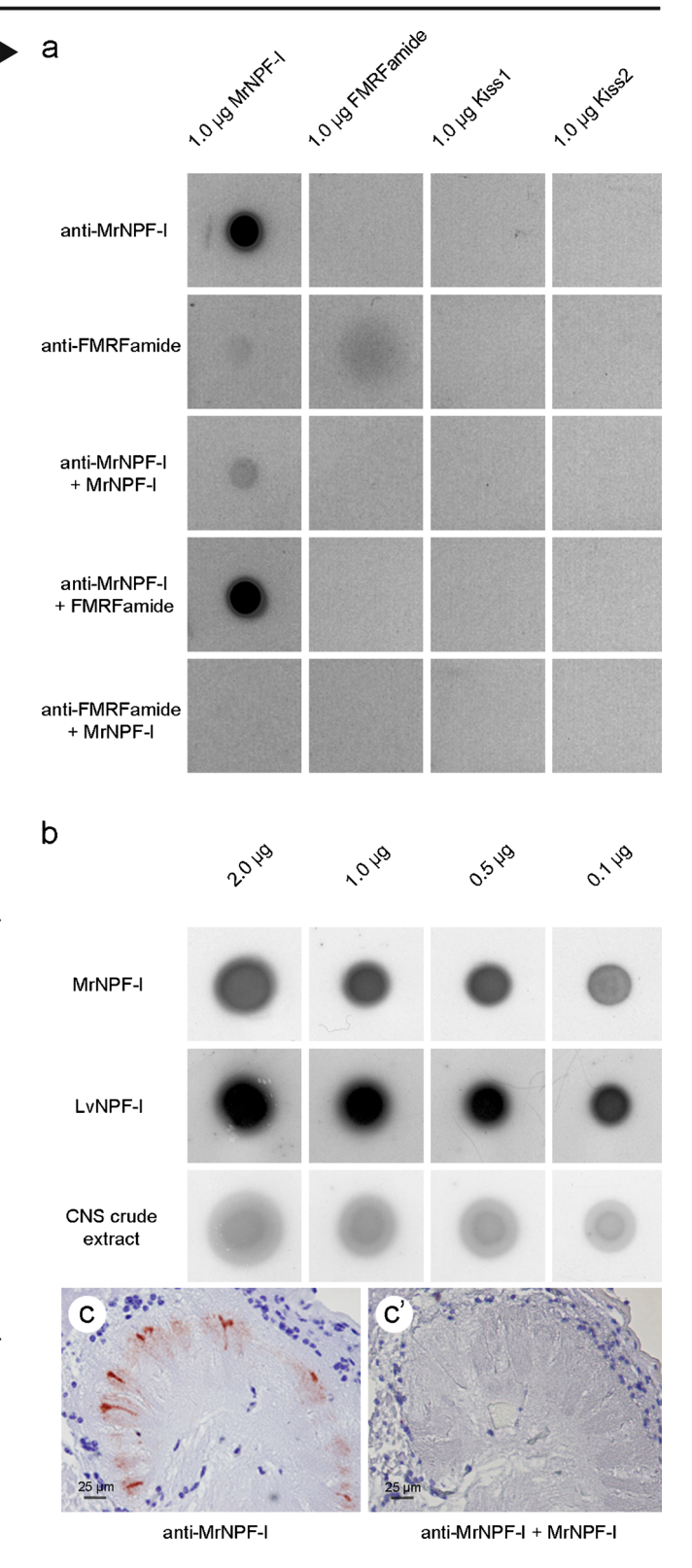
specific for MrNPF-I and strongly cross-reacted with LvNPF-I. Thus, this antibody was used for subsequent immunoperoxidase and immunofluorescence detections. Since the amino acid sequences of MrNPF-I and —II are identical, except for the insert in the mid-region of the latter as mentioned earlier, we assume that anti-MrNPF-I can detect both isoforms and henceforth, they will be referred to as MrNPFs.

# Immunohistochemical detection of MrNPFs in eyestalk and brain

The anatomical nomenclatures of the eyestalk and the brain (supraesophageal ganglion) were based on that described previously by Sandeman et al. (1992) and Tinikul et al. (2011a, 2011b). The regions of the eyestalk are demonstrated in a schematic diagram (Fig. 7a), which was used as the basis for mapping the distribution of MrNPFs in the eyestalk. Briefly, the neural tissue in the eyestalk is composed of two major regions: the optic ganglion and lateral protocerebrum. The optic ganglion consists of the lamina ganglionalis, medulla externa (ME) and medulla interna (MI) and each neuropil contains neuronal clusters 1, 2 and 3. The lateral protocerebrum is composed of the medulla terminalis (MT), hemi-elipsiod body, and neuronal clusters 4 and 5 (Fig. 7a, b).

In the optic lobe and lateral protocerebrum, MrNPF immunoreactivity (-ir) was intense in several neuropils and in neuronal clusters including the neurons of clusters 2 and 3 (Fig. 7c, d, e). MrNPF-ir was also present in the neurons of cluster 4 (X-organ; Fig. 7f). Intense immunoreactive fibers were detected in the neuropils of ME, MI and MT (Fig. 7g, h). Extremely intense immunoreactive fibers were also observed in the sinus gland (Fig. 7i). In contrast, no MrNPF-ir was detected in the control sections of the eyestalk (data not shown). The presence of MrNPF-ir in the eyestalk is summarized in Table 1.

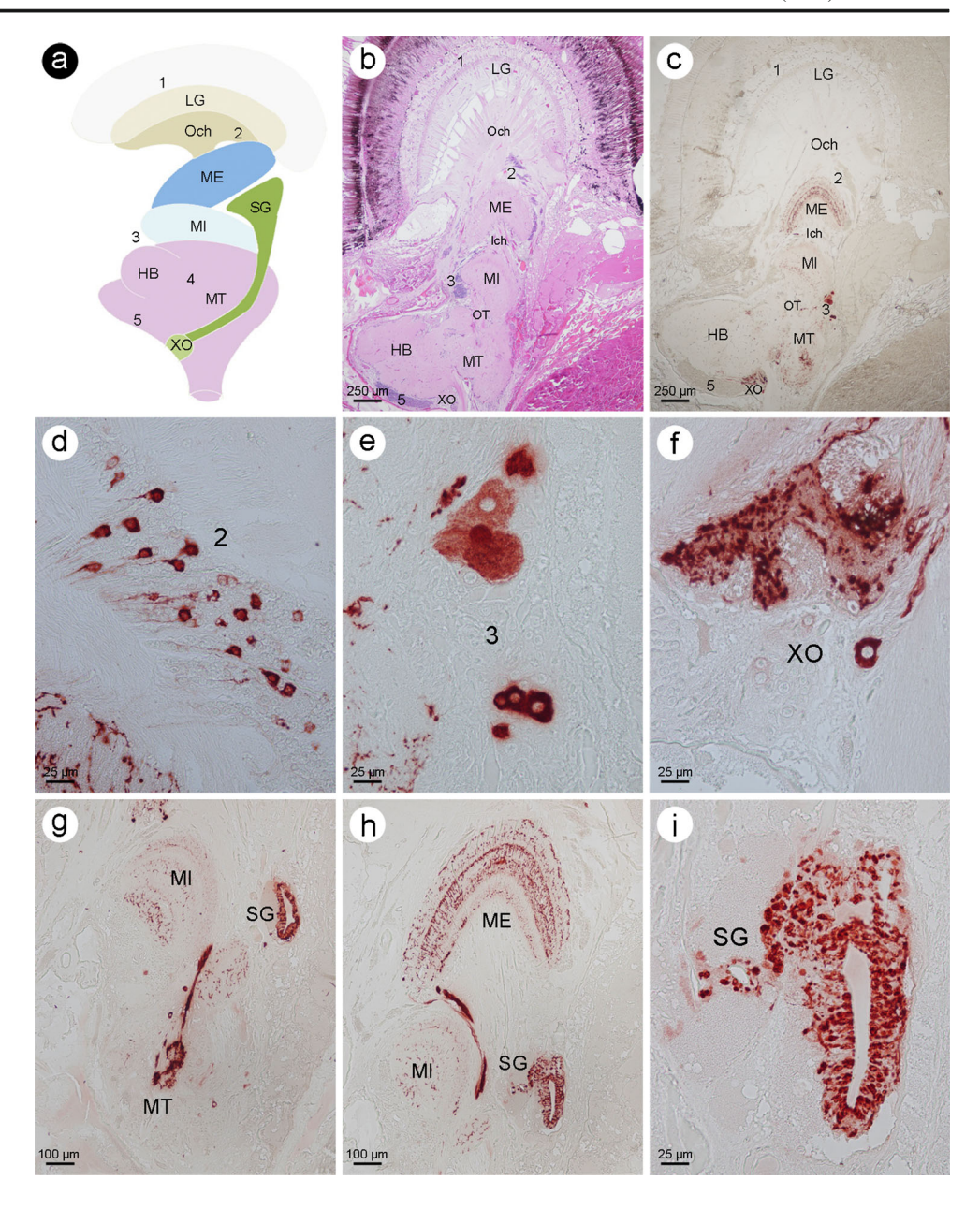
The brain is composed of three major parts: the medial protocerebrum, which contains the anterior medial protocerebral neuropils (AMPNs), posterior medial protocerebral neuropils (PMPNs), protocerebral bridge (PB), central body (CB), and neuronal clusters 6, 7 and 8; the



deutocerebrum containing several neuropils including the medial antenna I neuropil (MAN), lateral antenna I neuropil (LAN), ON and olfactory globular tract neuropil (OGTN) and neuronal clusters 9, 10, 11, 12 and 13; the tritocerebrum,



Fig. 7 Immunolocalization of MrNPF immunoreactivity (NPFir) in the eyestalk of M. rosenbergii. a Representation of the eyestalk of M. rosenbergii. **b** Sagittal section of the eyestalk stained with hematoxylin and eosin. c Similar section as in b showing the location of NPF-ir in various neuronal clusters (numbers) and neuropils. d, e High -magnification images of NPF-ir in neurons of clusters 2 and 3, respectively. f, i Highmagnification images of NPF-ir in the X-organ and sinus gland, respectively. g and h Projection fibers containing NPF-ir, extending from medulla terminalis to medulla externa (HB hemielipsoid body, Ich inner optic chiasm, LG lamina ganglionaris, ME medulla externa, MI medulla interna MT medulla terminalis, Och outer optic chiasm, OT optic tract, SG sinus gland, XO Xorgan)



which contains the tegumentary neuropil (TN) and antenna II neuropil (AnN) and neuronal clusters 14, 15, 16, and 17 (Fig. 8a).

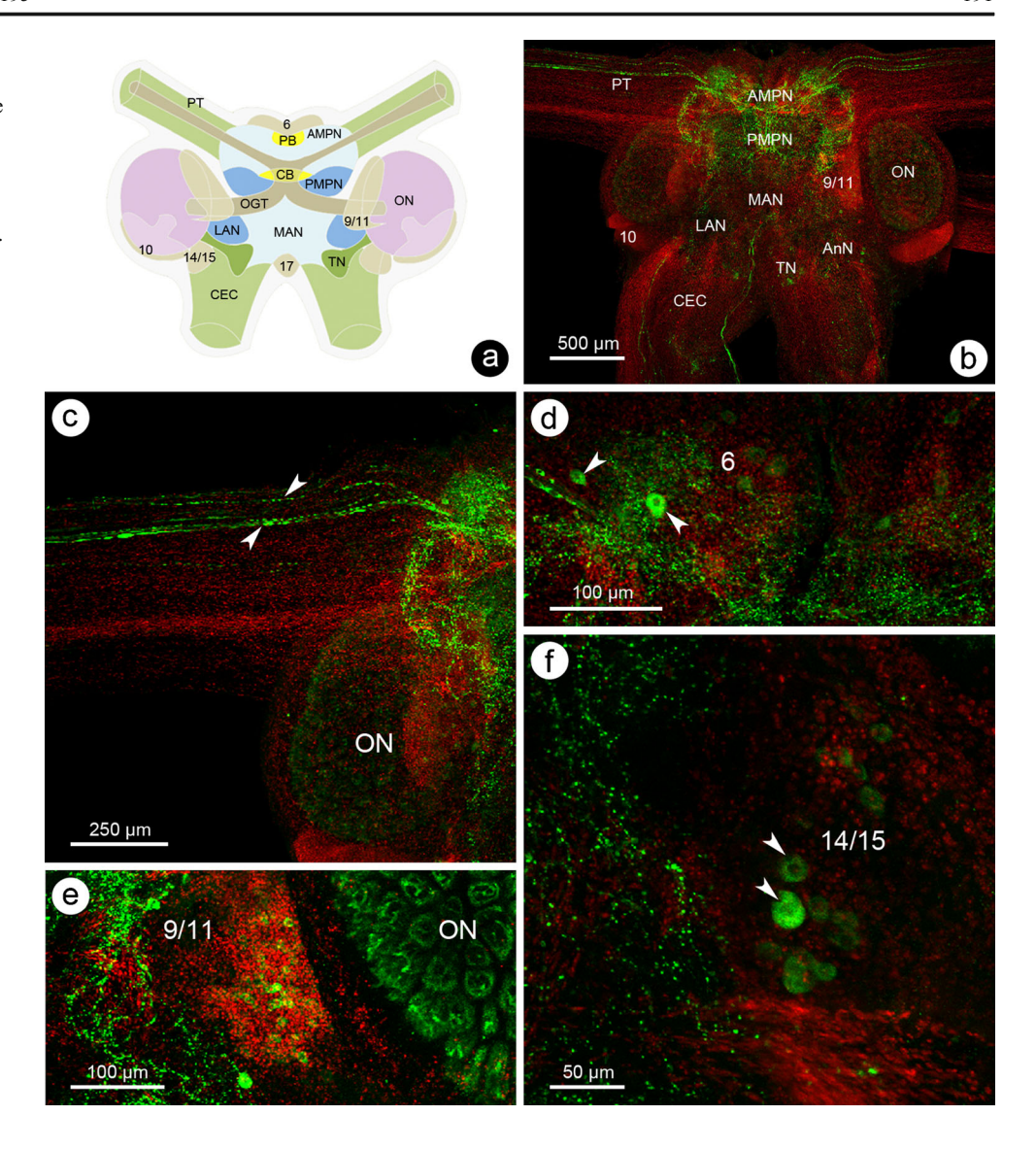
In the medial protocerebrum of whole-mount brain, strong MrNPF-ir was detected in many medium-sized neurons within cluster 6 (Fig. 8d). Intense immunoreactive fibers were observed in AMPN and PMPN (Fig. 8b) and moderately intense immunoreactive fibers were also detected in the PT, PB and CB neuropils (Fig. 8b, c). In the deutocerebrum, MrNPF-ir was detected in medium-sized neurons of clusters 9 and 11 (Fig. 8e) and strongly immunoreactive fibers were present in the ON and OGTN (Fig. 8e). Weak immunoreactive fibers were

detected in the MAN and LAN (Fig. 8b). In the tritocerebrum, strong MrNPF-ir neurons were detected in clusters 14, 15 and 16 (Fig. 8f) and intense immunoreactive fibers in the TN and AnN (Fig. 8b). The control brain sections showed no positive immunoreactivity (data not shown).

To confirm the observations made in the brain by whole-mount immunofluorescence, MrNPF-ir was further examined in brain sections by the immunoperoxidase technique. In the medial protocerebrum, MrNPF-ir was intense in neurons of cluster 6 (Fig. 9c). In the deutocerebrum, highly intense MrNPF-ir was observed in neurons of clusters 9 and 11 and the ON (Fig. 9a,



Fig. 8 Immunofluorescence detection of MrNPF-ir (green) in the brain whole-mount; nuclei are counterstained with To-Pro-3 (red). a Representation of the brain of M. rosenbergii. b Lowpower image showing MrNPF-ir present in all regions of the brain. c Protocerebral tract in protocerebrum (arrowheads) showing intense NPF-ir. d-f High-magnification images showing NPF-ir in neurons of clusters 6, 9/11, 14/15 (arrowheads) and olfactory neuropil (AMPN/PMPN anterior/ posterior medial protocerebral neuropils, PT protocerebral tract, PB protocerebral bridge, CB central body, ON olfactory neuropil, MAN/LAN medial/ lateral antenna I neuropils, OGT olfactory globular tract neuropil, TN tegumentary neuropil, AnN antenna II neuropil, CEC circumesophageal connective)



b, d). The tritocerebrum exhibited moderately intense MrNPF-ir in neurons of clusters 14 and 15 (Fig. 9e)

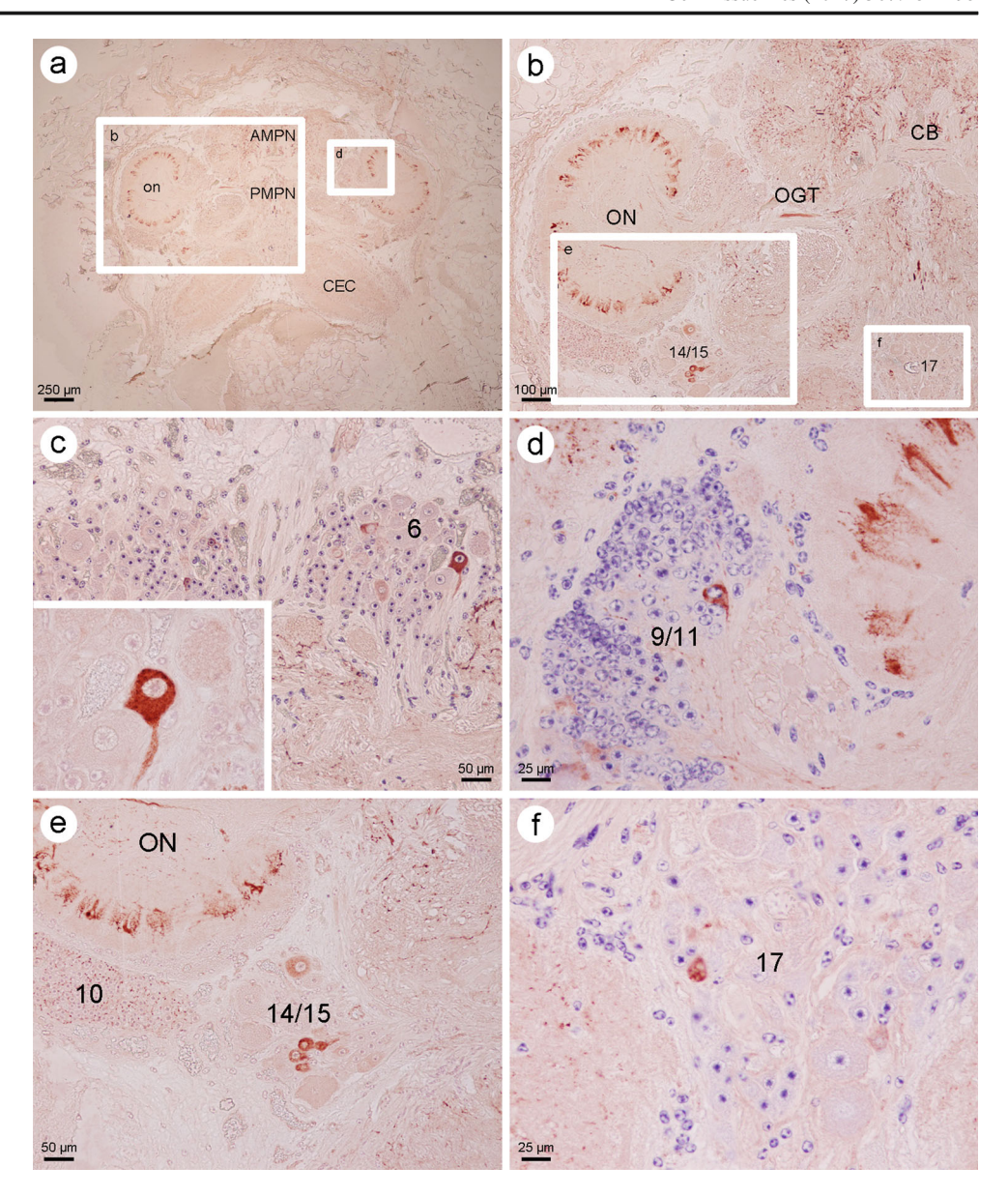
and clusters 17 (Fig. 9f). The presence of MrNPF-ir in the brain is summarized in Table 2.

Table 1 Distribution of *Macrobrachium rosenbergii* neuropeptide F (MrNPF) immunoreactivity (*MrNPF-ir*) in the eyestalk (+++ strong immunoreactivity, ++ moderate immunoreactivity, - no immunoreactivity, - no immunoreactivity, *LG* lamina ganglionaris, *ME* medulla externa, *MI* medulla interna, *MT* medulla terminalis, *HB* hemiellipsoid body, *SG* sinus gland, *S* small-sized neuron, *M* mediumsized neuron, *NA* not applicable)

Structure	Regions	Neuronal clusters/neuropils	Type of neurons	MrNPF-ir
Eyestalk	Optic ganglia	1	S	_
		2	S	++
		3	S, M	+++
		LG	NA	-
		ME	NA	++
		MI	NA	+
	Lateral protocerebrum	4	S, M	+++
		5	S	_
		SG	NA	+++
		MT	NA	++
		НВ	NA	-



Fig. 9 Immunolocalization of MrNPF in horizontal brain sections of M. rosenbergii. a Low-power image showing distribution of NPF-ir in various parts of the brain. b Mediumpower image showing MrNPF-ir in various neuronal clusters (numbers) and neuropils (CB central body, OGT olfactory globular tract neuropil, ON olfactory neuropil). c MrNPF-ir is present in neurons of cluster 6. Inset High-magnification image. d-f High-magnification images showing NPF-ir in neurons of clusters 9/11, 14/15 and 17; nuclei are counterstained by hematoxylin



## **Discussion**

Our recent transcriptomic analysis has revealed three isoforms of NPFs and four isoforms of sNPF in the CNS of female *M. rosenbergii* (MrNPF-I, NPF-II, NPF-III and four sNPF; Suwansa-Ard et al. 2015). MrNPF-I and -II each consists of a 29-amino-acid signal peptide followed by 32- and 69-amino-acid active peptides, cleaved at two dibasic cleavage sites. MrNPF-III is composed of a 23-amino-acid signal peptide and a 60-amino-acid active peptide, cleaved at a single dibasic cleavage site. MrNPF-I and -II active peptides show high sequence similarity (>90 %) with LvNPF-I and -II, whereas the MrNPF-III active peptide shows high similarity (66 %) with mollusc neuropeptide Y. Moreover, a precursor of the sNPF transcript has also been identified in the eyestalk and CNS transcriptomes and this sNPF precursor is predicted to be

cleaved at multiple sites to give rise to four active short peptides. In the present study, we validated the sequences of the two isoforms of NPFs and found that the full sequences are identical with those predicted from our earlier transcriptomic analysis (Suwansa-Ard et al. 2015). Interestingly, the MrNPF-I and -II precursor proteins, encoded by separate genes, show high similarity (91–95 %) to other prawns NPFs, i.e., those of L. vannamei and M. marginatus (Christie et al. 2011), whereas the mature NPF-I is almost identical, except for four amino acids (threonine, alanine, aspartic acid, and lysine, instead of serine, asparagine, glutamic acid, and asparagine, respectively) at the mid-region of the peptide. The MrNPF-I and -II precursors share 71 % amino acid identity, whereas the mature MrNPF-I and -II active peptide are identical, except for a 37amino-acid insert within the middle part of MrNPF-II. The insert of a 37-amino-acid sequence within MrNPF-II is typical



Table. 2 Distribution of MrNPFir in the brain of M. rosenbergii (+++ strong immunoreactivity, ++ moderate immunoreactivity. + weak immunoreactivity. - no immunoreactivity, AMPN/PMPN anterior/posterior medial protocerebral neuropils, PT protocerebral tract, PB protocerebral bridge, CB central body, ON olfactory neuropil, MAN/LAN medial/lateral antenna I neuropils, OGTN olfactory globular tract neuropil, TN tegumentary neuropil, AnN antenna II neuropil, S small-sized neuron, M medium-sized neuron, L large-sized neuron, NA not applicable)

Structure	Regions	Neuronal clusters/neuropils	Prominent type of neurons	MrNPF-ir
Brain	Median protocerebrum	6	S, M	+++
		7	M, L	_
		8	S	-
		AMPN/PMPN	NA	+++
		PT/PB/CB	NA	++
	Deutocerebrum	9/11	S, M	+++
		10	S	_
		12/13	S	_
		MAN/LAN	NA	+
		ON/OGTN	NA	++
	Tritocerebrum	14/15/16	S, M	++
		17	S, M	+
		TN/AnN	NA	+

for the second isoforms as also found in M. marginatus and L. vannamei (Christie et al. 2011). The MrNPF-II is almost identical to the NPF-II of M. marginatus and L. vannamei, except for 3 amino acids in the mid-region and 1 amino acid in the insert part of the mature peptide. Phylogenetically, when comparing the precursors of the prawns NPFs with those of Daphnia, a more primitive crustacean and with Drosophila and other insects, the similarity ranges from 72 % to 71 %, whereas both isoforms of the prawn active peptides are closely similar to those of Daphnia and insects with a range of 92-77 % (Fig. 4). This confirms that the active peptides of all arthropods and crustaceans are highly conserved. The receptors of both NPFs (NPFR1) have been cloned in Drosophila and show a high degree of conservation with that of the NPY receptor (Garczynski et al. 2002). Whether the prawn and insect NPFRs are also highly conserved remains to be explored. Incidentally, in our earlier work, we detected four isoforms of sMrNPF in the transcriptome of the brain of this species and suggested that these isoforms arise from a replication within a single gene (Suwansa-Ard et al. 2015); this again is similar to the situation in *Drosophila* in which four isoforms of sNPF have been found by RT-PCR (Carlsson et al. 2013). However, we have not yet been able to determine the sequence of the gene encoding the sMrNPFs.

Extensive localization studies have been carried out for *Drosophila* and insect NPFs and sNPF by both RT-PCR and immunohistochemical techniques. By and large, the NPFs and their receptors are localized in the brain, subesophageal ganglion, ventral nerve cord and midgut of larval *Drosophila* (Carlsson et al. 2013; Van Wielendaele et al. 2013). In the desert locust, *Schistocerca gregaria*, NPF has also been detected in the optic lobe (Van Wielendaele et al. 2013). Notably, the sNPF distribution in the brain is more wide spread than that of NPF implying its role as a neuromodulator acting together with other traditional neurotransmitters in addition to its paracrine/

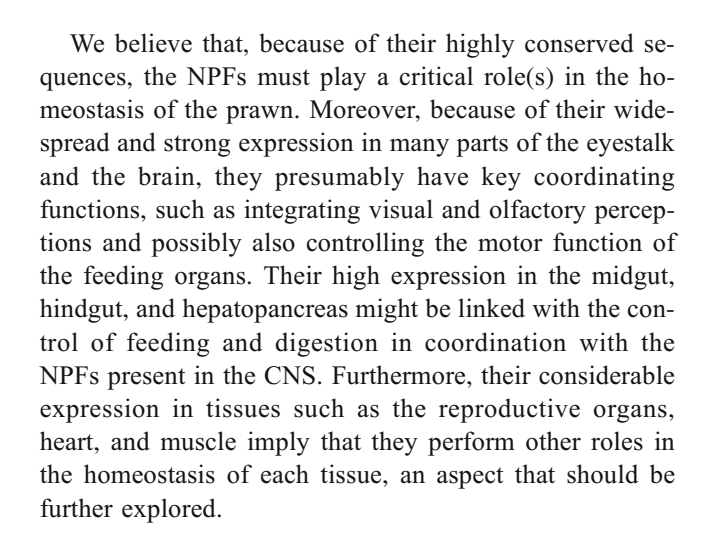
endocrine functions (Nassel and Wegener 2011). By contrast, in penaeus shrimps, NPF expression in tissue has only been determined by RT-PCR. Both NPF-I and -II are reported to be broadly distributed within CNS of L. vannamei and M. marginatus, including the optic ganglia of the eyestalk, brain and thoracic and abdominal ganglia. The transcript encoding NPF-I is weak in some and undetectable in other midgut samples. The transcript encoding NPF-II is present but with much weaker intensity in the above-mentioned parts of the CNS, except for the eyestalk and it is absent in the midgut of both species. The transcript of neither NPFs has been detected in muscle (Christie et al. 2011). In comparison, the distribution pattern and intensity of MrNPF-I and -II transcripts in various parts of the CNS of the freshwater prawn are similar to that of the two penaeus shrimps, with the highest intensity in the brain and thoracic ganglia and NPF-I showing a five- to seven-fold higher expression than NPF-II. However, we found that the presence of NPF-I and -II transcripts is widely spread in many parts of the gastrointestinal tract including the midgut, hindgut, and hepatopancreas, with NPF-I expression in the former two regions being about four-fold higher than the latter and the expression is as high as in the brain and thoracic ganglia. Surprisingly, in the present study, we also observed that NPF-I is strongly expressed in the testes, whereas in our earlier work, this peptide has also been reported to be strongly expressed in the ovaries (Suwansa-Ard et al. 2015). By comparison, the expression is much weaker in the spermatic duct. Other tissues that also express a considerable amount of NPF-I include the hematopoeitic tissue, heart and muscle. The widespread expression of NPFs in more tissues, especially the reproductive tissues, imply a more common role of NPF in tissue homeostasis other than just controlling feeding. One such activity is the role of NPFs in controlling the process of autophagy, which is responsible for the recruitment of nutrients from cells of all organs, especially the hepatopancreas



and muscle, in cases of limited food supply and starvation (manuscript in preparation).

In addition to the detection of the tissue expression by means of RT-PCR, we report, in this study, the detailed mapping of the NPFs by using immunohistochemical detection in both whole-mount and tissue sections of the brain and the eyestalk. The antibody that we used is highly specific for MrNPF-I, as practically no cross -reaction occurs with other RFamide peptides including FMRFamide and the Kiss peptides. Unfortunately, the antibody cannot differentiate between NPF-I and -II, because it was raised against the amino acid sequence of NPF-I, which is identical to the amino terminal part of NPF-II. Our specificity test indicates that this antibody does not react with the RFamide end, because when the anti FMRFamide is used, it reacts slightly with both NPF-I and FMRFamide (Fig. 6a) suggesting that this antibody reacts with the RFamide at the carboxy end of both NPF-I and FMRFamide. In contrast, anti-NPF-I only reacts with the NPF-I peptide, which suggests that the antibody reacts with the amino acid sequence upstream from the RFamide end. Since this sequence is identical in both isoforms of NPF, we suggest that the anti-NPF-I reacts with both isoforms. As shown in Table 2, MrNPFs are present in the optic ganglia of the eyestalk, i.e., neurons of clusters 2, 3 and 4 and the neuropils of ME and MT, indicating that these peptides are involved in mediating the transmission of visual signals from the eyestalk to the brain. Remarkably, strong immunoreactivity has been detected in the neurons of the X-organ and the sinus gland complex, implying that MrNPFs also play a role in controlling or acting together with the hormones in the CHH family, which control prawn reproduction and molting, including GIH, MIH and MOIH, which are known to be synthesized and released in the X-organ and sinus gland complex (Chung et al. 2010).

The strong expression of NPFs in neurons of cluster 6 and fibers within neuropils of AMPN, PMPN, PT, PB and CB of the medial protocerebrum implies further that these peptides help to integrate photoreception by the forebrain (protocerebrum) and olfactory reception by the midbrain (deutocerebrum). Indeed, the strong intensity of NPFs detected in the neurons of clusters 9 and 11 and fibers of the ON and OGTN neuropils, which are the key structures of the midbrain that receive olfactory stimuli (Kruangkum et al. 2013), further supports the notion that MrNPFs play a central role in mediating the reception of food odor, as is widely known in Drosophila (Nassel and Wegener 2011) and in integrating between visual and olfactory perceptions. Lastly, NPFs have been detected at moderate intensity in neurons of clusters 14, 15, and 16 and fibers in the TN and AnN of the tritocerebrum, which control the antennae and, together with the subesophageal ganglion, the mouth parts; this finding implies that NPFs exercise some control over the motor activity of the prawn feeding organs.



Acknowledgments This research was supported by a grant from the Office of Higher Education Commission (OHEC) and Mahidol University (MU) under the National Research University Initiatives and a OHEC-MU-Thailand Research Fund (TRF) Distinguished Research Professor Grant to Prasert Sobhon. This study was also supported by the Thailand Research Fund-the Royal Golden Jubilee Ph.D. Programme (TRF-RGJ Ph.D) co-funded by Mahidol University to Chaitip Wanichanon and Sirorat Thongrod, by National Research Council of Thailand (NRCT) scholarships (2016) to Sirorat Thongrod and by a TRF Research Career Development Grant (RSA5780011) (co-funded by the Thailand Research Fund and Mahidol University) to Yotsawan Tinikul. We extend our gratitude to Wilairat Kankuan and Tipsuda Thongbuakaew for their technical advice.

# References

Acuna-Goycolea C, Tamamaki N, Yanagawa Y, Obata K, Pol AN van den (2005) Mechanisms of neuropeptide Y, peptide YY, and pancreatic polypeptide inhibition of identified green fluorescent protein-expressing GABA neurons in the hypothalamic neuroendocrine arcuate nucleus. J Neurosci 25:7406–7419

Antonsen BL, Paul DH (2001) Serotonergic and octopaminergic systems in the squat lobster *Munida quadrispina* (Anomura, Galatheidae). J Comp Neurol 439:450–468

Broeck JV (2001) Neuropeptides and their precursors in the fruitfly, *Drosophila melanogaster*. Peptides 22:241–254

Cansell C, Denis RG, Joly-Amado A, Castel J, Luquet S (2012) Arcuate AgRP neurons and the regulation of energy balance. Front Endocrinol (Lausanne) 3:169

Carlsson MA, Enell LE, Nassel DR (2013) Distribution of short neuropeptide F and its receptor in neuronal circuits related to feeding in larval *Drosophila*. Cell Tissue Res 353:511–523

Chaudhri O, Small C, Bloom S (2006) Gastrointestinal hormones regulating appetite. Philos Trans R Soc Lond B Biol Sci 361:1187–1209

Christie AE, Cashman CR, Brennan HR, Ma M, Sousa GL, Li L, Stemmler EA, Dickinson PS (2008) Identification of putative crustacean neuropeptides using in silico analyses of publicly accessible expressed sequence tags. Gen Comp Endocrinol 156:246–264

Christie AE, Chapline MC, Jackson JM, Dowda JK, Hartline N, Malecha SR, Lenz PH (2011) Identification, tissue distribution and orexigenic activity of neuropeptide F (NPF) in penaeid shrimp. J Exp Biol 214:1386–1396



- Chung JS, Zmora N, Katayama H, Tsutsui N (2010) Crustacean hyperglycemic hormone (CHH) neuropeptides family: function, titer, and binding to target tissues. Gen Comp Endocrinol 166:447–454
- Field BC, Chaudhri OB, Bloom SR (2010) Bowels control brain: gut hormones and obesity. Nat Rev Endocrinol 6:444–453
- Garczynski SF, Brown MR, Shen P, Murray TF, Crim JW (2002) Characterization of a functional neuropeptide F receptor from *Drosophila melanogaster*. Peptides 23:773–780
- Gard AL, Lenz PH, Shaw JR, Christie AE (2009) Identification of putative peptide paracrines/hormones in the water flea *Daphnia pulex* (Crustacea; Branchiopoda; Cladocera) using transcriptomics and immunohistochemistry. Gen Comp Endocrinol 160:271–287
- Itskov PM, Ribeiro C (2013) The dilemmas of the gourmet fly: the molecular and neuronal mechanisms of feeding and nutrient decision making in *Drosophila*. Front Neurosci 7:12
- Karl T, Herzog H (2007) Behavioral profiling of NPY in aggression and neuropsychiatric diseases. Peptides 28:326–333
- Kornthong N, Cummins SF, Chotwiwatthanakun C, Khornchatri K, Engsusophon A, Hanna PJ, Sobhon P (2014) Identification of genes associated with reproduction in the Mud Crab (Scylla olivacea) and their differential expression following serotonin stimulation. PLoS One 9:e115867
- Krashes MJ, DasGupta S, Vreede A, White B, Armstrong JD, Waddell S (2009) A neural circuit mechanism integrating motivational state with memory expression in *Drosophila*. Cell 139:416–427
- Kruangkum T, Chotwiwatthanakun C, Vanichviriyakit R, Tinikul Y, Anuracpreeda P, Wanichanon C, Hanna PJ, Sobhon P (2013) Structure of the olfactory receptor organs, their GABAergic neural pathways, and modulation of mating behavior, in the giant freshwater prawn. Macrobrachium rosenbergii. Microsc Res Tech 76:572–587
- Lee KS, You KH, Choo JK, Han YM, Yu K (2004) Drosophila short neuropeptide F regulates food intake and body size. J Biol Chem 279:50781–50789
- Loh K, Herzog H, Shi YC (2015) Regulation of energy homeostasis by the NPY system. Trends Endocrinol Metab 26:125–135
- Nassel DR, Wegener C (2011) A comparative review of short and long neuropeptide F signaling in invertebrates: any similarities to vertebrate neuropeptide Y signaling? Peptides 32:1335–1355
- Palasoon R, Panasophonkul S, Sretarugsa P, Hanna P, Sobhon P, Chavadej J (2011) The distribution of APGWamide and RFamides in the central nervous system and ovary of the giant freshwater prawn, Macrobrachium rosenbergii. Invertebr Neurosci 11:29–42
- Root CM, Ko KI, Jafari A, Wang JW (2011) Presynaptic facilitation by neuropeptide signaling mediates odor-driven food search. Cell 145: 133–144
- Saetan J, Senarai T, Tamtin M, Weerachatyanukul W, Chavadej J, Hanna PJ, Parhar I, Sobhon P, Sretarugsa P (2013) Histological

- organization of the central nervous system and distribution of a gonadotropin-releasing hormone-like peptide in the blue crab, *Portunus pelagicus*. Cell Tissue Res 353:493–510
- Sandeman D, Sandeman R, Derby C, Schmidt M (1992) Morphology of the brain of crayfish, crabs and spiny lobsters: a common nomenclature for homologous structures. Biol Bull 183:304-326
- Sobrino Crespo C, Perianes Cachero A, Puebla Jimenez L, Barrios V, Arilla Ferreiro E (2014) Peptides and food intake. Front Endocrinol (Lausanne) 5:58
- Stanley S, Wynne K, McGowan B, Bloom S (2005) Hormonal regulation of food intake. Physiol Rev 85:1131–1158
- Suwansa-Ard S, Thongbuakaew T, Wang T, Zhao M, Elizur A, Hanna PJ, Sretarugsa P, Cummins SF, Sobhon P (2015) In silico neuropeptidome of female *Macrobrachium rosenbergii* based on transcriptome and peptide mining of eyestalk, central nervous system and ovary. PLoS One 10:e0123848
- Tinikul Y, Poljaroen J, Nuurai P, Anuracpreeda P, Chotwiwatthanakun C, Phoungpetchara I, Kornthong N, Poomtong T, Hanna PJ, Sobhon P (2011a) Existence and distribution of gonadotropin-releasing hormone-like peptides in the central nervous system and ovary of the Pacific white shrimp, *Litopenaeus vannamei*. Cell Tissue Res 343: 579-593
- Tinikul Y, Poljaroen J, Kornthong N, Chotwiwatthanakun C, Anuracpreeda P, Poomtong T, Hanna PJ, Sobhon P (2011b) Distribution and changes of serotonin and dopamine levels in the central nervous system and ovary of the Pacific white shrimp, *Litopenaeus vannamei*, during ovarian maturation cycle. Cell Tissue Res 345:103-124
- Tinikul Y, Poljaroen J, Tinikul R, Chotwiwatthanakun C, Anuracpreeda P, Hanna PJ, Sobhon P (2015) Alterations in the levels and distribution of octopamine in the central nervous system and ovary of the Pacific white shrimp, *Litopenaeus vannamei*, and its possible role in ovarian development. Gen Comp Endocrinol 210:12–22
- Tinikul Y, Poljaroen J, Tinikul R, Sobhon P (2016) Changes in the levels, expression, and their possible roles of serotonin and dopamine during embryonic development in the giant freshwater prawn, *Macrobrachium rosenbergii*. Gen Comp Endocrinol 225:71–80
- Van Wielendaele P, Wynant N, Dillen S, Badisco L, Marchal E, Vanden Broeck J (2013) In vivo effect of neuropeptide F on ecdysteroidogenesis in adult female desert locusts (*Schistocerca gregaria*). J Insect Physiol 59:624–630
- Wu Q, Wen T, Lee G, Park JH, Cai HN, Shen P (2003) Developmental control of foraging and social behavior by the *Drosophila* neuropeptide Y-like system. Neuron 39:147–161
- Wu Q, Zhao Z, Shen P (2005) Regulation of aversion to noxious food by Drosophila neuropeptide Y- and insulin-like systems. Nat Neurosci 8:1350–1355



FISEVIER

Contents lists available at ScienceDirect

# General and Comparative Endocrinology

journal homepage: www.elsevier.com/locate/ygcen



# Changes in the levels, expression, and possible roles of serotonin and dopamine during embryonic development in the giant freshwater prawn, *Macrobrachium rosenbergii*



Yotsawan Tinikul <sup>a,b,\*</sup>, Jaruwan Poljaroen <sup>a,b</sup>, Ruchanok Tinikul <sup>b</sup>, Prasert Sobhon <sup>a</sup>

- <sup>a</sup> Department of Anatomy, Faculty of Science, Mahidol University, Bangkok 10400, Thailand
- <sup>b</sup> Mahidol University, Nakhonsawan Campus, Nakhonsawan 60130, Thailand

#### ARTICLE INFO

Article history:
Received 5 May 2015
Revised 8 September 2015
Accepted 17 September 2015
Available online 21 September 2015

Keywords:
Serotonin
Dopamine
Embryonic development
Freshwater prawn
Neurotransmitter
Macrobrachium rosenbergii

#### ABSTRACT

We investigated the changes in the levels of serotonin (5-HT) and dopamine (DA), and their possible roles during embryonic development of the freshwater prawn, *Macrobrachium rosenbergii*. The 5-HT and DA concentrations were quantified using high performance liquid chromatography with electrochemical detection (HPLC-ECD). The levels of 5-HT and DA gradually increased from early developing embryos to late developing embryos. The 5-HT concentrations gradually increased from the pale yellow egg to orange egg stages, and reaching a maximum at the black egg stage. DA concentrations were much lower in the early embryos than those of 5-HT (P < 0.05), and gradually increased to reach the highest level at the black egg stage. Immunohistochemically, 5-HT was firstly detected in the early embryonic stages, whereas DA developed later than 5-HT. Functionally, 5-HT-treated female prawns at doses of  $2.5 \times 10^{-5}$ ,  $2.5 \times 10^{-6}$  and  $2.5 \times 10^{-7}$  mol/prawn, produced embryos with significantly shortened lengths of early embryonic stages, whereas DA-treated prawns at all three doses, exerted its effects by significantly lengthening the period of mid-embryonic stage onwards. These results suggest significant involvement of 5-HT and DA in embryonic developmental processes of this species.

© 2015 Elsevier Inc. All rights reserved.

# 1. Introduction

The giant freshwater prawn, Macrobrachium rosenbergii, is a highly valued aquatic animal for consumption that is cultured worldwide, including Thailand (Sandifer and Smith, 1985). The reproductive process and hormonal regulation of this species are not as well understood as in other decapod crustaceans, for examples, the crayfish, Procambarus clarkii, or the lobster, Homarus americanus, in which a number of neurohormones from the Xorgan-sinus gland complex, situated in the eyestalks, play roles in regulating the gonadal development (Fingerman, 1997; Benton et al., 1997; Chen et al., 2003; Prasad et al., 2014). In crustaceans, the synthesis and release of neurohormones are thought to be regulated by biogenic amines, including serotonin (5-HT) and dopamine (DA) (Richardson et al., 1991; Nagaraju et al., 2010; Nagaraju, 2011). 5-HT and DA are biogenic amines that play roles in regulating various physiological processes and reproduction (Beltz, 1999). 5-HT stimulates gonadal maturation in several decapod crustaceans, including the red swamp crayfish, *P. clarkii* (Kullkarni et al., 1992), the Pacific white shrimp, *Litopenaeus vannamei* (Vaca and Alfaro, 2000), the black tiger shrimp, *Penaeus monodon* (Wongprasert et al., 2006), and the freshwater prawn, *M. rosenbergii* (Tinikul et al., 2009b), whereas DA plays an opposite role (Tinikul et al., 2014). In *M. rosenbergii*, 5-HT shortens the embryonic development period, whereas DA shows an opposite effect (Tinikul et al., 2009a). However, there is a current lack of detailed studies about the specific actions of these two neurotransmitters on each embryonic developmental stage in *M. rosenbergii*.

The levels of 5-HT and DA have been quantitated in various regions of the CNS and ovaries of many decapod crustaceans, including *Pacifastacus leniusculus* (Elofsson et al., 1982), *M. rosenbergii* (Tinikul et al., 2008), and *L. vannamei* (Tinikul et al., 2011b). Major tissues that showed high levels of 5-HT and DA activities were the ovaries, brains, and thoracic ganglia. However, the levels of these two neurotransmitters during embryogenesis in *M. rosenbergii* are still not investigated, even though there are some previous works on immunohistochemical localization of biogenic amines during embryonic development in decapod crustaceans. In the lobster, *H. americanus*, 5-HT was detected in early embryonic development, and the serotonergic neurons in the brain and ventral nerve cord are fully developed by mid-embryonic life

<sup>\*</sup> Corresponding author at: Mahidol University, Nakhonsawan Campus, Phayuhakiri District, Nakhonsawan 60130, Thailand.

E-mail addresses: anatch2002@yahoo.com, yotsawan.tin@mahidol.ac.th, anatch2002@gmail.com (Y. Tinikul).

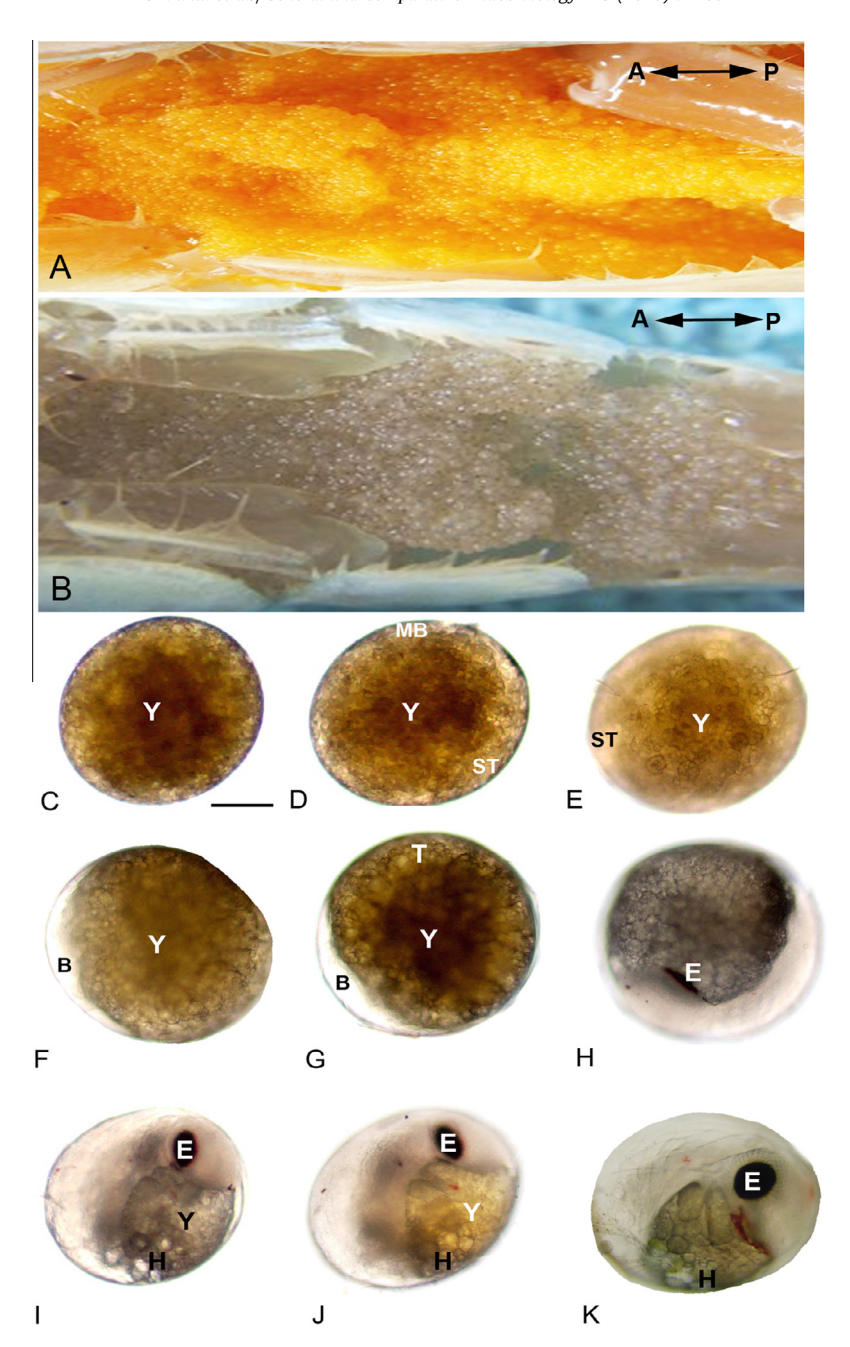


**Fig. 1.** Photographs of the ventral views of the brood chambers (A and B) and various stages of developing embryos (C–K) of the mature berried female *M. rosenbergii*. (A and B) The example micrographs of the ventral views of berried females at the mid-embryonic stages (orange egg stage; OE), and the late stage (gray egg stage; GE). The orientation of the prawn is given top right. (C and D) The bright yellow egg (BYE). (E) Deep yellow egg stage (DYE). (F and G) Orange egg stage (OE). (H and I) Brown egg stage (BE). (J) Gray egg stage (GE). (K) Black egg stage (BLE). A, anterior; B, blastocoel; E, eye; H, heart; MB, egg membrane; P, posterior; ST, small translucent region; T, trunk; Y, yolk. Scale bars: 100 μm. (For interpretation of the references to color in this figure legend, the reader is referred to the web version of this article.)

(Beltz, 1999). As well, it is proposed that 5-HT may play a developmental role in this decapod crustacean, and it is likely to be related to the functions of each compound at specific life stages (Benton et al., 1997). In *H. americanus*, the DA-ir staining was first detected in the brain and subesophageal ganglion of 50% of developmental stages, indicating that DA may be involved in embryogenesis in the lobster (Cournil et al., 1995). To our current knowledge, there is no detailed study regarding the existence, distribution, and variation in the levels of these biogenic amines during embryonic development in *M. rosenbergii*.

Therefore, the aim of this study was to quantify the changes in the levels and localize the distribution of 5-HT and DA during embryonic developmental stages by using HPLC and immunohistochemistry. In addition, the functional tests were undertaken to

assess the specific actions of these two neurotransmitters on each embryonic stage. The understanding how these neurotransmitters regulate embryonic development may assist in increasing the production of larvae of this species. Moreover, this study would provide valuable information to increase knowledge of evolutionary pathways of these two neurotransmitters during embryonic development in this crustacean species.

#### 2. Materials and methods

#### 2.1. Experimental animals

Mature female freshwater prawns (weighing on average about  $32.46\pm4.17~g$ ) were obtained from commercial farms, in Ayuthaya

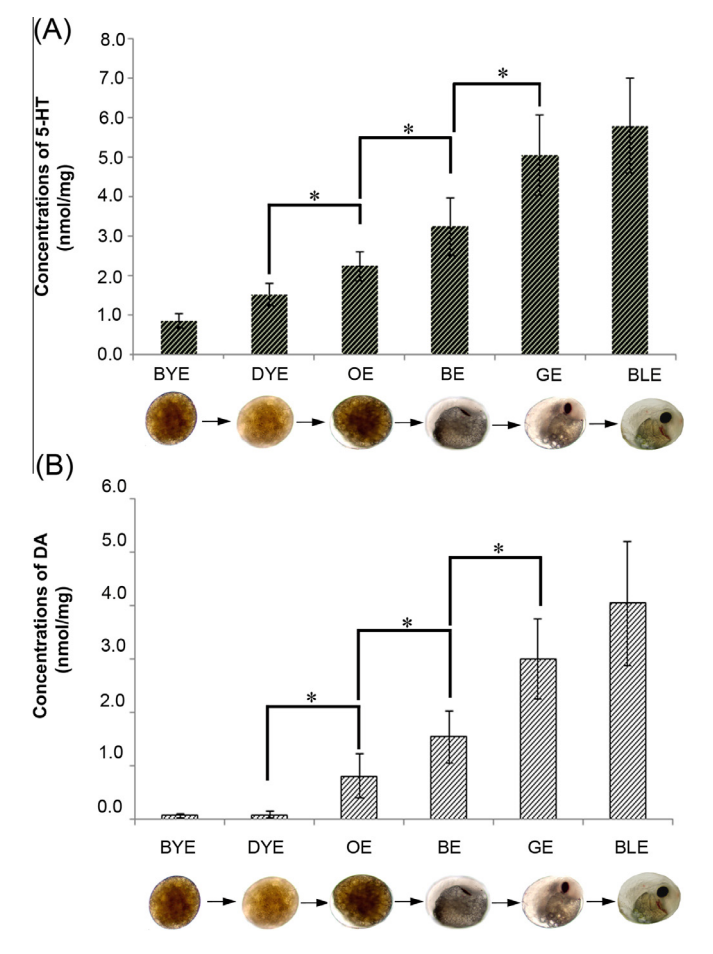


**Fig. 2.** (A) The changing concentrations of 5-HT in various embryonic stages, and (B) the concentrations of DA in various embryonic stages, as determined by HPLC. The concentration is expressed as nmol/mg of protein in the tissue extract. Numbers are means  $\pm$  SEM. Asterisks indicate significant differences at P < 0.05 in an analysis of variance. BE, brown egg; BLE, black egg; BYE, bright yellow egg; DYE, deep yellow egg; GE, gray egg; OE, orange egg. (For interpretation of the references to color in this figure legend, the reader is referred to the web version of this article.)

Province, Thailand. The prawns were kept in outdoor circular concrete tanks, each with 1.50 m diameter with the water depth at 0.80 m, and about 30% water was changed every 2 days. The prawns were fed with commercial pellets (Charoen Pokphand group, Thailand) twice a day. Aeration was given continuously. The plastic cages were added into every tanks (30 pieces per tank) for prawns to hide and to avoid any losses during molting from the cannibalistic behavior of this prawn species. The prawns were acclimatized under a photoperiod of 12:12 h light–dark for two weeks before beginning the experiments. Female prawns were selected and used in all experiments, as soon as they exhibited stage IV of the ovarian cycle. All prawns were cultured until they spawned, and the embryos were allowed to grow following the normal embryonic developmental cycle until reaching the final embryonic stage.

# 2.2. Samples collection and preparation

After they spawned, the mature berried females at various embryonic stages (at least n = 15 prawns) were sampled. The different embryonic stages from abdomen were carefully scraped from the female brood chambers. All spawned eggs were mixed with 3% sodium hypochlorite (NaClO) in distilled water to thoroughly disperse the eggs. At least 300 eggs were observed under

a stereo-microscope to determine the morphology and percentage of developing embryos. The embryonic stages were visually evaluated based on the color and morphological characteristics, which are seen through the abdomen in live females, as described by Müller et al. (2003), Manush et al. (2006), Tinikul et al. (2009a), and Habashy et al. (2012). After the dissection, the wet mass of all eggs was weighed, and later used for HPLC analyses and immunohistochemistry.

#### 2.3. Chemicals and reagents

All chemicals, including 5-HT and DA, were obtained from Sigma–Aldrich (St. Louis, MO, USA). Standard solutions were made up in freshly prepared ice-cold 0.1 M perchloric acid. Each of the standard solutions were prepared on the day of analysis and stored on ice between injections.

#### 2.4. Quantification of 5-HT and DA in the embryos

In the present study, the HPLC methods for quantification of 5-HT and DA concentrations in embryos were based on the method described by Tinikul et al. (2011b, 2015), with some modifications. After being dissected out and weighed, a lump of embryos was placed in 100 µl of 0.1 M perchloric acid and homogenized at 4 °C. The 5-HT and DA concentrations were detected electrochemically using a completely isocratic mode. Samples were injected onto a Brownlee C<sub>18</sub>-Aquapore OD-300 HPLC column  $(250 \times 4.6 \text{ mm i.d.})$ . A glassy carbon electrode, serving as the working electrode was set with an Ag/AgCl reference electrode. The sensitivity of the detector was maintained at 100 nA with full scale deflection. The potential of the detector was set at a range between +0.7 and +0.8 V. The mobile phase consisted of 75 mM NaH<sub>2</sub>PO<sub>4</sub>, 50 μM EDTA, 0.3 mM sodium octylsulphate, 2.5% acetonitrile, and 4% methanol. The pH was adjusted to 2.75 with orthophosphoric acid. The flow rate was kept constant at 0.7 ml/min. The mixture was sonicated and centrifuged at  $14,000 \times g$  at  $4 \,^{\circ}$ C. The supernatants were collected, and then filtered through a 0.22 um spin-x centrifugal filter tube before injection. Samples were injected into a 20 µl injection loop. Each sample was performed in triplicate. The signals from the electrochemical detector were recorded and integrated by using data analysis software (Millennium, Waters). The average concentrations of 5-HT and DA were estimated from three replicates. 5-HT and DA were quantified using the external standard method in which peaks corresponding to 5-HT and DA were detected in the extracts at the same elution times to their corresponding standards. In addition, standard solutions of 5-HT and DA were prepared and dissolved in ice-cold 0.1 M perchloric acid, and then filtered through a 0.45 µm filter and stored on ice during injections into the HPLC system. Furthermore, the identities of the peaks in each sample was verified by spiking known amount of 5-HT and DA standards into the tissue extracts in repeated separations. The Bio-Rad Protein Assay System (Mississauga, Canada) was employed for protein determination according to Bradford (1976). All samples were freshly prepared and analyzed within the same day.

### 2.5. Immunohistochemistry and specificities of antibodies

The dissected embryonic stages were fixed with 4% paraformaldehyde in 0.1 M phosphate-buffered saline (PBS) with 1% sodium meta-bisulfite (SMB) in PBS at 4 °C for 12 h. After fixation and paraffin embedding, the tissue sections were cut at 7–10  $\mu$ m thicknesses for the investigation of early embryonic stages, whereas the sections were cut at 10–20  $\mu$ m thicknesses for late embryonic stages. The sections were further mounted on slides coated with 3-aminopropyl triethoxy-silane solution

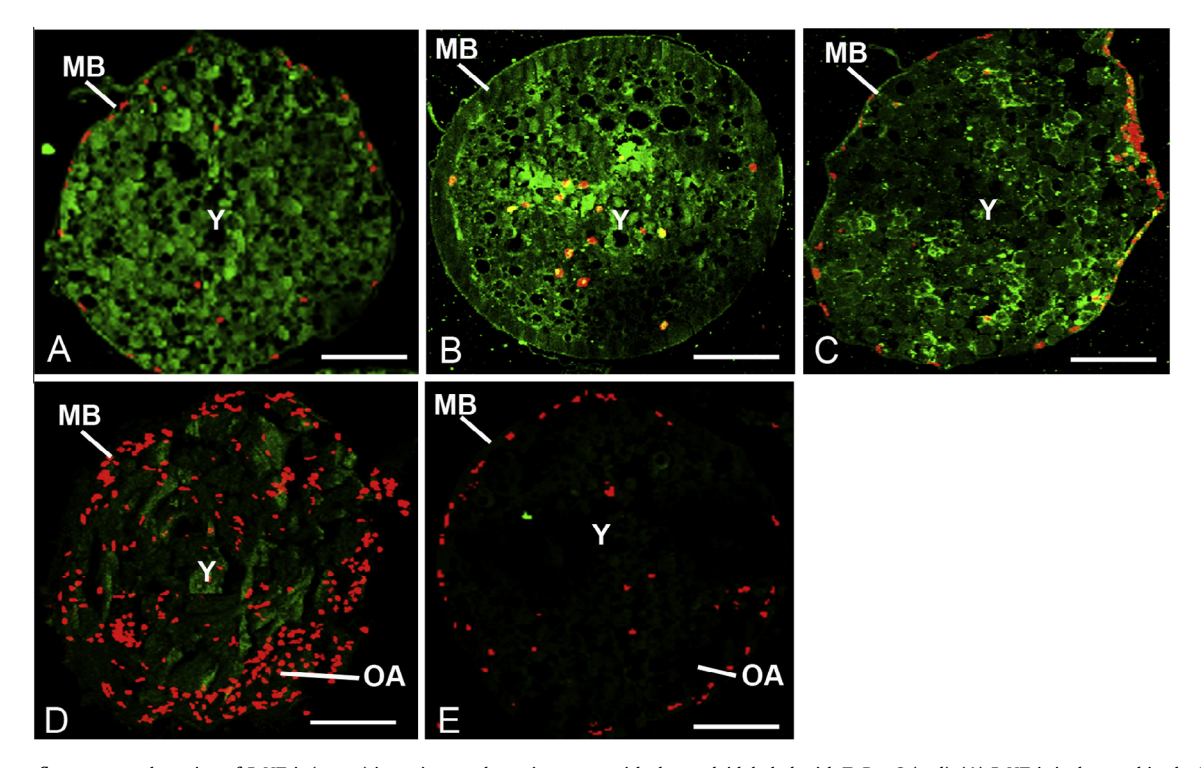


**Fig. 3.** Immunofluorescence detection of 5-HT-ir (green) in various embryonic stages, with the nuclei labeled with ToPro-3 (red). (A) 5-HT-ir is detected in the BYE stage (B and C) 5-HT-ir is present in the yolk of the DYE stage. (D) Intense 5-HT-ir is detected in the yolk of OE stages. (E) In the control sections, no immunofluorescence is detected. MB, egg membrane; OA, organ anlage; Y, yolk. Scale bars: 100 μm. (For interpretation of the references to color in this figure legend, the reader is referred to the web version of this article.)

(Sigma-Aldrich Co., St. Louis, MO, USA), and then processed for immunohistochemistry.

The immunohistochemical localization of 5-HT immunoreactivity (5-HT-ir) and DA immunoreactivity (DA-ir) during various embryonic stages, was performed based on that described previously (Tinikul et al., 2011a,b). Briefly, the sections were deparaffinized and rehydrated through a graded ethanol series for 10 min each. The sections were incubated with 1% glycine in PBS for 15 min. Subsequently, non-specific binding was blocked by immersing the sections in a blocking solution containing 10% normal goat serum (NGS) and 1% SMB in PBS with 0.4% triton-X (PBST), at room temperature for 2 h, in a moist chamber. The sections were then incubated with the primary antibodies, rabbit anti-5-HT (Chemicon International, USA), diluted 1:50 in the blocking solution, or rabbit anti-DA (Gemacbio, St. Jean d'Illac, France), diluted 1:100 in the blocking solution, at room temperature. The sections were washed three times with PBST, and then incubated in the secondary antibody, Alexa488-conjugated goat anti-rabbit IgG (Molecular Probes, Eugene, OR, USA), diluted 1:200 in the blocking solution, at room temperature for 2 h. In addition, the nuclei of cells in sections of embryos were stained with ToPro-3 (Molecular Probes), diluted at 1:2000 in the blocking solution. The sections were mounted in Vectashield (Vector Laboratory, Burlingame, CA, USA), viewed and images captured by an Olympus FV1000 confocal laser scanning microscope.

The specificities of the polyclonal antibodies against 5-HT and DA were tested by the manufacturer using standard immunohistochemical methods. The manufacturer has demonstrated that anti-5-HT and anti-DA antibodies did not cross-react with other biogenic amines. In the control sections, the specificities of anti-5-HT and anti-DA were ascertained by omitting the primary antibodies from the immunolocalization, or by pre-adsorption of the primary antibodies with 100  $\mu g/ml$  of synthetic 5-HT or DA (Sigma–Aldrich, St. Louis, MO, USA) at 4 °C for about 20 h, before staining (Tinikul et al., 2011b). In these controls, no immunostaining was observed.

## 2.6. Image analysis

The embryonic sections prepared for immunohistochemistry, were photographed with an Olympus Fluoview 1000 laserscanning confocal microscope (Olympus America, Center Valley, PA). Subsequently, the tissues were scanned sequentially for each fluorophore to obtain separate images for each label, and an overlayed image of all three channels for each optical section. These projected images were produced using subsets of the z-stacks. Furthermore, the digital images were exported and converted from the Olympus confocal system, and further transferred into Photoshop CS5 software (Adobe Systems Inc., San Jose, CA, USA), to adjust contrast and brightness to obtain optimal clarity. Images were not modified other than to balance brightness and contrast, as well as to remove irrelevant structures that interfered with visualization of our tissues using Adobe Photoshop CS5 (Adobe Systems, San Jose, USA). In addition, negative controls for each fluorochrome were scanned using the same parameter settings.

# 2.7. Investigation of the specific actions of 5-HT and DA on the development of embryonic stages

The methods and doses of 5-HT and DA used in this study were based on that described previously (Tinikul et al., 2009a, 2014), with some modifications. The experimental groups were divided into three groups and compared with the control group (with all groups having about 40–45 animals each). The first group was untreated control group (C), groups 2, 3 and 4 were injected with 5-HT and DA at doses of  $2.5 \times 10^{-5}$ ,  $2.5 \times 10^{-6}$  and  $2.5 \times 10^{-7}$ -mol/prawn, respectively, which were equivalent to the circulating concentrations of about 5, 0.5, and 0.05 mM, respectively, after dilution by the prawn hemolymph. 5-HT and DA were dissolved in crustacean physiological saline. The injected volumes of 5-HT and DA were 0.1 ml. All injections were performed at 4-day intervals. All prawns tolerated the injected doses of these two

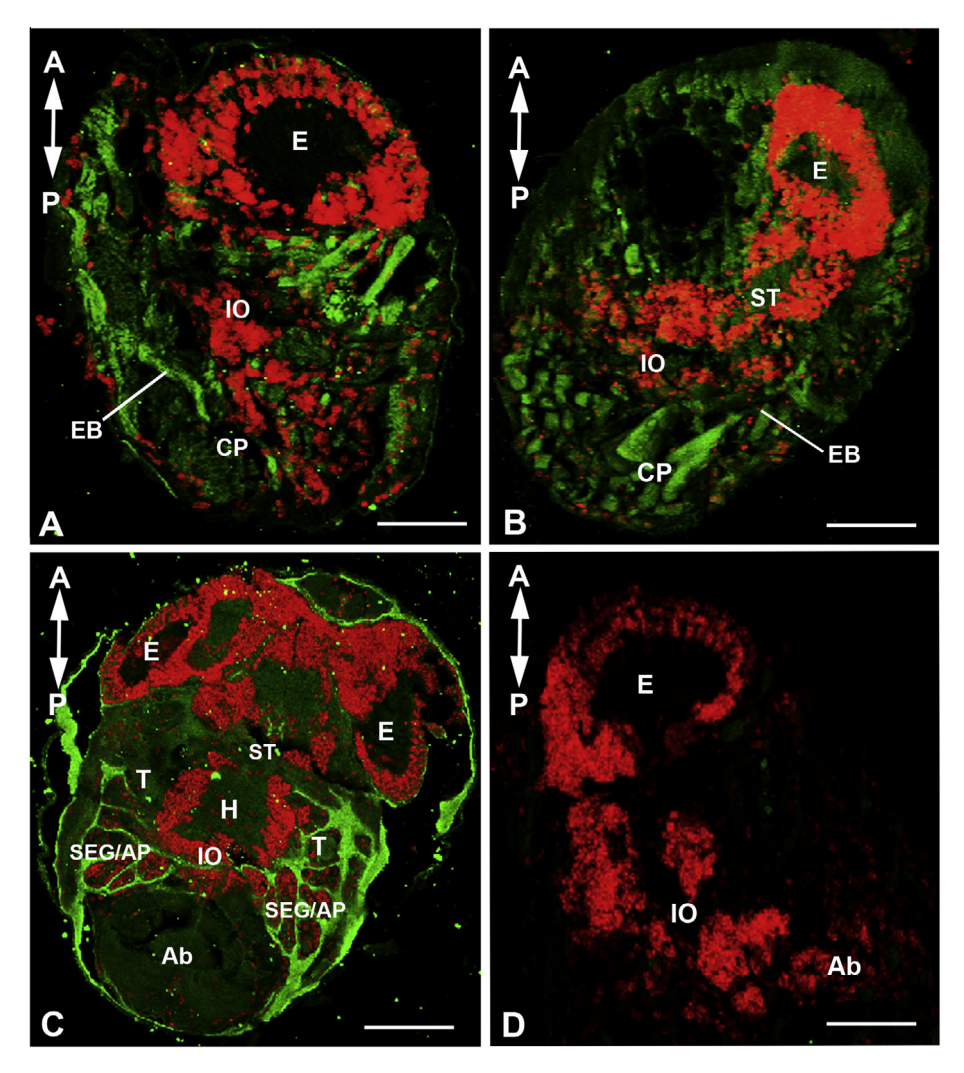


**Fig. 4.** Immunofluorescence detection of 5-HT-ir (green) in various embryonic stages, with nuclei labeled with ToPro-3 (red). The orientation of the embryos is given top left. (A) 5-HT-ir is present in the E, H, EB and CP at BE stage. (B and C) 5-HT-ir is detected in the EB, CP, SEG and AP at the GE and BLE stages. (D) In the control sections, no immunofluorescence is observed. A, anterior; Ab; abdomen; AP, appendages; E, eye; EB, elongated body; H, heart; IO, internal organs; P, posterior; SEG, segmented abdomen; ST, stomodaeum; T, trunk; Y, yolk. Scale bars: 100 μm. (For interpretation of the references to color in this figure legend, the reader is referred to the web version of this article.)

neurotransmitters without exhibiting any abnormal behavior. Measurements of total length and weight of the prawns were performed on every treatment day before injection. Prawns were identified in each group by tagging with plastic loops of different colors around the eyestalks. The injections were performed via an intramuscular route at the second abdominal segment using a 1 ml syringe fitted with  $26~\mathrm{G}\times1/2~(0.45\times12~\mathrm{mm})$  thin-wall needles (NIPRO). The experiment was performed in triplicate. The rest of the prawns were allowed to proceed until they spawned. After injections with 5-HT and DA, the quantity and quality of the spawned eggs were evaluated from the number of eggs per spawn and the percentage of fertilized eggs in order to ascertain that the embryonic development is normal. The embryonic developmental days after injections with these two neurotransmitters in comparison with the control group were carefully observed and recorded.

# 2.8. Statistical analyses

Experimental data were analyzed with SPSS program (version 12.0, SPSS Inc., Chicago, IL, USA) using one-way analysis of variance (ANOVA) and Tukey's post hoc test. The probability value less than

0.05 (P < 0.05) indicated the significant difference. Experimental data were presented as  $\overline{X} \pm S.E.M.$ .

## 3. Results

# 3.1. General morphology of the embryos resulted from fertilized eggs of M. rosenbergii

The general morphology of the embryonic stages of *M. rosenbergii* is demonstrated in Fig. 1A–K. These were used as the basis for the HPLC detection and mapping the distribution of 5-HT and DA during embryonic development. We have classified embryos into various stages based on the criteria described previously (New, 2002; Manush et al., 2006; Tinikul et al., 2009a). Representative micrographs of the ventral views of berried females showed the mid-embryonic stages (orange egg stage; OE) (Fig. 1A), and the late-embryonic stage (gray egg stage; GE) (Fig. 1B). The newly spawned eggs are elliptical in shape, and characterized by a bright yellow, then deep yellow to orange color, which gradually changes to brown, gray and finally black before hatching. The six main embryonic stages included the bright yellow egg stage (BYE), con-

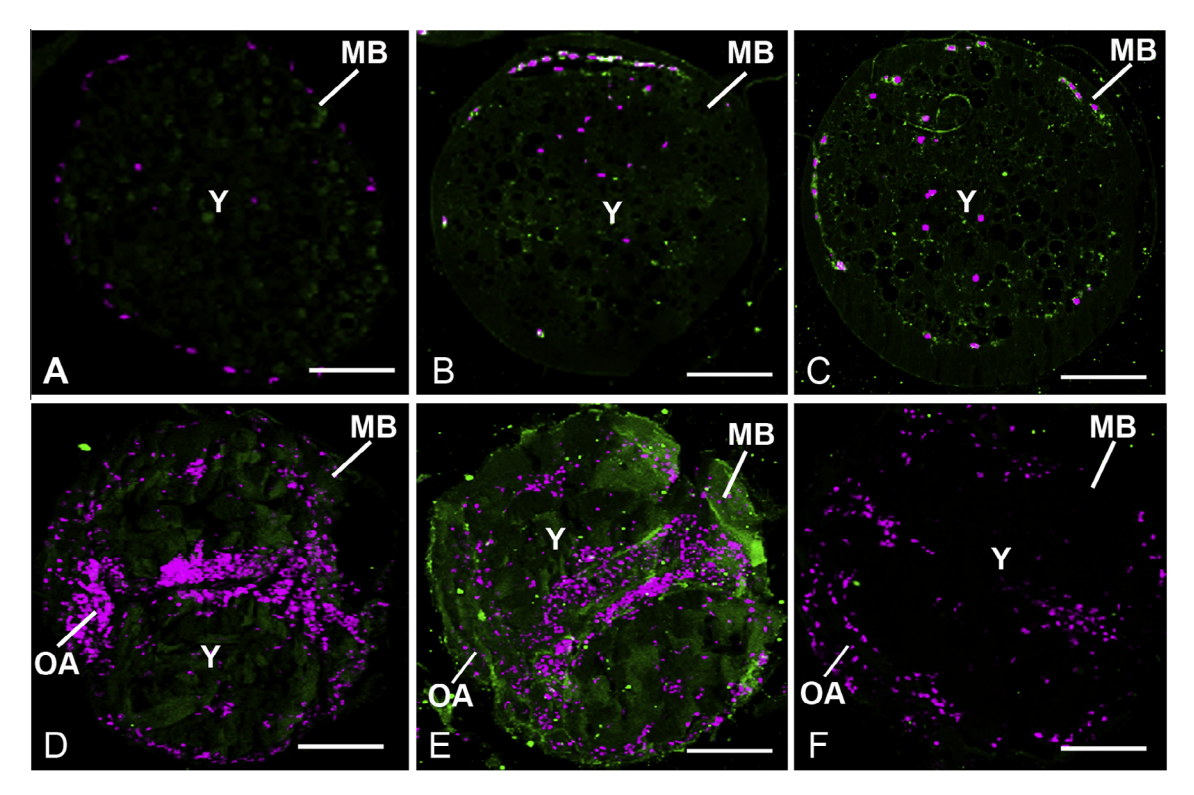


Fig. 5. Immunofluorescence detection of DA-ir (green) in various embryonic stages, with nuclei labeled with ToPro-3 (magenta). (A) DA-ir is present in the yolk of the BYE stage and (B and C) the DYE stage. (D and E) Intense DA-ir is detected in the yolk of OE stages. (F) In the control sections, no immunostaining is present. MB, egg membrane; OA, organ anlage; Y, yolk. Scale bars: 100 μm. (For interpretation of the references to color in this figure legend, the reader is referred to the web version of this article.)

taining mostly high density yolk masses, and a small translucent area (ST) on the egg surface (Fig. 1C and D). A later stage is the deep yellow egg stage (DYE), whose color is a deep yellow with blastocoel (B), clearly visible area in one pole of this embryonic stage (Fig. 1E and F). Later, the orange egg stage (OE), exhibits a clear area that extends to form the body and caudal region of the embryo (Fig. 1F and G). This is followed by the early brown egg stage (BE), which starts to form a pair of eye spots on the yolk area (Fig. 1H and I). At the late BE stage, the heart is firstly observed and starts beating (Fig. 1I). The dark eye spots are oval in shape. In the gray egg stage (GE), rudiments of appendages start to develop and the segmented abdomen is clearly visible (Fig. 1J). Finally, the black egg stage (BLE) is characterized by the presence of a pair of darkrounded eyes, the abdomen is enlarged and curves forward. The appendages are clearly visible before hatching (Fig. 1K).

# 3.2. Changes in the concentrations of 5-HT and DA in the embryonic stages

The 5-HT concentrations in the embryonic stages showed a gradual increase from the BYE stage, to reach the highest concentration at BLE stage (Fig. 2A). The concentration of 5-HT at BYE stage was  $0.86 \pm 0.18$  nmol/mg, and then it gradually increased through the DYE stage and OE stage  $(1.52 \pm 0.29$  and  $2.35 \pm 0.37$  nmol/mg, respectively), to a higher level at BE and GE stages  $(3.49 \pm 0.68$  and  $5.38 \pm 1.01$  nmol/mg, respectively). The highest 5-HT concentration was detected at BLE stage  $(6.05 \pm 1.29 \text{ nmol/mg})$ , which showed approximately a 7-fold increase over BYE stage. The differences were statistically significant (P < 0.05). In addition to the BLE stage, the 5-HT concentration at the BLE stage appeared to be higher than that of the GE stage, but not significantly different (P > 0.05). The 5-HT concentrations were about 2.7, 4, 6.2 times higher in the OE, BE and GE stages, respectively, than at BYE stage (P < 0.05) (Fig. 2A).

Very low DA concentrations were detected at the BYE stage  $(0.07 \pm 0.03 \text{ nmol/mg})$ , and DYE stage  $(0.09 \pm 0.01 \text{ nmol/mg})$ 

(Fig. 2B), whose the difference was not statistically significant (P > 0.05). The concentration of DA sharply increased at the OE stage, and it was  $0.81 \pm 0.24$  nmol/mg, and then about two times increased at the BE stage  $(1.54 \pm 0.49 \text{ nmol/mg})$ . DA levels increased steadily at successive stages, and became about a 2-fold increased at the GE stage  $(3.01 \pm 0.75 \text{ nmol/mg})$ . The DA concentration reached a maximal level at BLE stage  $(4.05 \pm 1.16 \text{ nmol/mg})$ , exhibiting approximately a 60- and 48-fold increases over BYE and DYE stages, respectively (P < 0.05). Interestingly, when comparing within same embryonic egg stages, the concentrations of DA were about 18.8, 2.9, 2.27 and 1.78 times lower in the DYE, OE, BE, GE and BLE than those of 5-HT, respectively (Fig. 2B).

# 3.3. The distribution of 5-HT and DA during embryonic developmental stages

The 5-HT-ir was detected in the yolk at the BYE stage (Fig. 3A), and it appeared to be more intense in the yolk and the membrane at the DYE stage (Fig. 3B and C). At the OE stage, 5-HT-ir was present in the yolk and the organ anlage (OA) (Fig. 3D). No positive fluorescence was observed in a control section taken from the DYE stage (Fig. 3E). At the BE stage, little 5-HT-ir was detected in the optic lobe area, including eye anlage (E) (Fig. 4A), but intense 5-HT-ir was detected in the elongated body (EB), and caudal papilla (CP) (Fig. 4B). In addition, 5-HT-ir was first observed in the stomodaeum (ST) and segmented abdomen (SEG) at the GE stage (Fig. 4B). Furthermore, intense 5-HT-ir was detected at the position of heart (H), SEG, and appendages (AP) (Fig. 4C). No 5-HT-ir was detected in a control section of any part of the late embryonic stages (Fig. 4D).

At BYE and DYE stages, DA-ir was detected with a very low intensity and was not clearly visible in the yolk (Fig. 5A–C). At the OE stage, DA-ir was clearly present in the yolk, and in some cases the OA showed moderate staining for DA-ir (Fig. 5D and E). The control sections of the OE stage did not show any positive fluorescence (Fig. 5F). At the BE stage, DA-ir was detected around

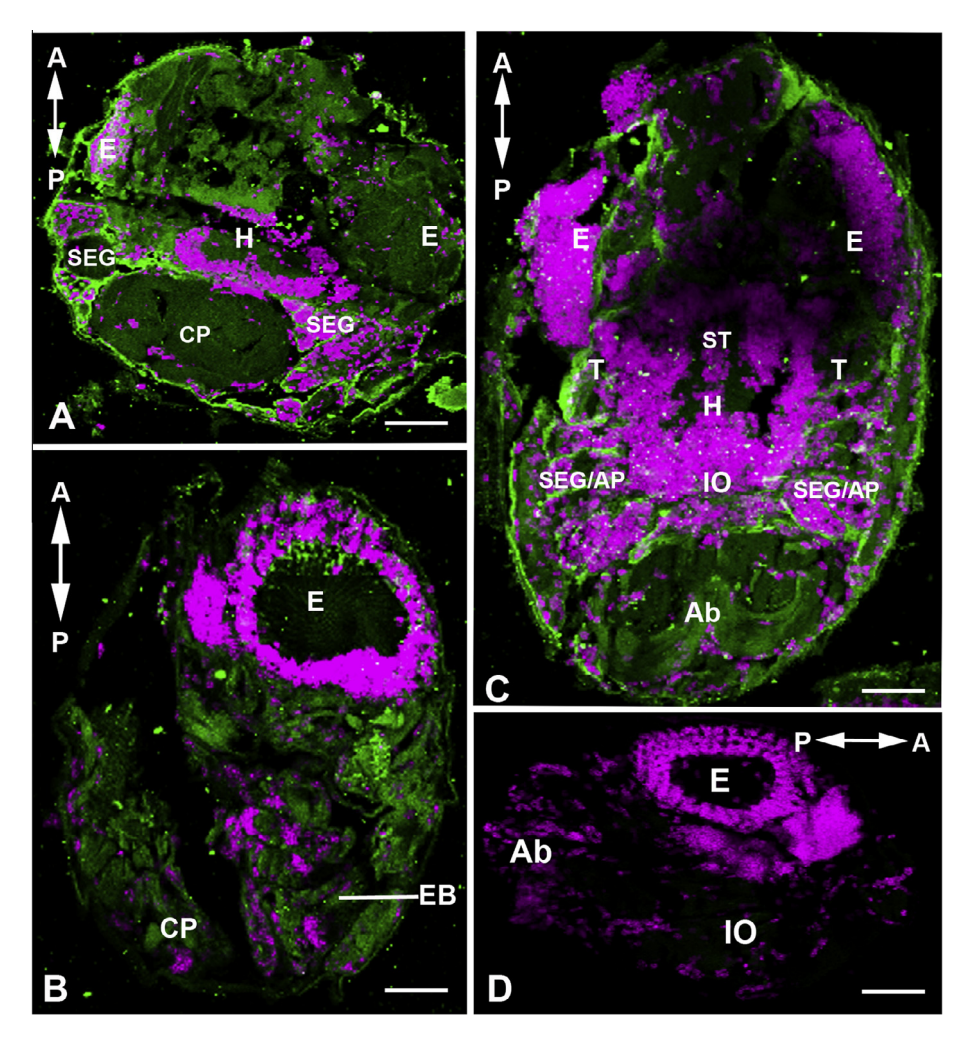


**Fig. 6.** Immunofluorescence detection of DA-ir (green) in the BE, GE, and BLE, with nuclei labeled with ToPro-3 (magenta). The orientation of the embryos is given top left (A–C) and top right (D). (A) DA-ir is present in the E, H, and EB at BE stage. (B) DA-ir is detected in the EB and CP at the GE stage, and (C) DA-ir is present in H, SEG, AP and IO at the BLE stage. (D) No immunofluorescence is detected in the control sections. A, anterior; Ab; abdomen; AP, appendages; E, eye; EB, elongated body; H, heart; IO, internal organs; P, posterior; SEG, segmented abdomen; ST, stomodaeum; T, trunk; Y, yolk. Scale bars: 100 μm. (For interpretation of the references to color in this figure legend, the reader is referred to the web version of this article.)

the E, H, EB and CP structures, and H (Fig. 6A), and strong DA-ir was detected at the periphery of their bodies. Each of the BE, GE, and BLE stages contained DA-ir, which were specifically scattered and intensely stained, compared with those in other early stages of the embryonic eggs (Fig. 6B and C). At the GE and BLE stage, we detected DA-ir in the SEG, CP and H. These DA-irs were continuous from the position of H, thorax regions and passing through the SEG (Fig. 6B and C). No DA-ir was detected in the control section of any part of the GE stage (Fig. 6D).

# 3.4. The specific actions of 5-HT and DA on the development of embryonic stages

The specific actions of 5-HT and DA on the lengths of development of each embryonic stage are shown in Fig. 7A and B. Generally, there were no differences between the 5-HT- and DA-injected groups, compared with the control group at the period from BYE to DYE (P > 0.05), as this period tends to be short (Fig. 7A). After treatment with 5-HT at doses of  $2.5 \times 10^{-5}$ ,  $2.5 \times 10^{-6}$  and  $2.5 \times 10^{-7}$  mol/prawn, the period from DYE stage to OE stage was shorter than that of the control group and was statistically significant (P < 0.05). 5-HT significantly reduced the time for the OE stage to reach the BE stage, they only took ( $3.85 \pm 0.35$ ,

 $3.91\pm0.58$ , and  $4.12\pm0.54$  days) for  $2.5\times10^{-5}$ ,  $2.5\times10^{-6}$  and  $2.5\times10^{-7}$  mol/prawn, respectively. The time from BE to GE stages was about half as long for the 5-HT at a dose of  $2.5\times10^{-5}$  mol/prawn ( $3.54\pm0.35$  days), compared with the control group ( $6.87\pm0.98$  days) (P<0.05). A similar effect was observed after injection of 5-HT at a dose of  $2.5\times10^{-5}$  mol/prawn, which significantly shortened GE to BLE stages ( $3.29\pm0.42$  days), compared with the control group ( $4.65\pm0.75$  days) (P<0.05) (Fig. 7A).

The lengths of BYE to DYE stages from prawns injected with DA at doses of  $2.5 \times 10^{-5}$ ,  $2.5 \times 10^{-6}$  and  $2.5 \times 10^{-7}$  mol/prawn, showed no statistical differences from the control group (P > 0.05) (Fig. 7B). Subsequently, the period from DYE to OE stages was a little longer ( $7.86 \pm 1.61$  and  $7.15 \pm 1.39$  days, respectively), compared with the control group ( $6.14 \pm 0.83$  days), but the difference was not statistically significant (P > 0.05) (Fig. 7B). Interestingly, the period from OE to BE stages (i.e.,  $12.44 \pm 1.43$ ,  $11.32 \pm 1.75$ , and  $9.96 \pm 1.81$  days, respectively) was longer than that of the control group ( $5.42 \pm 1.25$  days) (P < 0.05) (Fig. 7B). Similarly, the period from BE to GE stages was considerably longer, compared with the control group (P < 0.05). Finally, the time from GE to BLE stages after treatment with DA at doses of  $2.5 \times 10^{-5}$  and  $2.5 \times 10^{-6}$  mol/prawn was about two times longer ( $9.89 \pm 1.59$  and  $2.5 \times 10^{-6}$  mol/prawn was about two times longer ( $9.89 \pm 1.59$  and  $2.5 \times 10^{-6}$  mol/prawn was about two times longer ( $9.89 \pm 1.59$  and  $2.5 \times 10^{-6}$  mol/prawn was about two times longer ( $9.89 \pm 1.59$  and  $9.88 \pm 1.05$  days), compared with the control group ( $9.89 \pm 1.59$ ) and  $9.88 \pm 1.05$  days), compared with the control group ( $9.89 \pm 1.59$ ) and  $9.88 \pm 1.05$  days), compared with the control group ( $9.89 \pm 1.59$ ) and  $9.88 \pm 1.05$  days), compared with the control group ( $9.89 \pm 1.59$ ) and  $9.88 \pm 1.05$  days), compared with the control group ( $9.89 \pm 1.59$ ) and  $9.88 \pm 1.05$  days), compared with the control group ( $9.89 \pm 1.59$ ) and  $9.88 \pm 1.05$  days), compared with the control group ( $9.89 \pm 1.59$ ) and  $9.88 \pm 1.05$  days), compared with the control group ( $9.89 \pm 1.59$ ) and  $9.88 \pm 1.05$  days), compared with the control group ( $9.89 \pm 1.59$ ) and  $9.88 \pm 1.05$  days).

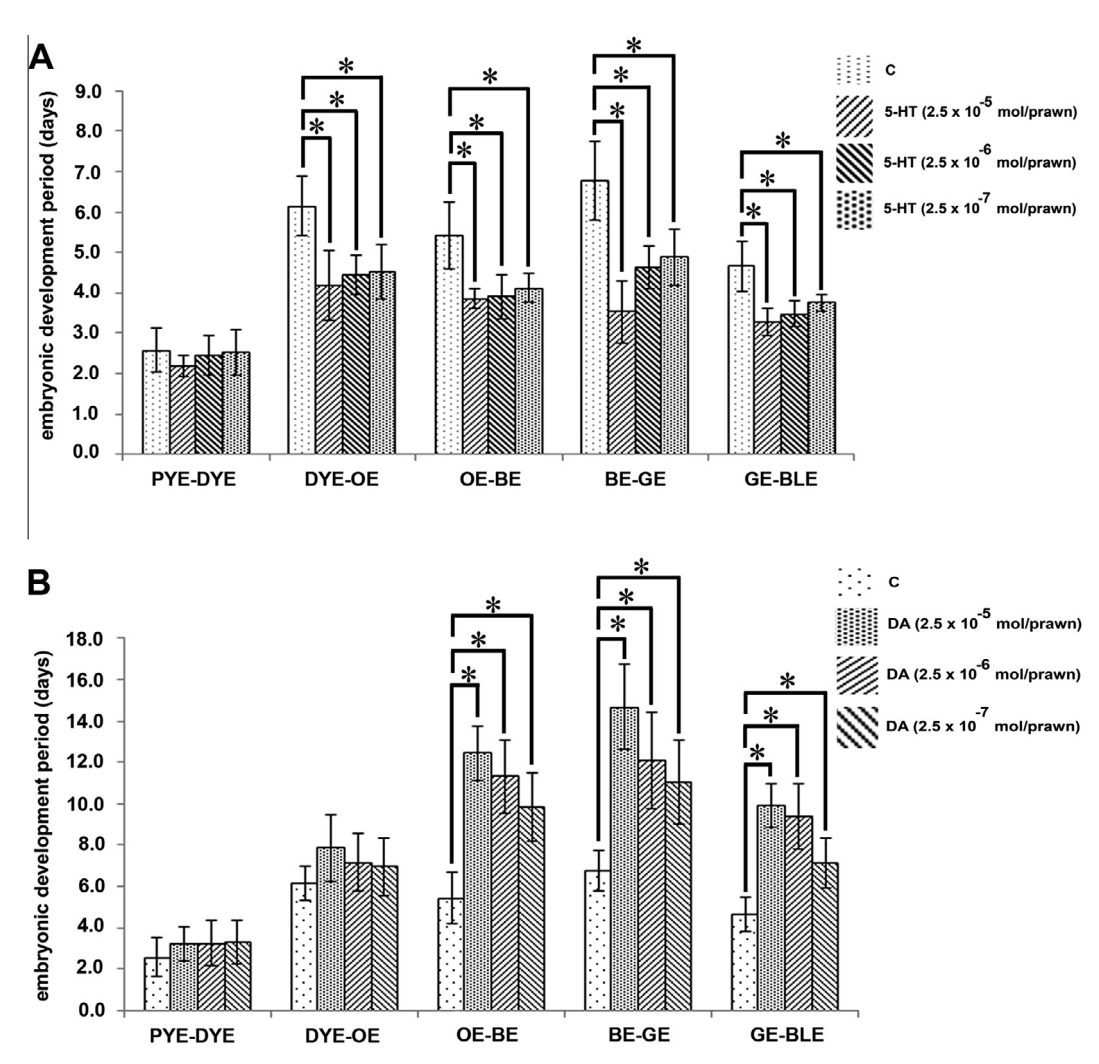


**Fig. 7.** The effects of 5-HT and DA on the development of each embryonic stage in *M. rosenbergii*. (A) Histograms showing that female prawns injected with 5-HT at doses of  $2.5 \times 10^{-5}$ ,  $2.5 \times 10^{-6}$  and  $2.5 \times 10^{-7}$  mol/prawn, exhibited significant shortening embryonic developmental period started from DYE to OE stages and onwards, compared with the control group. (B) After injections with DA at doses of  $2.5 \times 10^{-5}$ ,  $2.5 \times 10^{-6}$  and  $2.5 \times 10^{-7}$  mol/prawn, showed significant lengthening embryonic developmental period started from mid-embryonic stage onwards, compared with the control group. Each measurement is expressed as a mean  $\pm$  S.E.M. Asterisks indicate significant differences (P < 0.05) with respect to the control groups.

#### 4. Discussion

In this study, we reported for the first time in *M. rosenbergii* on the variation in concentrations and distribution of 5-HT and DA during embryogenesis. The 5-HT concentrations increased significantly at the early embryonic stages, while DA levels remained low. DA was clearly detected at about the mid-embryonic stage. 5-HT exerted its action by significantly decreasing durations of nearly all embryonic stages, whereas DA lengthened the durations of the mid-embryonic stages. This demonstrates the opposite actions of 5-HT and DA on embryonic development.

Several studies have reported on the varying concentrations of these two neurotransmitters during developmental processes in invertebrates, including decapod crustaceans. In the hookworm, *Nippostrongylus brasiliensis*, the fluctuation of 5-HT occurs in the embryonic and larval stages, suggesting that this amine may play important role during embryonic development (Goudey-Perrie et al., 1997). In the crayfish, *P. clarkii*, 5-HT levels in free larval stages were quantified using HPLC, with the total concentration of 5-HT being higher in the brain than in the eyestalks (Cervantes et al., 1999), which suggests that 5-HT may play an important role in embryonic development (Escamilla-Chimal

et al., 1998; Benton et al., 1997). In the sea urchin, DA showed a very low concentration at the blastula stage, and then it gradually increased from the late gastrula to late prism stages, and finally exhibited a sharp increase to reach a maximal concentration at late pluteus larva. This fluctuation in DA levels suggests a regulatory role for DA on the formation and transition of gastrula stage to the late embryonic stages (Anitole-Misleh and Brown, 2004). In addition, tyrosine, which is the precursor for synthesis of DA, exhibited a high concentration in the eyes and internal organs during embryogenesis, implying important roles of DA in accumulation of eye pigments and internal organ formation (Shen and Wang, 1990). Our present work demonstrates for the first time that the levels of 5-HT and DA fluctuate during the embryonic stages of M. rosenbergii, but the timing for the initial appearances of these two transmitters are different with the appearance of 5-HT at early embryonic stage, while DA appears later. The increases in 5-HT and DA to maximum levels by the late embryonic stages in M. rosenbergii, detected with HPLC analyses are in agreement with immunohistochemical data which demonstrated that the 5-HT-ir and DA-ir were more intense in the late embryonic stages. It is also possible that 5-HT and DA are important signaling molecules that regulate embryonic development of this species.

There have been reports regarding the presence and distribution of 5-HT and DA during embryonic development in invertebrates. In the sea urchin, 5-HT regulates cell divisions during cleavage and blastula stages, and promotes invagination to form the archenteron during gastrulation, suggesting that 5-HT is synthesized in fertilized eggs and early embryos so that it can regulate the processes of early embryogenesis (Buznikov et al., 2001). In addition, 5-HT could be an important molecule at the early embryonic stages that may be involved in expression of zygotic genes during the mid-blastula transition stages (Emanuelsson et al., 1988; Buznikov, 1990; Buznikov, 1991; Colas et al., 1999). In Drosophila, 5-HT also promotes the gastrulation during embryonic development, implying that 5-HT plays important role in the development of early embryos up to gastrulation stage (Colas et al., 1999). In the mollusk, Tritonia diomedea, 5-HT-ir was detected in cleaving embryos, indicating that 5-HT may be involved in the control of cleavage stage (Buznikov and Bezuglov, 2000). There are a few reports regarding the serotonergic system during embryonic development of crustaceans. In the crayfish, Cherax destructor, 5-HT was detected by the second postembryonic stage (Sandeman and Sandeman, 1990; Rieger and Harzsch, 2008). In the American lobster, H. americanus, 5-HT was firstly detected immunohistochemically in early embryonic stages, suggesting that 5-HT was synthesized early during embryogenesis (Beltz, 1999; Beltz et al., 2001). In the present study, we reported for the first time the existence and distribution of 5-HT in several embryonic stages of M. rosenbergii. Specifically, we detected 5-HTir in several regions and structures of different embryonic stages, including the yolk, cell membrane, and organ anlages, including the eye anlage, the elongated body, internal organs, and the heart, suggesting that 5-HT could be synthesized at early embryonic stages, and that it may be involved in regulating the utilization of yolk, and serving in regulating the cleavage stage, as well as in organ formation, for example, the invagination of the archenteron during gastrulation, as reported earlier in the sea urchin (Colas et al., 1999).

DA has been detected during embryonic stages of many invertebrate species, including decapod crustaceans. In the sea urchin and the starfish. DA-ir was detected in the zygotes, cells of cleavage and blastula stages, indicating that DA may be involved in the control of cell divisions during these stages (Buznikov et al., 1996). In H. americanus, the DA-ir staining was first detected at about the mid-embryonic stages, indicating that the onset of DA is later than 5-HT (Cournil et al., 1995). DA-ir was detected in the stomatogastric ganglion and other internal organs, suggesting that DA may be involved in the growth of stomach and exerts its activity during the lobster embryogenesis (Pulver et al., 2003). In Calanus finmarchicus, DA biosynthetic enzyme-encoding transcripts were present across six developmental stages. This suggests that the synthesis of DA occurs during early naupliar life (Christie et al., 2014). In the present study, we also reported the initial appearance and tissue distribution of DA at about the mid-embryonic stages of M. rosenbergii embryos. The timing of the first appearance of DA in embryonic stages of M. rosenbergii was similar to those of other crustacean species, though slightly earlier than in H. americanus. Specifically, DA-ir was detected in the yolk and organ anlages, which was similar to those found in the sea urchin, suggesting that DA might be involved in regulating the utilization of yolk and the development of organs during the stages of a rapid growth of the embryos, as reported in H. americanus. In M. rosenbergii, DA-ir was also detected in the eye anlage and internal organs, implying that DA might be involved in regulating in the development of these organs (Zhao et al., 1998; Yao et al., 2006).

There have been reports on the actions of 5-HT and DA during development in invertebrates and in a few decapod crustaceans. In the sea urchin, it was found that 5-HT stimulates cleavage divisions, while DA inhibits cell divisions during these processes, implying their opposite actions during embryonic development (Buznikov

and Bezuglov, 2000; Buznikov et al., 2001). Moreover, 5-HT receptors were up-regulated in the mid-blastula stage, which was correlated with the rapid cell division, resulting in the formation of additional cell layers in the blastula wall in the sea urchin (Buznikov et al., 2001). In H. americanus, the critical role of 5-HT in the embryonic development was demonstrated by pharmacological depletion of 5-HT using 5,7-dihydroxytryptamine, which resulted a long-term reduction of 5-HT that significantly slowed the growth of olfactory and accessory lobes of the brain, suggesting that 5-HT may play a role in the brain development (Benton et al., 1997). In M. rosenbergii, prawn larvae exposed to 5-HT showed significantly reduced lengths of all larval stages and enhanced the transformation post-larval stage, compared with the control group (Tangvuthipong and Damrongphol, 2006). Previously, we found that injecting 5-HT into adult female M. rosenbergii broodstocks also shortened the whole length of embryonic development, whereas injecting DA showed an opposite effect, suggesting these two neurotransmitters act antagonistically with regard to the embryonic development (Tinikul et al., 2009a,b). However, that study did not detail the specific actions of 5-HT and DA on the lengths of each embryonic developmental stage. In the present study, we further demonstrated that the injection of 5-HT to female broodstocks significantly decreased the lengths of embryonic development from early to late embryonic stages, whereas DA-injected groups significantly lengthened the embryonic development from the mid to late stages, compared with the control group. It is possible that 5-HT may stimulate the development of early embryonic stages, while DA exercises opposite control as demonstrated in the sea urchin (Buznikov and Bezuglov, 2000; Buznikov et al., 2001). In addition, 5-HT has been reported to stimulate the release of a number of other neurohormones in decapod crustaceans, particularly crustacean hyperglycemic hormone (CHH) during early development. We postulate that 5-HT may regulate the release of the CHH which stimulates glycogenolysis in muscles and the midgut to promote early development, and supports fast growth during embryonic stages in crustaceans (Kallen et al., 1988). Our results indicate the dynamic balance of these two neurotransmitters acting together during embryonic development, which may be necessary for setting the normal rhythm and pattern of embryonic formation in this prawn species. The precise molecular mechanisms of 5-HT and DA actions in embryonic development of this decapod crustacean needed to be clarified by further studies.

### **Conflict of interest**

All authors have no conflict of interest.

#### Acknowledgments

This research was supported by a TRF Research Career Development Grant (RSA5780011) to Yotsawan Tinikul (co-funded by the Thailand Research Fund and Mahidol University), and a Distinguished Research Professor Grant to Prasert Sobhon (jointly funded by the Thailand Research Fund, the Commission on Higher Education, and Mahidol University). We thank the Center of Nanoimaging (CNI), Faculty of Science, Mahidol University, for the use of a confocal microscope and technical assistance. We are grateful to Assoc. Prof. Chaitip Wanichanon and Mr. Anurak Prabyai for useful suggestions and technical assistance.

#### References

Anitole-Misleh, K.G., Brown, K.M., 2004. Developmental regulation of catecholamine levels during sea urchin embryo morphogenesis. Comp. Biochem. Physiol. Part A 137, 39–50.

Beltz, B.S., 1999. Distribution and functional anatomy of amine-containing neurons in decapod crustaceans. Microsc. Res. Tech. 44, 105–120.

- Beltz, B.S., Benton, J.L., Sullivan, J.M., 2001. Transient uptake of serotonin by newborn olfactory projection neurons. Proc. Natl. Acad. Sci. U.S.A. 98, 12730– 12735.
- Benton, J.L., Huber, R., Ruchhoeft, M., Helluy, S., Beltz, B.S., 1997. Serotonin depletion by 5,7-dihydroxytryptamine alters deutocerebral development in the lobster, *Homarus americanus*. J. Neurobiol. 33, 357–373.
- Bradford, M.M., 1976. A rapid and sensitive method for the quantitation of microgram quantities of protein utilizing the principle of protein-dye binding. Anal. Biochem. 72, 248–254.
- Buznikov, G.A., 1990. Neurotransmitters in Embryogenesis. Harwood Academic Press, USA.
- Buznikov, G.A., 1991. The biogenic monoamines as regulators of early (pre-nervous) embryogenesis: new data. In: Timiras, P.S. et al. (Eds.), Plasticity and Regeneration of the Nervous System. Plenum, New York, pp. 33–48.
- Buznikov, G.A., Bezuglov, V.V., 2000. 5-Hydroxytryptamides and 3-hydroxytyramides of polyenoic fatty acids as a tool for studying the prenervous biogenic monoamines functions. Russ. J. Physiol. 86, 1093–1108 (In Russian)
- Buznikov, G.A., Lambert, H.W., Lauder, J.M., 1996. From oocyte to neuron: do neurotransmitters function in the same way throughout development? Cell. Mol. Neurobiol. 16, 532–559.
- Buznikov, G.A., Lambert, H.W., Lauder, J.M., 2001. Serotonin and serotonin-like substances as regulators of early embryogenesis and morphogenesis. Cell Tissue Res. 305. 177–186.
- Cervantes, O.C., Battelle, B.A., Moles, M.L.F., 1999. Rhythmic changes in the serotonin content of the brain and eyestalk of crayfish during development. J. Exp. Biol. 202, 2823–2830.
- Chen, Y.N., Fan, H.F., Hsieh, S.L., Kuo, C.M., 2003. Physiological involvement of DA in ovarian development of the freshwater giant prawn, *Macrobrachium rosenbergii*. Aquaculture 228, 383–395.
- Christie, A.E., Fontanilla, T.M., Roncalli, V., Cieslak, M.C., Lenz, P.H., 2014. Identification and developmental expression of the enzymes responsible for dopamine, histamine octopamine and serotonin biosynthesis in the copepod crustacean *Calanus finmarchicus*. Gen. Comp. Endocrinol. 195, 28–39.
- Colas, J.F., Launay, J.M., Maroteaux, L., 1999. Maternal and zygotic control of serotonin biosynthesis are both necessary for *Drosophila* germband extension. Mech. Dev. 87, 67–76.
- Cournil, I., Casasnovas, B., Helluy, S.M., Beltz, B.S., 1995. Dopamine in the lobster *Homarus gammarus*: Il dopamine-immunoreactive neurons and development of the nervous system. J. Comp. Neurol. 362, 1–16.
- Elofsson, R., Laxmyr, L., Rosengren, E., Hansson, C., 1982. Identification and quantitative measurement of biogenic amines and DOPA in the central nervous system and hemolymph of the crayfish *Pacifastacus leniusculus* (Crustacea), Comp. Biochem, Physiol. Part C 71, 195–201.
- Emanuelsson, H., Carlberg, M., Lowkvist, B., 1988. Presence of serotonin in early chick embryos. Cell Differ. 24, 191–200.
- Escamilla-Chimal, E.G., García-Rivera, C.C., Aguilar-Morales, M., Romero-Díaz, V., Fanjul-Moles, M.L., 1998. The retina of crayfish *Procambarus clarkii* during development shows serotonin and tryptophan hydroxylase-like immunoreactivity daily changes. Biol. Rhythm Res. 29, 471–479.
- Fingerman, M., 1997. Roles of neurotransmitters in regulating the reproductive hormone release and gonadal maturation in decapod crustaceans. Invertebr. Reprod. Dev. 31, 47–54.
- Goudey-Perrie, F., Grosclaude, J.M., Nembo, B., Burreteau, H., Jacquot, F.C., Gayral, P., 1997. Levels of biogenic amines in larvae and adults of the rat hookworm, *Nippostrongylus brasiliensis* (Nematoda). Comp. Biochem. Physiol. Part A 118, 615–622
- Habashy, M.M., Sharshar, K.M., Hassan, M.M.S., 2012. Morphological and histological studies on the embryonic development of the freshwater prawn, *Macrobrachium rosenbergii* (Crustacea, Decapoda). JOBAZ 65, 157–165.
- Kallen, J.L., Rigiani, N.R., Trompenaars, H.J.A.J., 1988. Aspects of entrainment of CHH cell activity and hemolymph glucose levels in crayfish. Biol. Bull. 175, 137–143.
- Kullkarni, G.K., Nagabhushanam, R., Amaldoss, G., Jaiswal, R.G., Fingerman, M., 1992. In vitro stimulation of ovarian development in the red swamp crayfish, Procambarus clarkii (Girard), by 5-hydroxytryptamine. Invertebr. Reprod. Dev. 21, 231–240.
- Manush, S.M., Pal, A.K., Das, T., Mukherjee, S.C., 2006. The influence of temperatures ranging from 25 to 36 °C on developmental rates, morphometrics and survival of freshwater prawn (*Macrobrachium rosenbergii*) embryos. Aquaculture 256, 529–536.
- Müller, Y.M.R., Nazari, E.M., Simões-Costa, M.S., 2003. Embryonic stages of the freshwater prawn, *Macrobrachium olfersii* (Decapoda, Palaemonidae). J. Crustacean. Biol. 23, 869–875.
- Nagaraju, G.P., 2011. Reproductive regulators in decapod crustaceans: an overview. J. Exp. Biol. 214 (1), 3–16.

- Nagaraju, G.P., Prasad, G.L.V., Taliaferro-Smith, L., Aruna, B.V., Naik, B.R., Sekhar, Y. N., 2010. Computational analysis of the structural basis of ligand binding to the crustacean retinoid X receptor. Comp. Biochem. Physiol. Part D 5, 317–324.
- New, M.B., 2002. Farming freshwater prawns: a manual for the culture of the giant river prawn (*Macrobrachium rosenbergii*). FAO Fisheries Technical Paper 428, 1–10
- Prasad, G.L.V., Naik, B.R., Ko, J.E., Nagaraju, G.P., 2014. Effects of naloxone, serotonin, and dopamine on reproduction of the freshwater crab *Barytelphusa guerini*. J. Exp. Zool. 321A, 173–182.
- Pulver, S.R., Thirumalai, V., Richards, K.S., Marder, E., 2003. Dopamine and histamine in the developing stomatogastric system of the lobster *Homarus americanus*. J. Comp. Neurol. 462, 400–414.
- Richardson, H.G.D., Decaraman, M., Fingerman, M., 1991. The effect of biogenic amines on ovarian development in fiddler crab, *Uca pugilator*. Comp. Biochem. Physiol. Part C 99, 53–56.
- Rieger, V., Harzsch, S., 2008. Embryonic development of the histaminergic system in the ventral nerve cord of the marbled crayfish (Marmorkrebs). Tissue Cell 40, 113–126
- Sandeman, R., Sandeman, D.C., 1990. Development and identified neural systems in the crayfish brain. In: Wiese, K., Krenz, W.D., Tautz, J., Reichert, H., Mulloney, B. (Eds.), Frontiers in Crustacean Neurobiology. Birkhaüser, Basel, pp. 498–508.
- Sandifer, P.A., Smith, T.J., 1985. Freshwater Prawn: Crustacean and Mollusk Aquaculture in the United States. A Publishing Company Inc., Westport, USA, pp. 1–15.
- Shen, T., Wang, J.Y., 1990. Biochemistry [M]. Higher Education Publisher, pp. 67–86.
  Tangvuthipong, P., Damrongphol, P., 2006. 5-Hydroxytryptamine enhances larval development of the giant freshwater prawn, *Macrobrachium rosenbergii*.
  Aquaculture 251, 567–572.
- Tinikul, Y., Mercier, A.J., Soonklang, N., Sobhon, P., 2008. Changes in the levels of serotonin and dopamine in the central nervous system and ovary, and their possible roles in the ovarian development in the giant freshwater prawn, *Macrobrachium rosenbergii*. Gen. Comp. Endocrinol. 158, 250–258.
- Tinikul, Y., Soonthornsumrith, B., Phoungpetchara, I., Poljareon, J., Meeratana, P., Duangsuwan, P., Soonklang, N., Mercier, A.J., Sobhon, P., 2009a. Effects of serotonin, dopamine, octopamine, and spiperone on ovarian maturation and embryonic development in the giant freshwater prawn, *Macrobrachium rosenbergii* (De Man, 1879). Crustaceana 82, 1007–1022.
- Tinikul, Y., Mercier, A.J., Sobhon, P., 2009b. Distribution of dopamine and octopamine in the central nervous system and ovary during the ovarian maturation cycle in the giant freshwater prawn, *Macrobrachium rosenbergii*. Tissue Cell 41, 430–442.
- Tinikul, Y., Poljaroen, J., Nuurai, P., Anuracpreeda, P., Chotwiwatthanakun, C., Phoungpetchara, I., Kornthong, N., Poomtong, T., Hanna, P.J., Sobhon, P., 2011a. Existence and distribution of gonadotropin-releasing hormone-like peptides in the central nervous system and ovary in the Pacific white shrimp, *Litopenaeus vannamei*. Cell Tissue Res. 343, 579–593.
- Tinikul, Y., Poljaroen, J., Kornthong, N., Chotwiwatthanakun, C., Anuracpreeda, P., Poomtong, T., Hanna, P.J., Sobhon, P., 2011b. Distribution and changes of serotonin and dopamine levels in the central nervous system and ovary of the Pacific white shrimp, *Litopenaeus vannamei*, during ovarian maturation cycle. Cell Tissue Res. 345, 103–124.
- Tinikul, Y., Poljaroen, J., Tinikul, R., Anuracpreeda, P., Chotwiwatthanakun, C., Senin, N., Poomtong, T., Hanna, P.J., Sobhon, P., 2014. Effects of gonadotropin-releasing hormones and dopamine on ovarian maturation and their presence in the ovary during ovarian development of the Pacific white shrimp, *Litopenaeus vannamei*. Aquaculture 420–421, 79–88.
- Tinikul, Y., Poljaroen, J., Tinikul, R., Chotwiwatthanakun, C., Anuracpreeda, P., Hanna, P.J., Sobhon, P., 2015. Alterations in the levels and distribution of octopamine in the central nervous system and ovary of the Pacific white shrimp, *Litopenaeus vannamei*, and its possible role in ovarian development. Gen. Comp. Endocrinol. 210, 12–22.
- Vaca, A.A., Alfaro, J., 2000. Ovarian maturation and spawning in the white shrimp, *Penaeus vannamei*, by serotonin injection. Aquaculture 182, 373–385.
- Wongprasert, K., Asuvapongpatana, S., Poltana, P., Tiensuwan, M., Withyachumnarnkul, B., 2006. Serotonin stimulates ovarian maturation and spawning in the black tiger shrimp *Penaeus monodon*. Aquaculture 261, 1447– 1454
- Yao, J.J., Zhao, Y.L., Wang, Q., Zhou, Z.L., Hu, X.C., Duan, X.W., An, C.G., 2006. Biochemical compositions and digestive enzyme activities during the embryonic development of prawn, *Macrobrachium rosenbergii*. Aquaculture 253, 573–582.
- Zhao, Y.L., Wang, Q., Du, N.S.H., Lai, W., 1998. Embryonic development of the giant fresh water prawn, *Macrobrachium rosenbergii* (Crustacea: Decapoda): I. Morphogenesis of external structures of embryo (Chinese). Acta Zool. Sin. 44, 249–256.